Fluorescent Bioanalytical Platforms

Based on Graphene Oxide

산화그래핀을 이용한 형광기반의 생분자 분석

플랫폼의 개발

2015 년 2 월

서울대학교 대학원

화학부 나노바이오화학 전공

이 지 언

Fluorescent Bioanalytical Platforms

Based on Graphene Oxide

by

Jieon Lee

Supervisor: Prof. Dal-Hee Min

February, 2015

Department of Chemistry

Graduate School

Seoul National University

Fluorescent Bioanalytical Platforms Based on Graphene Oxide

산화그래핀을 이용한 형광기반의 생분자 분석 플랫폼의 개발

지도교수 민 달 희

이 논문을 이학박사학위논문으로 제출함

2015 년 1 월

서울대학교 대학원

화학부 나노바이오화학 전공

이 지 언

이 지 언 의 박사학위논문을 인준함

2015 년 1 월

위 원 장　　　홍 종 인 (인)

부 위 원 장　　민 달 희 (인)

위　　　원　　남 좌 민 (인)

위　　　원　　김 석 희 (인)

위　　　원　　박 희 성 (인)

Abstract

Jieon Lee

Department of chemistry

The Graduate School

Seoul National University

Detection of biomolecules that were considered as important biological targets is a crucial tool in the field of clinical diagnosis and drug discovery. In general, most of the typical methods such as gel electrophoresis, immunoassay, antibody based assay have been showed relatively low specificity and sensitivity compared to required specifications for high level bio-analysis. These systems are laborious, time/cost-consuming, and not suitable for high throughput assay. Recently, alternative approaches have been developed based on nanomaterials such as gold nanoparticles, mesoporous silica nanoparticles and carbon based materials for noticeable improvement of the sensing performance. These nanomaterials have been applied in fluorescence, electrochemistry, mass spectrometry or SERS (Surface Enhanced Raman Scattering) based biosensors. These systems also enabled more rapid, cost and time-effective analysis, compared with conventional methods, thus they can provide a means in the field of target related basic research and further applications.

Herein, we report fluorescent sensing systems based on graphene oxide (GO)

for quantitative analysis of various biomarkers in clinical diagnosis and drug discovery. GO, a water-soluble version of graphene, has come into the spotlight in development of bioanalytical system due to its remarkable electronic, mechanical and thermal properties. Among these properties, the general strategy in this study relies on the fluorescence-quenching capability of GO for fluorescent molecules within short distance (~ 20 nm). By using fluorescent probes or substrates, this GO-based platforms allow real-time measurement and quantitative analysis for various biomolecules such as nucleic acids and enzymes in short time. In this study, we developed 5 bioanalytical platforms which were classified into two categories according to each purpose: 1) nucleic acid detection platforms for analysis of double stranded DNA, single stranded DNA or RNA, single nucleotide polymorphism (SNP), 2) enzyme assay platforms for analysis of DNA exonuclease and protein kinase. Commonly, they could overcome the limitations of classical approaches and showed various applicability for further application. We believe that the present platforms will become an important assay tool in the field of personalized diagnostics, drug discovery and individual biomolecules related basic research.

Table of Contents

List of Figures

1. Introduction

1.1 Nanotechnology for Bio-Application

Nanoscale materials recently have been developed and harnessed in diverse biological applications due to their large surface area, small size and unique properties.[1] Significantly, the field of biological analysis has actively employed various kinds of nanomaterials such as metallic nanoparticles,[2] quantum dots,[3] magnetic nanoparticles,[4] silica[5] or carbon based nanomaterials[6], fitting for each purpose. These sensors were designed based on understanding at a molecular level how it works, resulting in noticeable improvement of the sensing performance compared to conventional systems.

For example, various carbon materials have been applied in fluorescence,[6a] electochemistry,[7] mass spectrometry[8] or surface enhanced raman scattering (SERS)[9] based biosensors, presenting improved sensitivity and specificity. These systems also enabled more rapid, cost and time-effective analysis, compared with conventional methods, thus they can provide a means in the field of target related basic research and further applications. Therefore, it is worth to develop biological analysis platforms using nanotechnology.

1.2 Graphene Oxide

In 2004, Chernogolovka discovered graphene planes detached by scotch tape and improved its high electric conductivity.[10] The isolated atomic plane of graphite is a 2-dimensional nanomaterial with extraordinary electronic, thermal, and mechanical properties.[11] Since then, graphene has stimulated intense interest and has been extensively studied theoretically and experimentally in various fields. Graphene oxide (GO) is a water dispersible version of graphene presenting oxygen-containing functional groups such as hydroxyl, carboxyl, and epoxy groups.[12] On the basis of the unique properties of graphene and amphiphilicity, GO has been recently harnessed in diverse biological applications such as drug delivery,[13] catalysis[14] and biosensor[15] in the last decade. In 2009, Guo-Nan Chen firstly demonstrated that GO can be used in a fluorometric assay for fast, sensitive, and selective detection of biomolecules and this platform is cost-effective compared to platform based on carbon nanotube.[15] General strategy in this application relies on the strong binding of single stranded nucleic acid with GO through pi-pi stacking and/or hydrogen bonding interactions and the fluorescence-quenching capability of GO. Since then, many studies based on GO have been processed in the field of bio-analysis for further applications such as live cell imaging[16] and enzymatic assay.[17] Here, we have suggested improved strategies for analysis of biomolecules that were considered as important biological targets in the field of clinical diagnosis and drug discovery.

2

1.3 Description of Researches

1.3.1 Direct, Sequence-Specific Detection of dsDNA Based on Peptide Nucleic Acid and Graphene Oxide without Requiring Denaturation[18]

Direct, sequence-specific dsDNA detection system was developed without requiring any thermal denaturing step. Our strategy utilizes peptide nucleic acid (PNA) and graphene oxide (GO) as a probe and as a fluorescence quencher, respectively. Unlike other dsDNA sensors based on complementary DNA probes, PNA in combination with GO provided tighter turn-on signal control with very low background signal and high sensitivity and sequence selectivity even in the presence of serum proteins.
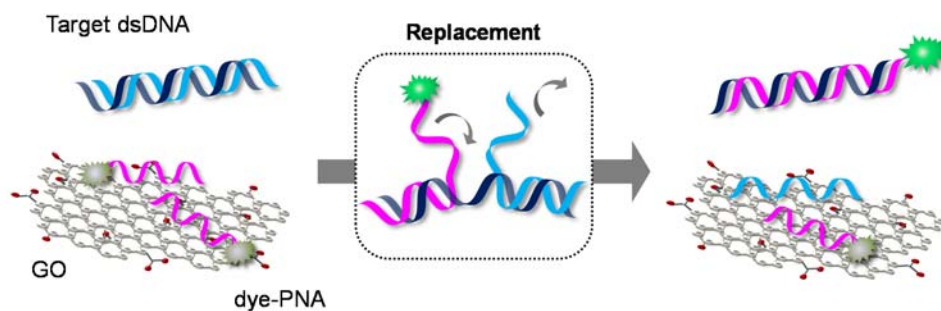
Scheme 1.1   A strategy for direct detection of dsDNA using PNA and GO.

1.3.2 Bovine Serum Albumin: A Simple Strategy for Practical Applications of PNA in Bioanalysis

We employed bovine serum albumin (BSA) in PNA applications as an additive for preventing its adsorption on hydrophobic surfaces and increasing the ratio of soluble PNA in a solution. Moreover, the usage of BSA can be extended to blocking the adsorption of PNA/DNA duplex on graphene oxide (GO) surface, which is very effective for improving the performance of nucleic acid biosensing platform based on PNA and GO.
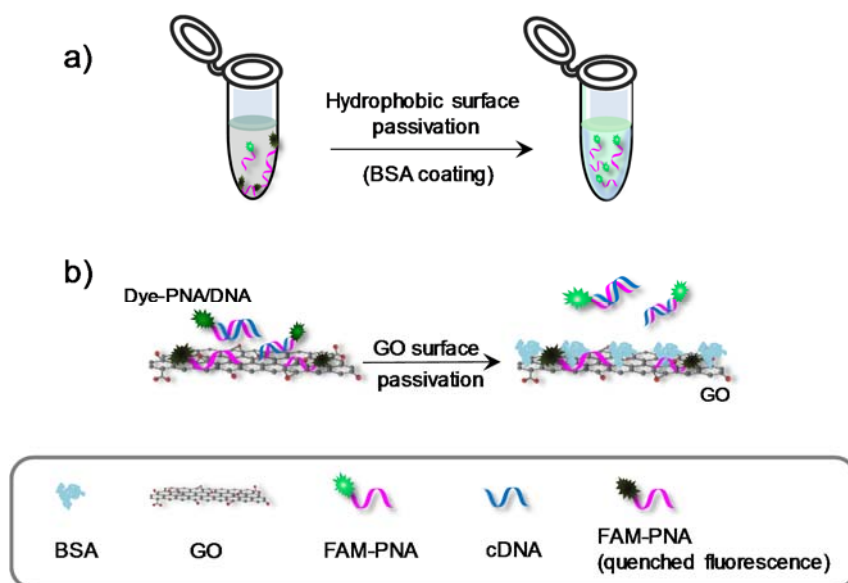
Scheme 1.2   BSA blocking to (a) prevent the nonspecific adsorption of PNA on hydrophobic surface and (b) inhibit the adsorption of PNA/DNA duplex on GO surface in GO-based biosensing platform using PNA probe.

1.3.3 A New Strategy for Nucleic Acid Detection with High Sequence Specificity Using Graphene Oxide and Peptide Nucleic Acid

In this study, a robust strategy for extremely high sequence specific nucleic acid detection was suggested by using dye conjugated pep-tide nucleic acid and graphene oxide. By controlling the dissociation temperature of pre-hybridized PNA/target in the presence of GO, fluorescence intensity for mismatched target was selectively quenched and thus we can measure the signal for perfect matched target quantitatively.
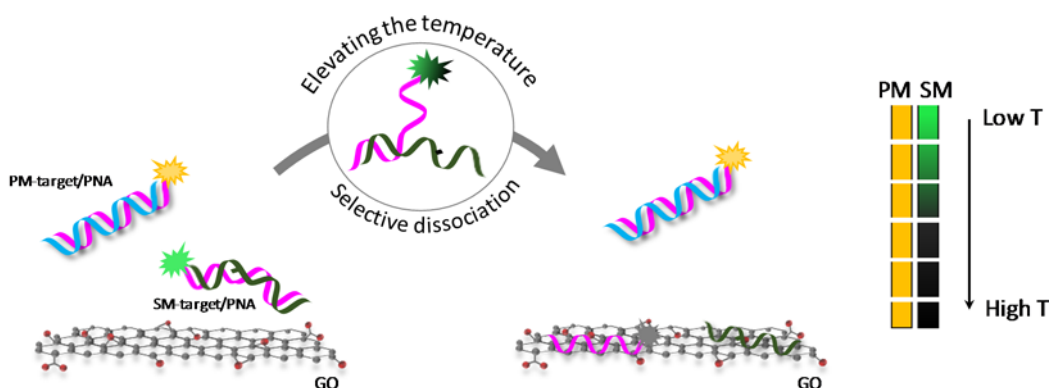
Scheme 1.3   A strategy for single mismatch discrimination in miRNA using PNA and GO (PM : perfect matched target, SM : single mismatched target)

1.3.4 A Simple DNA Exonuclease Activity Assay Based on Graphene Oxide[19]

A new DNA exonuclease activity assay method was developed based on the preferential binding of single-stranded DNA (ssDNA) over double-stranded DNA (dsDNA) to graphene oxide (GO) (Scheme 1.1). By measuring the quenching and recovery of fluorescence of dye conjugated to double strand part, exonuclease activity can be assayed. This GO-based approach allows a simple and quantitative activity measurement in a short time at a low cost compared to conventional methods.
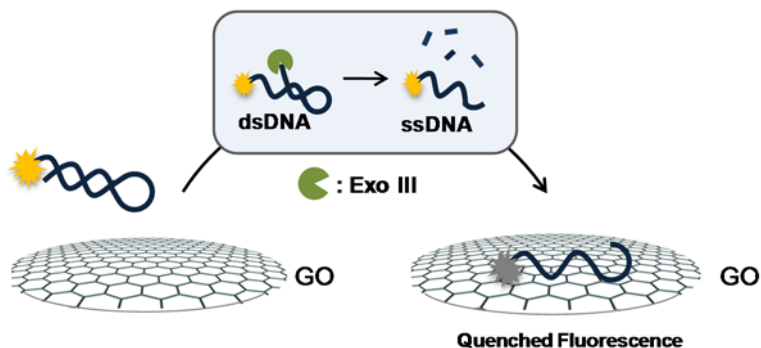
Scheme 1.4   A strategy for 3'→5' DNA exonuclease activity assay based on GO.

1.3.5 Robust and Quantitative Platform for Multiplexed Protein Kinase Inhibitor Screening

This new platform for protein kinase activity assay was established by using TiO_2 decorated graphene oxide, which is applicable in high throughput inhibitor screening. On the basis of strong affinity of TiO_2 for phosphate group and fluorescence super-quenching ability of GO, phosphorylation of substrate by protein kinase was quantitatively detected in a short time. Utility of the present platform was proven by discovering the inhibitors through multiplexed inhibitor screening for two protein kinase using hundreds of bioactive compounds.
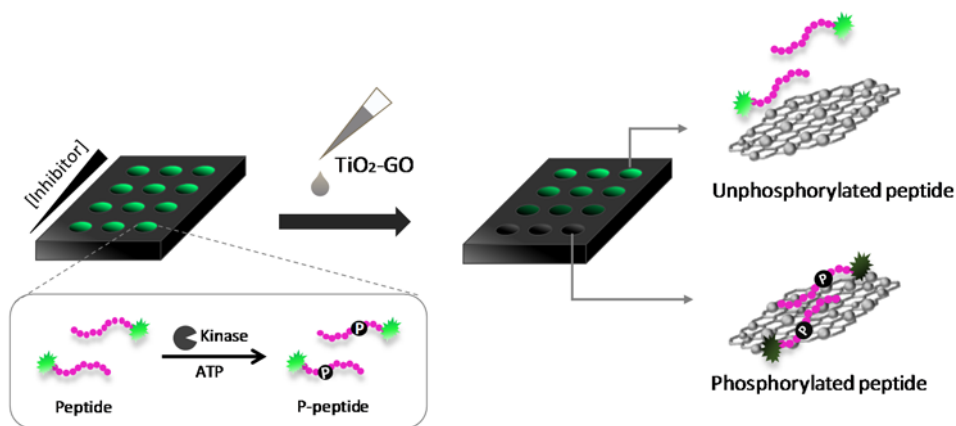
Scheme 1.5   A strategy for protein kinase activity assay using TiO_2 decorated GO.

1.4 Reference

1. a) De, M.; Ghosh, P. S.; Rotello, V. M., 2008, *Adv. Mat*. **20**, 4225-4241. b) Nel, A. E., Madler, L., Velegol, D., Xia, T., Hoek, E. M. V., Somasundaran, P., Klaessig, F., Castranova, V., Thompson, M., 2009, *Nat. Mater.* **8**, 543-557. c) Cheng, L. C., Jiang, X. M., Wang, J., Chen, C. Y. ,Liu, R. S., 2013, *Nanoscale* **5**, 3547-3569.

2. Jain, P. K., Huang, X. H., El-Sayed, I. H., El-Sayed, M. A., 2008, *Acc. Chem. Res*. **41**, 1578-1586.

3. Medintz, I. L., Uyeda, H. T., Goldman, E. R., Mattoussi, H., 2005, *Nat. Mater*. **4**, 435-446.

4. Lu, A. H., Salabas, E. L., Schuth, F., 2007, *Angew. Chem. Int. Ed*. **46**, 1222-1244.

5. Lin, V. S. Y., Lai, C. Y., Huang, J. G., Song, S. A., Xu, S., 2001, *J. Am. Chem. Soc*., **123**, 11510-11511.

6. a) Chung, C., Kim, Y. K., Shin, D., Ryoo, S. R., Hong, B. H., Min, D. H., 2013, *Acc. Chem. Res*., **46**, 2211-2221., b) Balasubramanian, K., Burghard, M., 2006, *Anal. Bioanal*. Chem. **385**, 452-468.

7. Wang, J., 2005, *Electoanalysis* **17**, 7-14.

8. Lee, J., Kim, Y. K., Min, D. H., 2010, *J. Am. Chem. Soc.,* **132**, 14714-14717.

9. Schedin, F., Lidorikis, E., Lombardo, A., Kravets, V. G., Geim, A. K., Grigorenko, A. N., Novoselov, K. S., Ferrari, A. C., 2010, *ACS Nano* **4**, 5617-5626.

10. Novoselov, K. S., Geim, A. K., Morozov, S. V., Jiang, D., Zhang, Y., Dubonos, S. V., Grigorieva, I. V., Firsov, A. A., 2004, *Science* **306**, 666–669.

11. Geim, A. K., Novoselov, K. S., 2007, *Nat. Mater*. **6**, 183-191.

12. Li, D., Muller, M. B., Gilje, S., Kaner, R. B., Wallace, G. G., 2008, *Nat. Nanotechnol*. **3**, 101-105.

13. Liu, Z.; Robinson, J. T.; Sun, X.; Dai, H., 2008, *J. Am. Chem. Soc*. **130**, 10876-10877.

14. Pyun, J., 2011, *Angew. Chem. Int. Ed*. **50**, 46-48.

15. Lu, C. H.; Yang, H. H.; Zhu, C. L.; Chen, X.; Chen, G. N., 2009, *Angew. Chem. Int. Ed*. **48**, 4785-4787.

16. Ryoo, S.-R., Lee, J., Yeo, J., Na, H.-K., Kim, Y.-K., Jang, H., Lee, J. H., Han, S. W., Lee, Y., Kim, V. N., Min, D.-H. 2013, *ACS Nano* **7**, 5882-5891.

17. Jang, H., Kim, Y.-K., Kwon, H.-M., Yeo, W.-S., Kim, D.-E., Min, D.-H., 2010, *Angew. Chem. Int. Ed*. **49**, 5703-5707.

18. Lee, J., Park, I.-S., Jung, E., Lee, Y., Min, D.-H., 2014, *Biosens. Bioelecron*. **62**, 140-144.

19. Lee, J., Min, D.-H., 2012, *Analyst* **137**, 2024-2026.

2. A Direct, Sequence-Specific Detection of dsDNA Based on Peptide Nucleic Acid and Graphene Oxide without Requiring Denaturation

2.1 Introduction

DNA detection is important in diagnosis and monitoring the fatal infections caused by viruses such as hepatitis virus, human immunodeficiency virus (HIV), ebola virus (EV) and severe acute respiratory syndrome (SARS) corona virus as well as diseases associated with genetic alterations.[1-3] Conventional DNA detection methods, such as southern blot,[4] fluorescence in situ hybridization (FISH),[5] polymerase chain reaction (PCR)[6] and DNA microarray[7,8] are based on the sequence specific recognition of single stranded nucleic acid through Watson-Crick base pairing. Recently, alternative approaches based on nanomaterials have been developed for simple and fast DNA detection.[9-11]

In general, denaturing procedure is necessary to separate two DNA strands prior to sensing of the target DNA by hybridization with probe molecule or sequence because target DNA usually exists in duplex form with complementary strand. In such a case, spontaneous reannealing of original two DNA strands could disturb the hybridization of the target DNA with probe and lower the efficiency of target detection. Recently, several approaches that do not require

denaturation and/or rehybridization have been proposed. These direct detection methods utilized double-stranded DNA (dsDNA) binding probes such as zinc finger DNA binding proteins,[12] pyrrole-imidazole polyamides (PAs)[13,14] for binding at minor groove of dsDNA and triplex-forming oligonucleotides (TFOs)[15] for Hoogsteen hydrogen bonding at major groove of dsDNA. However, these approaches have drawbacks such as low chemical stability of protein as a probe and limitation in recognition length or sequence. Therefore, it is important to establish a robust, versatile and efficient sensing platform for direct dsDNA detection.

Graphene is a 2D carbon material with remarkable electronic, thermal, and mechanical properties.[16-18] Graphene oxide (GO), a water-soluble derivative of graphene, has been recently harnessed in diverse biological applications such as drug delivery, catalysis, enzyme activity assay and biosensor.[10,19-26] General strategy in these applications relies on the strong binding of single stranded nucleic acid and/or hydrophobic molecules with GO through pi-pi stacking and/or hydrogen bonding interactions and the fluorescence-quenching capability of GO.[27-30]

Here, we report a direct dsDNA detection method based on the end invasion of peptide nucleic acid (PNA) towards dsDNA and preferential binding of GO to single-stranded PNA (ssPNA) over DNA/PNA duplex. PNA is a DNA analogue which has amide bonds instead of phosphate backbone.[31,32] It hybridizes with

complementary DNA or RNA with high sequence specificity in short time. The duplex of PNA with natural nucleic acid has high stability in various buffered conditions and at high temperature, basically due to the uncharged neutral backbone of PNA. Typically, DNA/PNA duplex shows at least 1°C higher melting temperature per base pair than DNA duplex.[33] In addition to its widely known favorable properties as a biological probe, PNA could also interact with negatively charged GO stronger than negatively charged nucleic acids and construct stable PNA/GO complex, showing lower background signals due to less non-specific desorption of probe nucleic acid from GO.[34-36]

The present strategy starts with preparation of a fluorescent dye conjugated PNA probe and a target dsDNA which consists of an upper strand as an actual target DNA for PNA probe recognition and a bottom strand complementary to target DNA. Upon incubation of dsDNA with PNA probe, the PNA binds at the end of upper strand because the hydrogen bonding at the terminal base pair of DNA duplex is weaker than internal one. Due to the superior binding affinity of PNA to complementary DNA, branch migration for strand replacement occurs gradually. Finally, the bottom DNA strand is dissociated from original DNA duplex and PNA/DNA duplex is formed.[37-39] Upon addition of GO to this mixture, free PNA probe, not PNA/DNA duplex, preferentially binds onto GO through pi-pi stacking interaction and hydrogen bonding formation, and subsequently, the fluorescence of the dye conjugated PNA probe is quenched by energy transfer to

GO. Therefore, only PNAs forming duplexes with target DNA emit the fluorescence signal, and thus, the initial concentration of the target dsDNA could
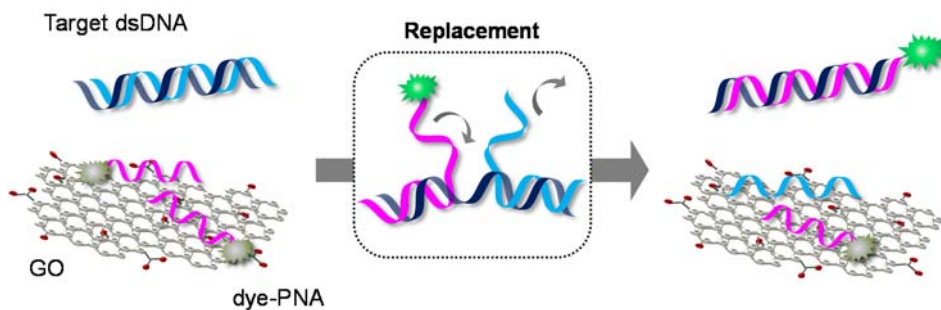
be quantitatively analyzed (Scheme 2.1).

Scheme 2.1   A strategy for direct detection of dsDNA using PNA and GO.

2.2 Result

Before the demonstration of the present dsDNA sensor based on PNA and GO,
the DNA strand replacement from dsDNA by PNA was first examined by
resolving the PNA/DNA duplex and intact dsDNA using nondenaturing
polyacrylamide gel electrophoresis (native - PAGE). Due to less negative charge
of PNA/DNA duplex compared to DNA/DNA duplex, the band of the hetero
duplex appeared at upper region, implying slower migration than DNA duplex in
the gel. When the PNA probe was added to dsDNA, PNA was expected to first
bind to the end site of dsDNA, followed by branch migration and complete
hybridization between PNA and DNA along with separation of bottom strand
DNA (Figure 2.1a). Next, we determined the optimal GO[40] concentration for
quenching the fluorescence of fluorescein amidite (FAM) labeled ssPNA probe (5'
- FAM–TTT GAG GGA AGT TAC GCT TAT - 3').
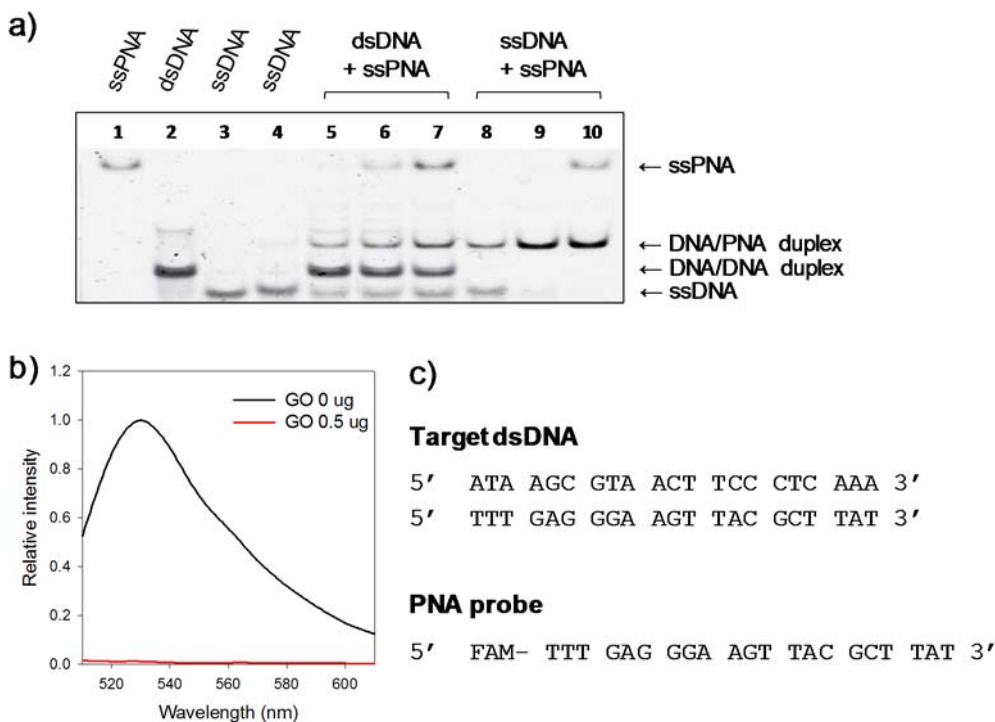
Figure 2.1 Target strand invasion and GO adsorption of PNA strands. a) Gel electrophoresis was performed on a 15% native -PAGE. Lanes 1-4 show each 10 pmol of ssPNA, dsDNA, ssDNA (bottom strand) and ssDNA (upper strand). Lanes 5-7 show 10 pmol of dsDNA incubated with 5, 10, 20 pmol of PNA. Lanes 8-10 show 10 pmol of ssDNA (upper strand) incubated with 5, 10, 20 pmol of PNA. b) Fluorescence spectra of FAM labeled PNA in the presence of GO (0 μg and 0.5 μg, respectively).   c) Sequences of target dsDNA and FAM labeled PNA probe.

We found that the fluorescence of FAM-PNA probe was quenched up to ~98% in the presence of GO (0.5 μg), giving maximum quenching efficiency under the experimental condition (Figure 2.1b). We then performed PNA/GO

based fluorometric detection of dsDNA. Various concentrations of target dsDNA solutions ranging from 0 to 400 nM were mixed with FAM-PNA probe and then, GO solution was added. The fluorescence emission spectra of the mixed solutions of dsDNA, FAM-PNA and GO showed the dsDNA concentration dependent fluorescence enhancement with high sequence specificity showing no notable fluorescence intensity from a mixture containing scrambled dsDNA in place of target dsDNA (Figure 2.2a). This sensor showed a linear fluorescence increase between 0 and 2000 pM with the detection limit of 260 pM according to the equation, LOD = 3.3 (SD / S) (LOD: limit of detection, SD: standard deviation, S: slope of the calibration curve) (Figure 2.2b).
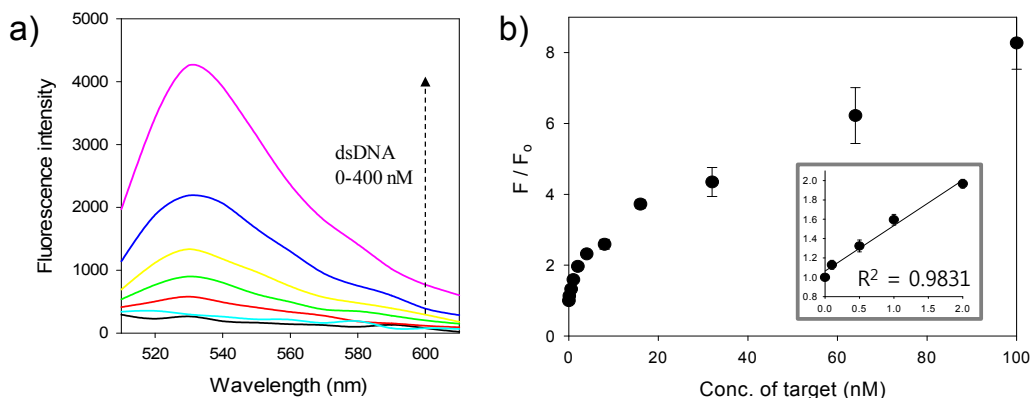
Figure 2.2   Direct dsDNA detection in buffered solution. a) Fluorescence spectra of FAM-PNA probe in the presence of various concentrations of dsDNA target and scrambled dsDNA 400 nM in buffered solution with addition of GO. b) Fluorescence intensity enhancement (F/F_0) with a wide concentration ranges of target dsDNA from 0 to 100 nM (F: fluorescence intensity of PNA probe hybridized with target, F0: fluorescence intensity of PNA probe without target).

As a control, we performed same experiment with FAM-DNA probe in place of FAM-PNA probe. FAM-DNA probe showed significant signal increase upon addition of scrambled DNA followed by addition of GO, which is estimated as ~50% of the fluorescence intensity measured from the mixture of FAM-DNA probe, perfect matched target DNA and GO. The control data suggested that DNA probe is much less attractive for this type of direct, sequence-specific, quantitative detection of dsDNA due to high background fluorescence (Figure 2.3).
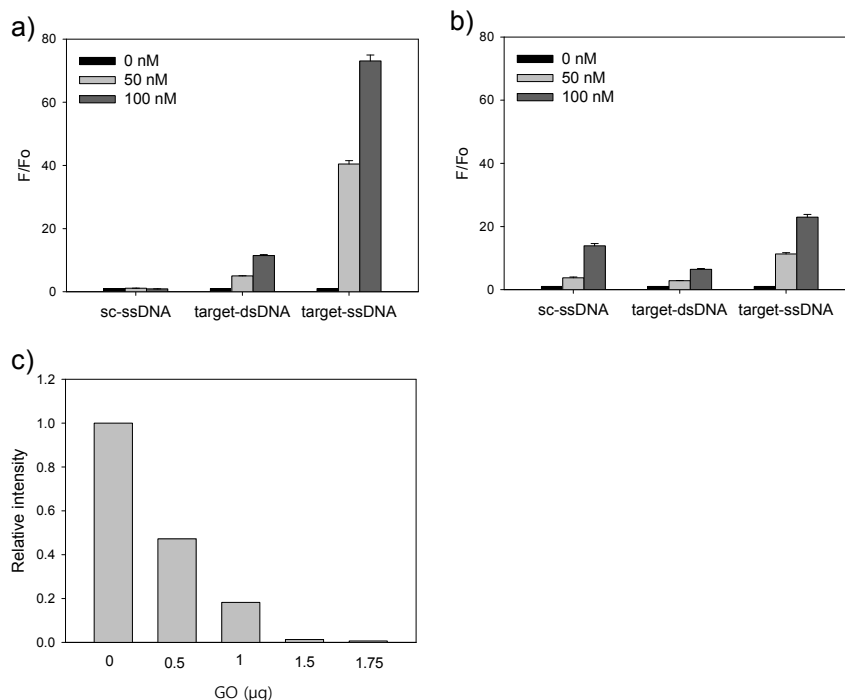
Figure 2.3 Comparison between DNA probe and PNA probe in dsDNA detection. Fluorescence intensity enhancement (F/F_0) of a) PNA probe and b) DNA probe in the presence of scrambled ssDNA, target dsDNA, target ssDNA (0, 5, 10 pmol, respectively). c) Relative fluorescence intensity of FAM dye labeled DNA(10 pmol) in the presence of GO. For dsDNA detection using DNA probe, reaction mixture was prepared by 100 nM FAM labeled DNA probe incubated with the annealed target dsDNA in 1XPBS. After incubation at room temperature for 1hr, 3 μL of 500 μg/ml GO stock was added to mixture for adsorption of ssDNA on GO surface, which was 3-fold higher than PNA probe used system.

Furthermore, to investigate the applicability for direct sensing of dsDNA in serum containing biological samples, we repeated the dsDNA detection in buffered solutions containing 10% fetal bovine serum (FBS). Under the condition, the sensor also exhibited a linear fluorescence increase in the same concentration

18

range of target DNA (0 ~ 2000 pM) with a slightly higher detection limit of 400

pM according to the equation, LOD = 3.3 (SD / S) (Figure 2.4).
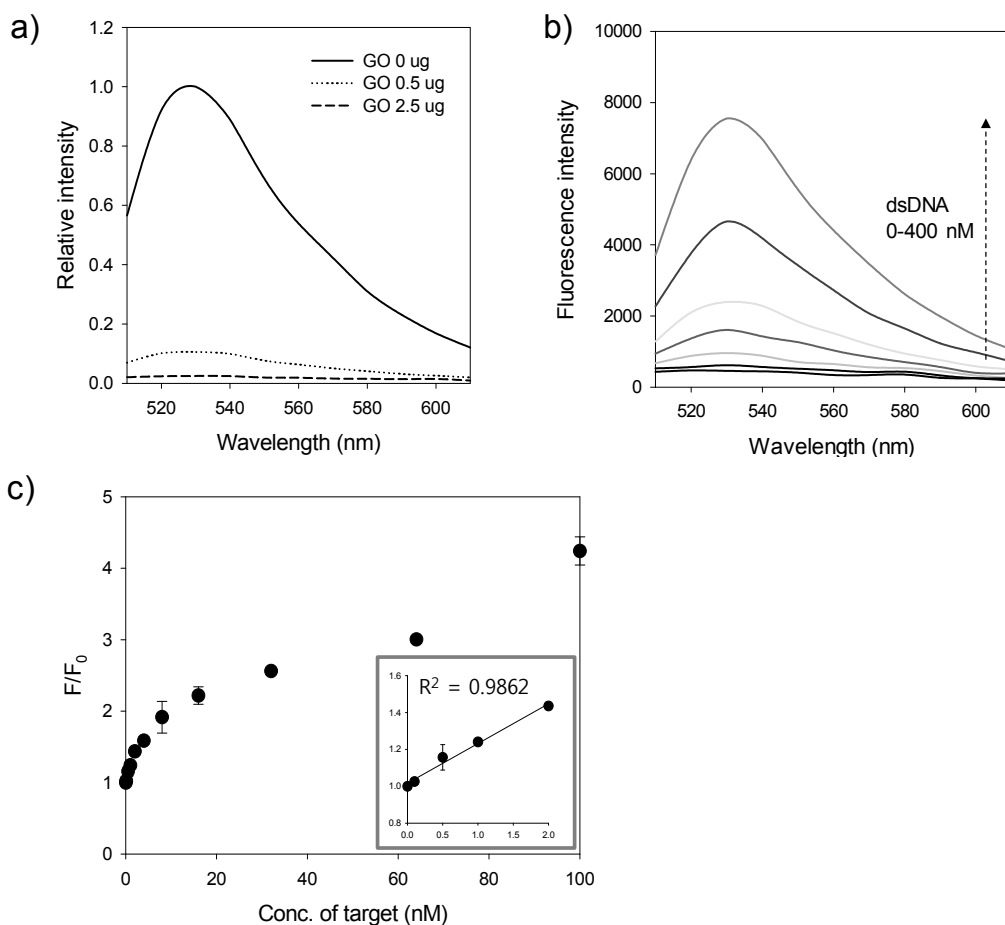
Figure 2.4 Direct dsDNA detection in serum containing colution a) Relative fluorescence spectra of FAM conjugated to PNA incubated with GO (0 μg, 0.5 μg and 2.5 μg, respectively) in a buffered solution containing 10 % FBS. b) Fluorescence spectra of PNA probe in presence of various concentration of dsDNA target and scrambled dsDNA 400nM in bufffered solution containing 10% FBS. c) Fluorescence intensity enhancement (F/F_0) with wide concentration range of target in buffered solution containing 10% FBS.

Next, we performed discrimination test between perfect matched target sequence and mismatched DNAs possessing one or three base pair (bp) mismatches. Precise recognition of few base mismatches in DNA sequences having very high sequence similarity is important because it provides information on genetic mutation, DNA damage and single-nucleotide polymorphism (SNP).[41-43] One and three bp mismatched DNAs were designed based on transversion mismatch at internal bases (A↔T). As expected, the mismatched target DNA showed lower fluorescence intensity than perfect matched target upon addition of FAM-PNA and GO (Figure 2.5a). Specifically, single bp mismatch in the middle of the upper target strand induced the decrease of the F/F_0 value down to 57% compared to that from the perfect matched target DNA. Furthermore, the F/F_0 values decreased to ~35% with three bp mismatches, and down to below ~1% with scrambled dsDNA (in the mixture of 100 nM each target and 100 nM PNA probe) (Figure 2.5b).
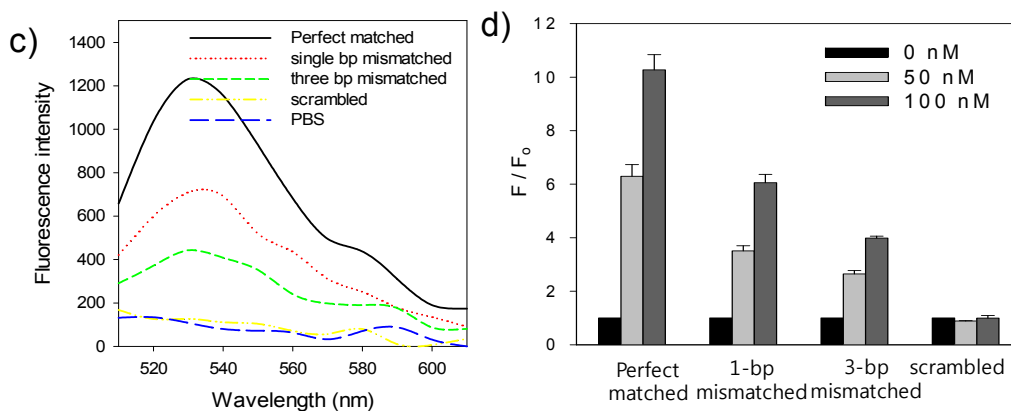
Figure 2.5 Mismatch discrimination. a) Fluorescence spectra of PNA probe in the presence of target dsDNA, single base pair mismatched, three base pair mismatched dsDNA and scrambled sequence dsDNA with addition of GO. b) A bar graph showing fluorescence intensity enhancement (F/F_0) with matched, mismatched dsDNA target (0, 50, 100 nM, respectively).

Finally, we demonstrated the capability of multiple target detection in a single solution. We chose three target genes related to viral diseases for multiplex sensing: hepatitis A virus Vall7 polyprotein gene (HVA), human immunodeficiency virus (HIV) and hepatitis B virus surface antigen gene (HVB). Target dsDNAs having 15 bp with unique sequences derived from the three fatal viruses were then prepared and conjugated with three different fluorescent dyes—FAM, ROX (6-carboxyl-X-rhodamine) and Cy5 (cyanine 5) which showed emission maxima of 518 (green), 608 (orange) and 670 nm (red) with excitation at 492, 587 and 650 nm, respectively. For multiple dsDNA detection, each target dsDNA or different combinations of three dsDNA (200 nM) were added to the

21

mixture of the three dye labelled PNA probes (each concentration=100 nM),

followed by addition of GO (Figure 2.6).
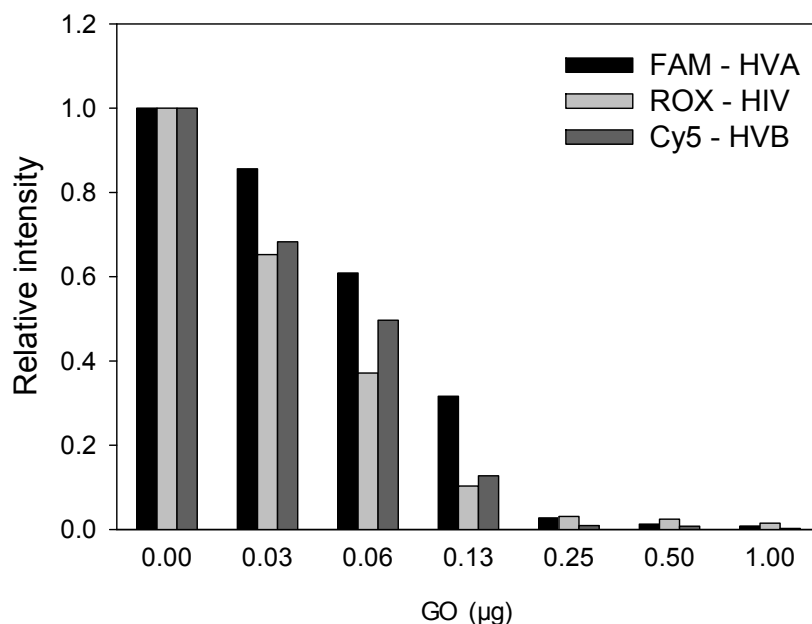
Figure 2.6   Relative fluorescence intensity of each three dye labeled PNAs in
the presence of GO. FAM, ROX and Cy5 was conjugated to each PNA probe for
HVA, HIV and HVB, respectively.

As expected, green, orange and red fluorescence emission spectra and images

were obtained only in the sample containing each corresponding HVA, HIV and

HVB target dsDNA (Figure 2.7).
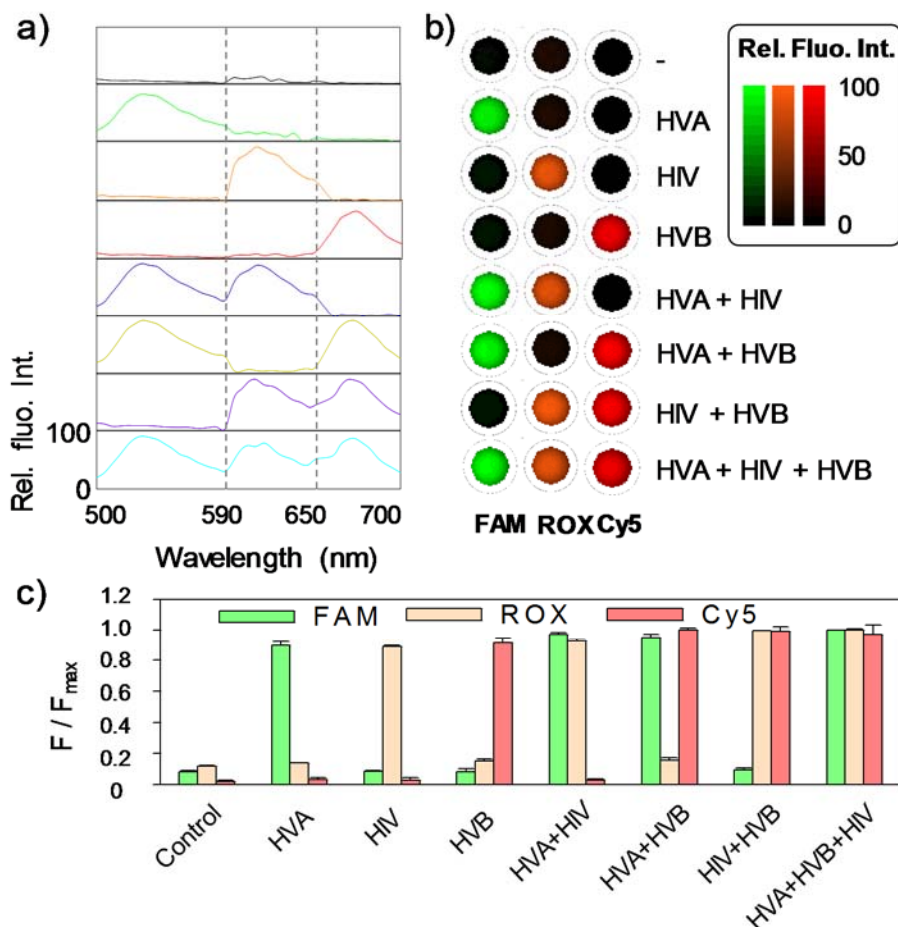
Figure 2.7 Multiple target detection of three viral genes in a single solution. a) Fluorescence spectra of three dye labeled PNAs in the presence of 200 nM target dsDNA in a buffered solution. b) Fluorescent images of reaction mixtures for multiple detection. Column 1: fluorescence signal of FAM-HVA; Column 2: fluorescence signal of FAM-HVB; Column 3: fluorescence signal of FAM-HIV in the presence of 200 nM of each target. c) A bar graph showing relative fluorescence intensity of three dye labeled PNAs in the presence of each target dsDNA (200 nM) (F : fluorescence intensity of PNA probe with target, Fmax : Maximum fluorescence intensity of each PNA probe observed in the presence of perfect matched duplex target).

2.3 Conclusion

In conclusion, we developed a new GO-based platform for direct and robust dsDNA detection using PNA probe. To the best of our knowledge, this is first study on sequence-specific, quantitative and direct detection of dsDNA based on GO. The present dsDNA sensor utilized the unique properties of PNA and GO. First, PNA could invade at the temini of the complementary strand of target dsDNA without sequence limitations, followed by strand replacement based on its higher binding affinity to complementary DNA than DNA probes. Second, GO showed outstanding adsorption ability for uncharged ssPNA compared to other biomolecules such as proteins and naturally occurring nucleic acids. Also, GO quenched the fluorescence of a dye that is attached to the PNA probe effectively. By combining PNA probe with GO, quantitative fluorometric dsDNA sensing was enabled even in the serum containing samples without a wide variation of LOD, which was impossible to achieve by using DNA probe. This combination of PNA and GO overcome drawbacks of conventional DNA or RNA probes and thus, would make the applicable field of GO based sensors broader. We believe that this new direct GO-based dsDNA sensor using PNA probe will become an important tool in the field of personalized medicine and diagnostics of viral diseases and genetic disorders in the future.

2.4 Material and Methods

Materials.   Graphite nanofibers was purchased from Catalytic Materials LLC (USA). Sulfuric acid (H_2SO_4) was purchased from Samchun chemical (Seoul, Korea). Hydrogen peroxide (30% in water) (H_2O_2) was purchased from Junsei (Japan). Potassium permanganate ($KMnO_4$), Potassium persulfate ($K_2S_2O_8$) and Phosphorus pentoxide (P_2O_5) were purchased from Sigma-Aldrich (MO, USA). Fatal bovine serum (FBS) was purchased from Welgene (Daegu, Korea). DNA strands were purchased from Genotech (Daejeon, Korea). PNA probes were purchased from Panagene (Daejeon, Korea). Fluorescence intensity and fluorescence image were obtained by fluorometer SynergyMx (Biotek, UK).

Preparation of graphene oxide.   Graphene oxide (GO) was synthesized by using Hummers method with pre-oxidation treatment, using graphite nanofiber as starting material. First, concentrated H_2SO_4 (5 ml) was heated to 80 °C in a round bottom flask, then $K_2S_2O_8$ (0.15 g) and P_2O_5 (0.15 g) were added in a round bottom flask, keeping at 80 °C for 4.5 hours. After the mixture was cooled, the reaction mixture was diluted with deionized (DI) water. This solution was filtered and rinsed with DI water (100 ml) for removing remained reactants. Obtained pre-oxidized graphite nanofibers were dried in air. Then, the dried solid was transferred into a 50 ml round bottom flask and concentrated H_2SO_4 was added (25 ml). Then the mixture was chilled to 0 °C using an ice bath. $KMnO_4$ (1 g) was

added to the mixture slowly with stirring, keeping the temperature below 10 °C. After mixing, the flask was placed in 35 °C water bath for 12 hours. The mixture was transferred into an Erlenmeyer flask (500 ml) in an ice bath. DI water (100 ml) was added to the flask slowly with stirring. During this step, keeping the temperature below 55 °C was needed. After that, 5 ml of 30 % H_2O_2 solution was added to the mixture, of which the color turned into bright yellow. This mixture was collected, centrifuged and then, rinsed with 3.4% HCl solution and acetone to get rid of residual salts and acid. Obtained solid GO was dried under vacuum before use. To get the GO solution, GO was dissolved in water, then the solution was centrifuged at 3000 rpm for 30 min to remove large chunks.

Sequence information.

DNA strands for mismatch discrimination:

	Upper strand	Bottom strand
Perfect matched dsDNA	5' ATA AGC GTA ACT TCC CTC AAA 3'	5' TTT GAG GGA AGT TAC GCT TAT 3'
Single bp mismatched	5' ATA AGC GTA TCT TCC CTC AAA 3'	5' TTT GAG GGA AGA TAC GCT TAT 3'
Three bp mismatched	5' ATA AGC GAA TCT ACC CTC AAA 3'	5' TTT GAG GGT AGA TTC GCT TAT 3'
Scrambled dsDNA	5' TAG CTT ATC AGA CTG ATG TTG A 3'	5' TCA ACA TCA GTC TGA TAA GCT A 3'

DNA strands for multiplex dsDNA detection:

	Upper strand	Bottom strand
HVA	5' TTA GAG TTG CAT GGA 3'	5' TCC ATG CAA CTC TAA 3'
HIV	5' TAA CAT GAC CTG GAT3	5' ATC AGG TCA TG TTA 3'
HVB	5' ATG GAT GAT GTG GTA 3'	5' TAC CAC ATC ATC CAT 3'

PNA probes

PNA probe (21mer)	5' FAM – TTT GAG GGA AGT TAC GCT TAT 3'
HVA probe (15mer)	5' FAM – TCC ATG CAA CTC TAA 3'
HIV probe (15mer)	5' ROX – ATC AGG TCA TG TTA 3'
HVB probe (15mer)	5' Cy5 – TAC CAC ATC ATC CAT 3'

Detection of dsDNA using Peptide Nucleic Acid and Graphene Oxide.

To prepare duplex DNA target, 2.5 μL of 100 μM upper strand DNA was mixed

with and a 1.1-fold excess of bottom strand DNA in pH 8.0 buffer containing 50

mM Tris-HCl and 50 mM NaCl. Then, the mixture was annealed by heating to 90℃

for 5 min and followed by slow cooling at room temperature for 1 hr. For dsDNA

detection, reaction mixture was prepared by 100 nM FAM labeled PNA probe

incubated with various concentration of annealed target dsDNA in 1XPBS

containing BSA (pH 7.2 buffer containing NaCl 137 mM, KCl 2.7 mM, BSA

0.01%). After incubation at room temperature for 1hr, 1 μL of 500 μg/ml GO

stock was added to mixture. Fluorescence intensity was measured at 520 nm.

Multiple target detection using Peptide Nucleic Acid and Graphene Oxide. For multiple target detection, dsDNA target was incubated with the PNA probes mixture containing each 10 pmol of FAM-HVA probe, ROX-HIV probe and Cy5-HVB probe in 1XPBS. After incubation at room temperature for 1hr, 1.25 µL of 500 µg/ml GO stock was added to mixture. FAM-PNA, ROX-PNA and Cy5-PNA were excited at 492 nm, 587 nm and 650 nm in a homogeneous solution. Fluorescence intensities of each probes were measured at 518, 608, and 670 nm, respectively.

2.5 Reference

1. Dejean, A., Lugassy, C., Zafrani, S., Tiollais, P., Brechot, C., 1984. *J. Gen. Virol.* **65**, 651-655.

2. Barany, F., 1991. *Proc. Natl. Acad. Sci. U.S.A.* **88**, 189-193.

3. Mahony, J. B., 2008. *Clin. Microbiol. Rev.* **21**, 716-747.

4. Southern, E. M., 1975. *J. Mol. Bio.* **98**, 503-517.

5. Levsky, J. M., Singer, R. H., 2003. *J. Cell. Sci.* **116**, 2833-2938.

6. Chen, S. C., Halliday, C. L., Meyer, W., 2002. *Med. Mycol.* **40**, 333-357.

7. Heller, M., 2002. *J. Annu. Rev. Biomed. Eng.* **4**, 129-153.

8. Hatakeyama, H., Ito, E.; Yamamoto, M., Akita, H., Hayashi, Y., Kajimoto, K., Kaji, N., Baba, Y., Harashima, H., 2011. *Mol. Ther.* **19**, 1487-1498.

9. Elghanian, R., Storhoff, J. J., Mucic, R. C., Letsinger, R. L., Mirkin, C. A., 1997. *Science* **277**, 1078-1081.

10. Lu, C. H., Yang, H. H., Zhu, C. L., Chen, X., Chen, G. N., 2009. *Angew. Chem. Int. Ed.* **48**, 4785-4787.

11. Song, Y., Wang, X., Zhao, C., Qu, K., Ren, J., Qu, X., 2010. *Chem. Eur. J.* **16**, 3617-3621.

12. Segal, D. J., Barbas III, C. F., 2001. *Curr. Opin. Biotechnol.* **12**, 632-637.

13. Mrksich, M., Wade, W. S., Dwyer, T. J., Geierstanger, B. H., Wemmer, D. E., Dervan, P. B., 1992. *Proc. Natl. Acad. Sci. U.S.A.* **89**, 7586-7590.

14. Dervan, P. B., 2001. *Bioorg. Med. Chem.* **9**, 2215-2235.

15. Chan, P. P., Glazer, P. M., 1997. *J. Mol. Med.* **75**, 267-282.

16. Novoselov, K. S., Geim, A. K., Morozov, S. V., Jiang, D., Zhang, Y., Dubonos, S. V., Grigorieva, I. V., Firsov, A. A., 2004. *Science* **306**, 666-669.

17. Allen, M. J., Tung, V. C., Kaner, R. B., 2010. *Chem. Rev.* **110**, 132-145.

18. Kim, F., Cote, L. J., Huang, J., 2010. *Adv. Mater.* **22**, 1954-1958.

19. Liu, Z., Robinson, J. T., Sun, X., Dai, H., 2008. *J. Am. Chem. Soc.* **130**, 10876-10877.

20. Jang, H., Kim, Y.-K., Kwon, H.-M., Yeo, W.-S., Kim, D.-E., Min, D.-H., 2010. *Angew. Chem. Int. Ed*. **49**, 5703-5707.

21. Lee, J., Kim, Y.-K., Min, D.-H., 2010. *J. Am. Chem. Soc*. **132**, 14714-14717.

22. Zhu, Y., Murali, S., Cai, W., Li, X., Suk, J. W., Potts, J. R., Ruoff, R. S., 2010. *Adv. Mater*. **22**, 3906-3924.

23. Pyun, J., 2011. *Angew. Chem. Int. Ed*. **50**, 46-48.

24. Chung, C., Kim, Y.-K., Shin, D., Ryoo, S.-R., Hong, B. H., Min, D.-H., 2013. A*cc. Chem. Res*. **46**, 2211-2224.

25. Kim, S., Ryoo, S.-R., Na, H.-K., Kim, Y.-K., Choi, B.-S., Lee, Y., Kim, D.-E., Min, D.-H., 2013. *Chem. Commun*. **49**, 8241-8243.

26. Na, H.-K., Kim, M.-H., Lee, J., Kim, Y.-K., Jang, H., Lee, K. E., Park, H., Heo, W. D., Jeon, H., Choi, I. S., Lee, Y., Min, D.-H., 2013. *Nanoscale* **5**, 1669-1677.

27. Swathi, R. S., Sebastian, K. L., 2008. *J. Chem. Phys*. **129**, 054703-054709.

28. Swathi, R. S., Sebastian, K. L., 2009. *J. Chem. Phys*. **130**, 086101-086103.

29. He, S., Song, B., Li, D., Zhu, C., Qi, W., Wen, Y., Wang, L., Song, S., li, H., Fan, C., 2010. *Adv. Funct. Mater*. 20, 453-459.

30. Wu, M., Kempaiah, R., Huang, P.-J. J., Maheshwari, V., Liu, J., 2011. *Langmuir*, **27**, 2731-2738.

31. Nielsen, P. E., Egholm, M., Berg, R. H., Buchardt, O., 1991. *Science* **254**, 1497-1500.

32. Hyrup, B., Nielsen, P. E., 1996. *Bioorg. Med. Chem*. **4**, 5-23.

33. Jang, H., Kim, J., Choi, J. J., Son, Y., Park, H. J., 2010. *Clin. Microbiol*. **48**, 3127-3131.

34. Kotikam, V., Fernandes, M., Kumar, V. A., 2012. *Phys. Chem. Chem. Phys*. **14**, 15003-15006.

35. Guo, S., Du, D., Tang, L., Ning, Y., Yao, Q., Zhang, G. J., 2013. *Analyst* **138**, 3216-3220.

36. Ryoo, S.-R., Lee, J., Yeo, J., Na, H.-K., Kim, Y.-K., Jang, H., Lee, J. H., Han, S. W., Lee, Y., Kim, V. N., Min, D.-H., 2013. *ACS Nano* **7**, 5882-5891.

37. Lesignoli, E., Germini, A., Corradini, R., Sforza, S., Galavema, G., Dossena, A., Marchelli, R., 2001. J. Chromatogr. A. **922**, 177-185.

38. Smolina, I. V., Demidov, V. V., Soldatenkov, V. A., Chasovskikh, S. G., Frank-Kamenetskii, M. D., 2005. *Nucleic Acids Res*. **33**, e146.

39. Kuhn, H., Frank-Kamenetskii, M. D., 2008. *Nucleic Acids Res*. **36**, e40.

40. Luo, J., Cote, L. J., Tung, V. C., Tan, A. T., Goins, P. E., Wu, J., Huang, J., 2010. *J. Am. Chem. Soc*. **132**, 17667-17669.

41. Harfe, B. D., Jinks-Robertson, S., 2000. *Annu. Rev. Genet*. **34**, 359-399.

42. Fedier, A., Fink, D., 2004. Int. J. Oncol. **24**, 1039-1047.

43. Barreiro, L. B., Laval, G., Quach, H., Patin, E., Quintana-Murci, L., 2008, *Nat. Genet*. **40**, 340-345.

3. Bovine Serum Albumin: A Simple Strategy for Practical Applications of PNA in Bioanalysis

3.1 Introduction

Peptide nucleic acid (PNA) is a DNA mimic composed of natural nucleobases and pseudo-peptide backbone.[1,2] Being a polyamide based molecule, PNA exhibits high thermal/chemical stability as well as resistance to nuclease-mediated degradation. In addition, the electrically neutral backbone enables PNA to hybridize with complementary DNA or RNA with high affinity and specificity. Therefore, PNA can be employed as not only a potent tool for molecular biology and genetic diagnostics, but also a powerful anti-sense drug candidate. Recently, many researchers demonstrated various nanomaterial based biosensors in combination with PNA.[3-6] For example, a graphene oxide (GO) based sensing system using PNA probe was developed for target specific bio-detection, enzyme activity assay, duplex nucleic acid detection as well as live cell imaging of biomolecules.[6-10] However, despite of a lot of merits of PNA, its applications have been limited by its poor solubility in aqueous solution which induces self-aggregation or nonspecific adsorption on hydrophobic solid supports that are commonly used in biological applications such as polystyrene (PS) plates and plastic tubes.[2,11] Generally, a mixed solution of PNA and solvent should be heated over 60 °C to dissolve PNA to make a stock solution. PNA at nanomolar

concentrations prepared for working solutions easily loses its function since the PNA in diluted solutions get adsorbed on vessel walls over time. Thus, to enhance the solubility of PNA and prevent self-aggregation, many approaches have been developed such as direct backbone modifications or conjugation of solubility enhancers utilizing charged amino acids, hydrophilic linkers or natural nucleic acids.[12-15] Moreover, organic solvents such as dimethylformamide and dimethyl sulfoxide have been used for dissolving PNA.[16-18] However, apart from the self-aggregation of PNA, nonspecific adsorption of PNA on hydrophobic support has been relatively overlooked during PNA applications and could not be adequately overcome with structural modifications of PNA or usage of organic solvents. In addition, the excessive modifications or the high volume ratio of organic solvents could induce poor performance of PNA and other side effects in biological experiments.[19,20]

Here, we employed bovine serum albumin (BSA) as an additive to prevent the nonspecific adsorption of PNA on a hydrophobic surface and to enhance its solubility in aqueous media and thus, improved the yield of target-specific hybridization (Scheme 3.1a). BSA is one of the serum albumin proteins, which is widely used blocking agent due to its high efficiency, cost effectiveness and biocompatibility in various bioanalytical experiments.[21] Because BSA has both hydro-phobic and hydrophilic parts on the surface, it can prevent nonspecific protein-surface interactions or protein-protein interactions in diverse biochemical

applications such as ELISA and immunoblottings.[22-25] Therefore, the usage of BSA can be a simple, effective method as a remedy to reduce a main shortcoming of PNA. Furthermore, we extended the application of BSA to GO/PNA based oligonucleotide sensors to improve sensing performance by preventing the interaction between PNA/DNA duplex and GO as well as the adsorption of PNA on hydrophobic surface (Scheme 3.1b).
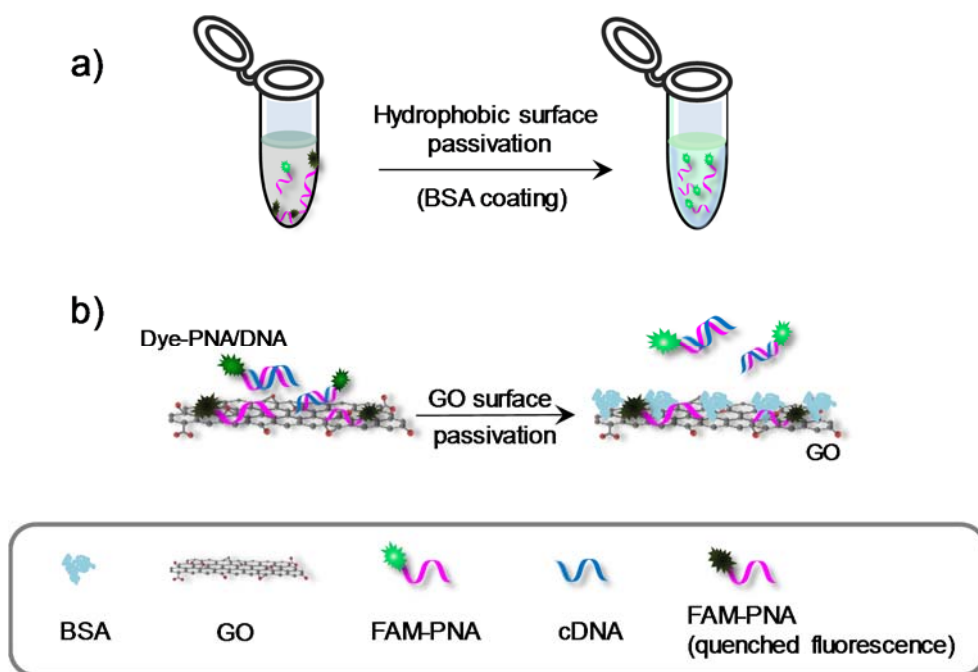
Scheme 3.1 BSA blocking to a) prevent the nonspecific adsorption of PNA on hydrophobic surface and b) inhibit the adsorption of PNA/DNA duplex on GO surface in GO-based biosensing platform using PNA probe.

3.2 Result

In the present study, the degree of PNA adsorption on a hydrophobic surface was judged by monitoring changes in the fluorescence emission intensity of the dye-labelled PNA in solution. In the PNA structure, ethylene glycol linker (O), one of the solubility enhancers, was utilized to minimize the possibility of self-aggregation of PNAs as well as to give space between the fluorescein amidite (FAM) moiety and the PNA strand. The 200 nM F-PNA (5' FAM–OO–TTT GAG GGA AGT TAC GCT TAT–3') in a phosphate buffered saline (PBS, pH 7.4) was prepared by dilution of a 100 μM F-PNA stock solution. The fluorescence intensity of the diluted F-PNA solution gradually decreased down to ~18% of the original intensity over 5 hrs when the solution was incubated in a 96 well black PS plate (Figure 3.1a,b). On the other hand, the intensity of F-PNA incubated with 0.01% BSA very slightly decreased for initial 1 hr and maintained at ~90% of initial intensity in the same PS plate. As a control, when DNA probes were used in place of PNA, the same trend, ~10% decrease of initial fluorescence intensity over time, was observed regardless of BSA addition (Figure 3.1c). The degree of fluorescence intensity decrease of F-PNA was dependent on BSA concentration and maximum prevention of nonspecific adsorption was observed above as little as 0.002% BSA (Figure 3.1e,f). The decay of fluorescence intensity of F-PNA solution was accompanied by slight red-shift of emission

35

spectrum, suggesting that the decline of intensity could be due to the aggregation of F-PNA on a container surface by adsorption (Figure 3.1d).
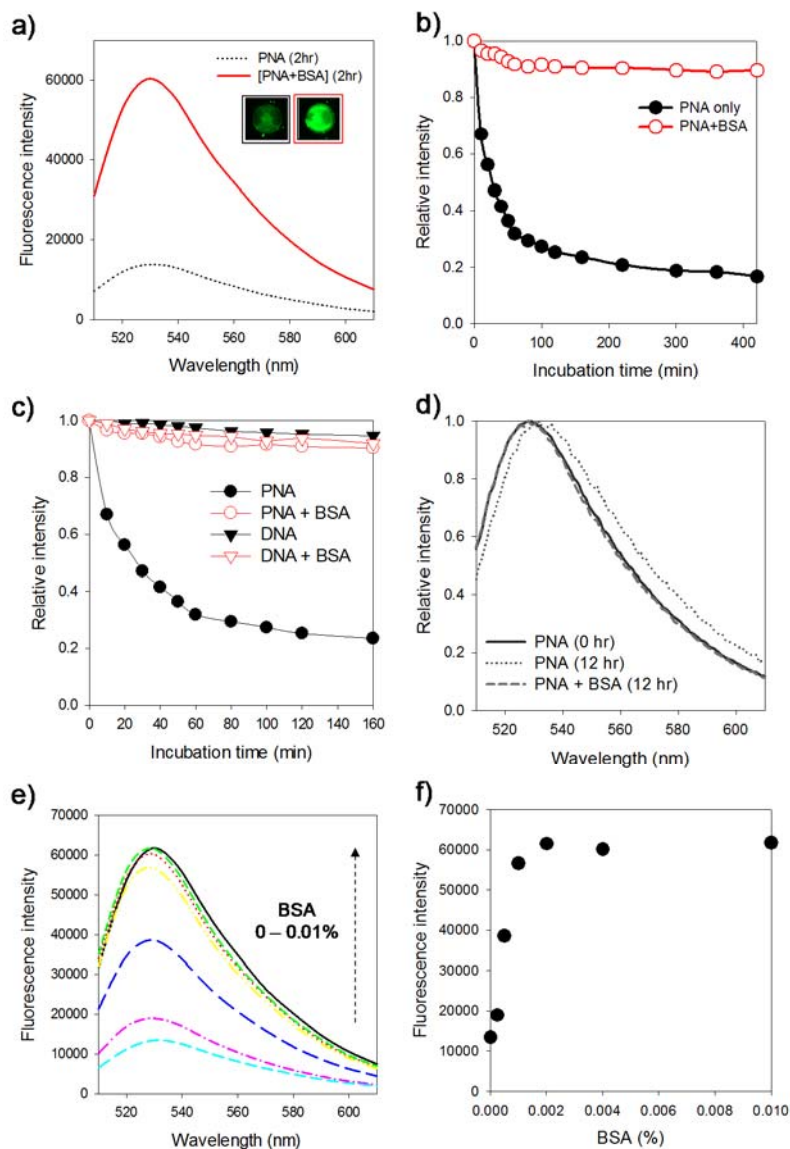
Figure 3.1 Prevention of PNA adsorption on hydrophobic surface by BSA. a) Fluorescence spectra and b) time-dependent relative fluorescence intensity of F-PNA in buffered solution containing BSA 0 % and 0.01 %. c) Time-dependent relative fluorescence intensity of F-PNA and F-DNA in buffer solution containing BSA 0% and 0.01%. d) Fluorescence spectra of F-PNA in buffer solution containing 0% and 0.01% BSA. The emission spectum of PNA solution without BSA was shifted by about 4 nm to red, whereas PNA solution with BSA didn't show the emission shift even after 12hr incubation. e) Fluorescence spectra and f) intensity of F-PNA in presence of various concentration of BSA.

37

To investigate the adsorption of F-PNA on the surface, we compared the fluorescence signal from the container wells (96 well black plate) before and after removing the F-PNA solution following 3 hrs incubation. In the case of F-PNA solution omitting BSA, the similar fluorescence intensity to the incubated solution was measured in the vacant container even after transferring out the solution and several washing. However, F-PNA solutions with BSA showed much lower fluorescence intensity from the empty container, BSA concentration dependently, after removing the solution. The tendency was also correlated with surface coverage of BSA on a PS surface characterized by AFM (Figure 3.2).
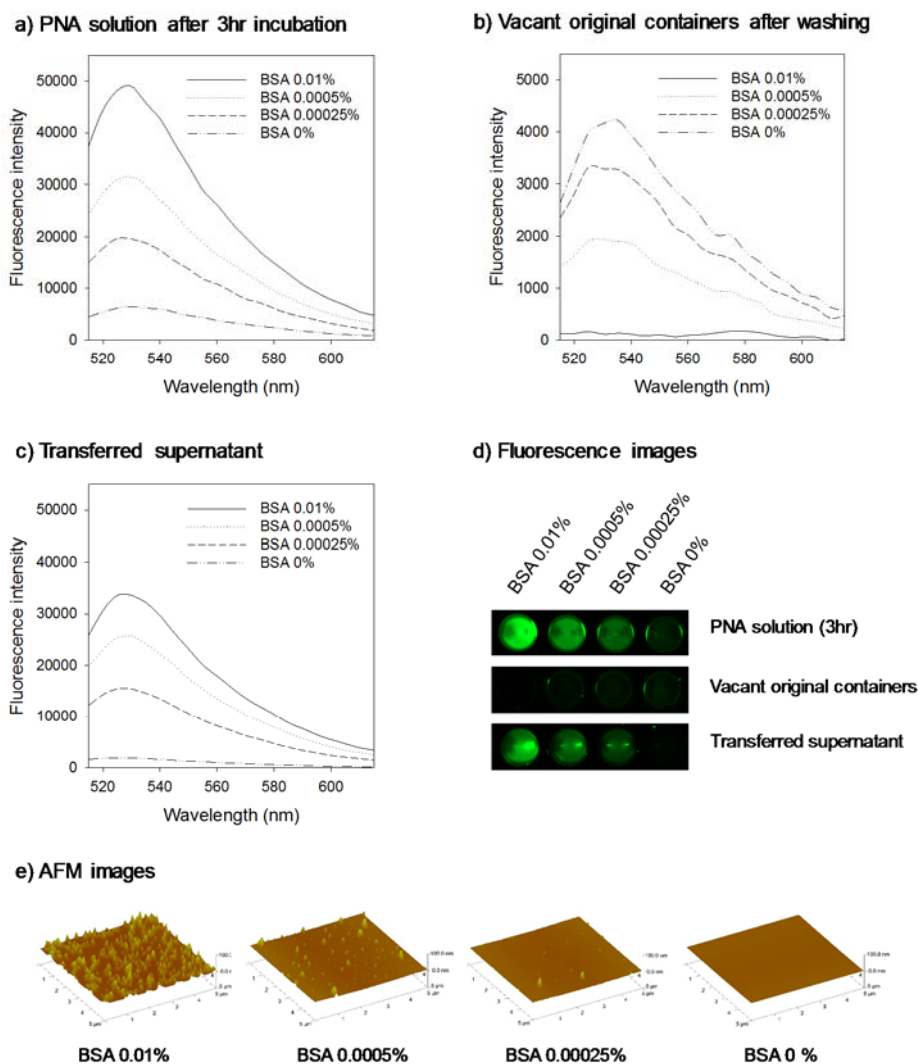
Figure 3.2 BSA concentration dependent blocking effect on hydrophobic surface. a) Fluorescence spectra of F-PNA incubated in a buffered solution containing BSA for 3 hr. The incubated PNA solutions were transferred to new containers and the emptied containers were washed with PBS twice. Fluorescence spectra of b) vacant containers and c) transferred supernatant. d) Fluorescence images of PNA solution, vacant container and transferred supernatant in the presence of various concentration of BSA. e) AFM images showing the gradient adsorption of BSA on polystyrene surfaces when polystyrene coated wafers were immersed in a buffered solution containing various concentrations of BSA for 1hr.

The result indicated that the nonspecific adsorption of PNA on hydrophobic surface can be prevented by BSA blocking. Furthermore, a post-addition of BSA to the adsorbed F-PNA on the hydrophobic support resulted in the gradual recovery of fluorescence intensity until the equilibrium was reached, indicating that BSA could induce desorption of the F-PNA from a solid surface into the solution as well as the inhibition of the adsorption of F-PNA to a solid surface (Figure 3.3).
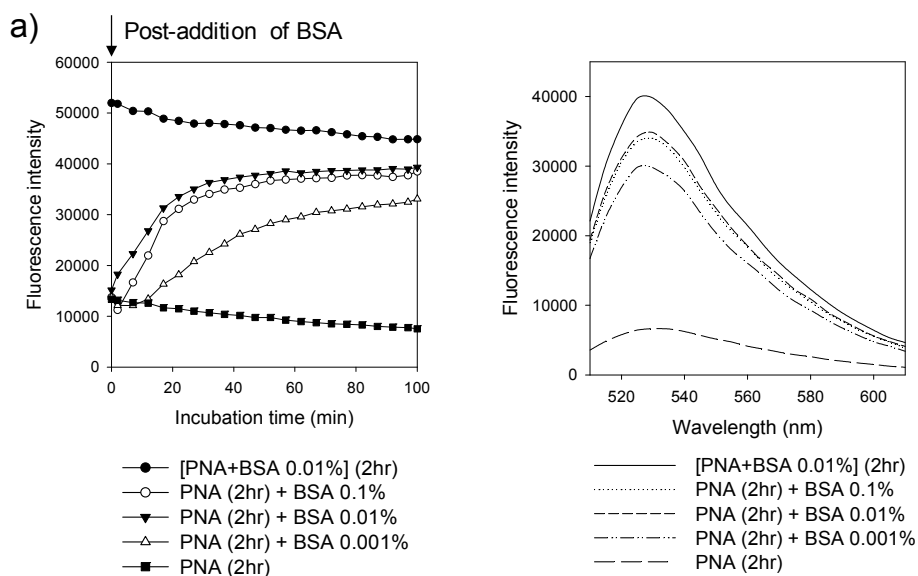
Figure 3.3   PNA strand desorption by BSA. a) Time-dependent fluorescence recovery from non-specifically adsorbed PNA on the hydrophobic surface upon addition of BSA. b) Fluorescence spectra of F-PNA after 100 min from the BSA addition.

Next, we utilized GO for identifying how much percentage of PNA strands were available as a probe in a hydrophobic container in the presence of BSA. GO, a water-dispersible graphene derivative, having a hexagonal lattice of sp^2 carbons and oxygen containing functional groups was pre-pared by using a modified Hummers method.[26-29] GO has high affinity to hydrophobic molecules as well as efficient fluorescence quenching of dyes near its surface.[7,30,31] Thus, the nucleobases of single stranded PNA (ssPNA) can be adsorbed on the GO surface, inducing the fluorescence quenching of the dye conjugated to PNA. Upon the addition of GO to F-PNA solutions incubated in a hydrophobic container without and with 0.01% BSA showed the decrease in the fluorescence intensity, corresponding to 18 and 91% of the initial intensity of F-PNA, respectively (Figure 3.4a,b).
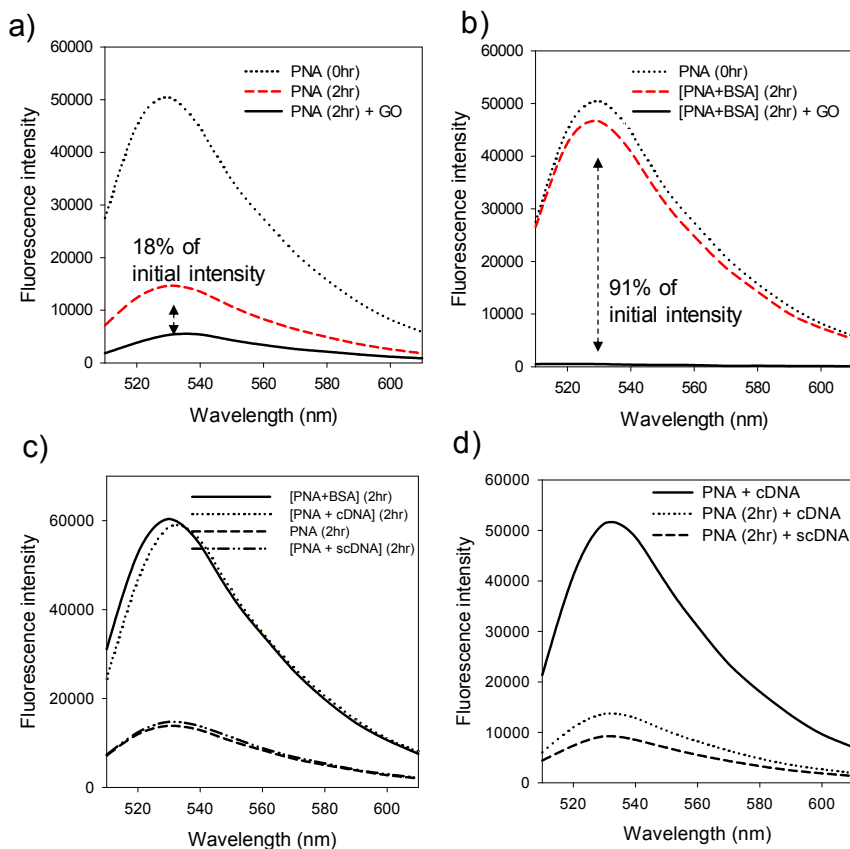
Figure 3.4 ssPNA strands in solution in the presence of BSA. Fluorescence spectra of F-PNA a) in buffered solution and b) in BSA containing buffered solution, in the presence of GO. c) Fluorescence spectra of F-PNA, F-PNA/DNA duplex, F-PNA with scramble sequenced DNA and F-PNA with BSA in buffered solution. d) Comparison of fluorescence spectra of F-PNA with the addition of cDNA between before and after incubating in hydrophobic container.

We could assume that each percentage represented the proportion of ssPNA in each solution that was able to interact with GO, exhibiting exposed bases, and that the PNA adsorbed on the hydrophobic surface cannot function as a probe for hybridization. To examine capability of F-PNA for sequence specific hybridization with target nucleic acid, we next per-formed an experiment in which equal molar amount of complimentary DNA (cDNA) was added before and after F-PNA incubation in a hydrophobic container. The pre-hybridized F-PNA/DNA duplex was highly soluble due to the polyanionic backbone of DNA and maintained the almost uniform fluorescence intensity, which was nearly identical with F-PNA solution containing 0.01% BSA. However, the F-PNA solution that was incubated in the container for 2 hrs, followed by the addition of cDNA, showed much lower fluorescence intensity compared to the pre-hybridized F-PNA/DNA duplex (Figure 3.4c,d). These results suggested that the adsorbed F-PNA on a hydrophobic support cannot play a role as a probe for hybridization with complementary tar-get sequence.

To further investigate the problems occurred by nonspecific adsorption of PNA in biosensor application, we carried out a dsDNA detection using GO and PNA probe in the presence of BSA on the basis of end invasion of PNA to-wards dsDNA (Figure 3.5).[10] In this method, a dye labeled PNA probe was incubated with target dsDNA for the formation of PNA/DNA duplex, followed by GO addition for the adsorption of excess ssPNA and subsequent fluorescence

43

quenching of the dye conjugated to PNA. In contrast to BSA containing samples, BSA free sample showed a high background signal and target concentration independent F/F_0 values, presenting the unfeasibility of dsDNA detection without BSA. This result indicated that nonspecifically adsorbed dye-labeled PNA could give high background signal in a fluorometric biosensing platform.
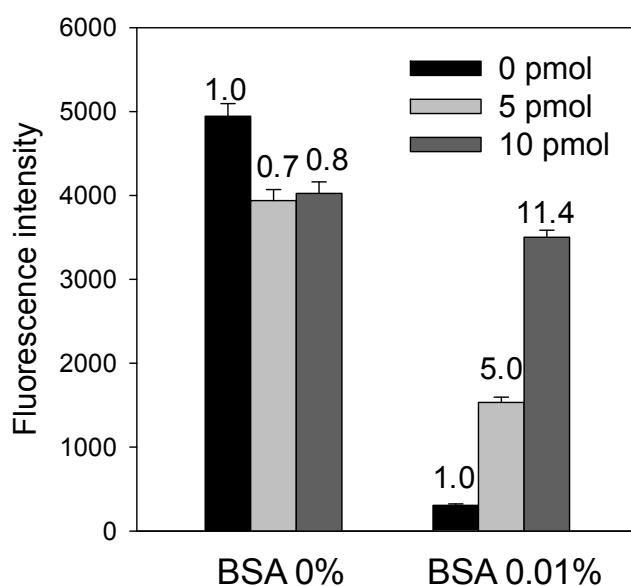
Figure 3.5 Direct dsDNA detection using PNA probe in the presence of 0 and 0.01% BSA. F/F_0 values were shown above the corresponding bar graph. For direct dsDNA detection using PNA probe, a mixture was prepared by adding 10 pmol FAM labelled PNA probe to annealed target dsDNA in PBS containing 0 and 0.01% BSA. After incubation at room temperature for 1hr, 1 μg of GO was added to the mixture for adsorption of ssPNA on GO surface and fluorescence quenching. BSA free sample represented high background signal and unfeasibility of dsDNA detection. On the other hand, BSA containing sample showed negligible background signal and target concentration dependent F/F_0 values, indicating reliable dsDNA detection using PNA probe.

We next performed an experiment to reveal BSA effect on the adsorption of F-PNA on a hydrophobic solid surface by varying the concentration of F-PNA. Lower concentration of F-PNA showed more significant decreases in fluorescence intensities after incubation in the absence of BSA. It indicated that the portion of adsorbed F-PNA was higher with low concentration of F-PNA on the hydrophobic support probably due to the relatively larger surface contact area per PNA. However, the F-PNA solution containing BSA maintained the fluorescence signal over 80% of initial intensity regardless of F-PNA concentration (Figure 3.6a). Because the concentration of F-PNA probes used in actual experiments is usually in nanomolar range, simply adding 0.01% BSA to a PNA solution can be very useful to various F-PNA applications by preventing the adsorption of PNA on a hydrophobic support. To be practical, it will be more convenient if a concentrated stock solution of PNA is made as a mixture with BSA at a proper concentration and used directly for dilution to make each working solution since additional pi-petting of BSA solution for each sample every time could be cumbersome and inefficient. We found that the 100-fold diluted F-PNA solution from the 20 μM F-PNA stock solution containing 0.5% BSA exhibited a constant fluorescence intensity without notable decrease in fluorescence intensity (Figure 3.6b).
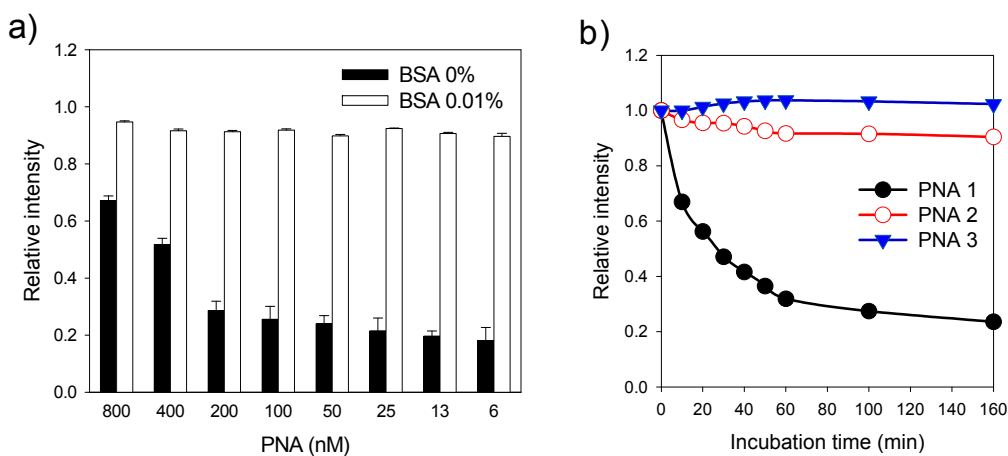
Figure 3.6 Further utility of BSA in PNA applications. a) Relative fluorescence intensity (F_0 min = 1) of various concentrations of F-PNA with and without 0.01% BSA. b) Time dependent fluorescence intensity of three types of PNAs (20 nM), PNA1: diluted from a 20 μM PNA stock, PNA2: diluted from a 20 μM PNA stock, followed by addition of BSA, PNA3: diluted from 20 μM PNA stock containing 0.5% BSA.

We then investigated the sequence-specific tar-get DNA binding ability of F-PNA probe with varying concentrations of BSA. The PNA/DNA duplex was first prepared by mixing equal molar amount of both strands in a buffered solution containing various concentrations of BSA. The duplex was characterized by using non-denaturing poly-acrylamide gel electrophoresis (native-PAGE). Due to less negative charge of F-PNA/DNA duplex compared to DNA/DNA duplex, the band of hetero duplex appeared at upper region showing slower migration than DNA duplex in the gel. The functionality of F-PNA wasn't affected by BSA even though the concentration of BSA was raised up to 1% in F-PNA solution (Figure

3.7a). The co-incubation of F-PNA with BSA in a stock solution was similarly effective in pre-venting F-PNA adsorption with the typical blocking method in that a high concentration of BSA is treated on the support and rinsed away before assay. Both of the methods allowed much higher fluorescence of F-PNA compared to F-PNA solution without BSA, regardless of the type of surface materials (Figure 3.7b). Taken together, we found that BSA in a PNA stock solution can play an important role in a simple and practical usage of PNA.
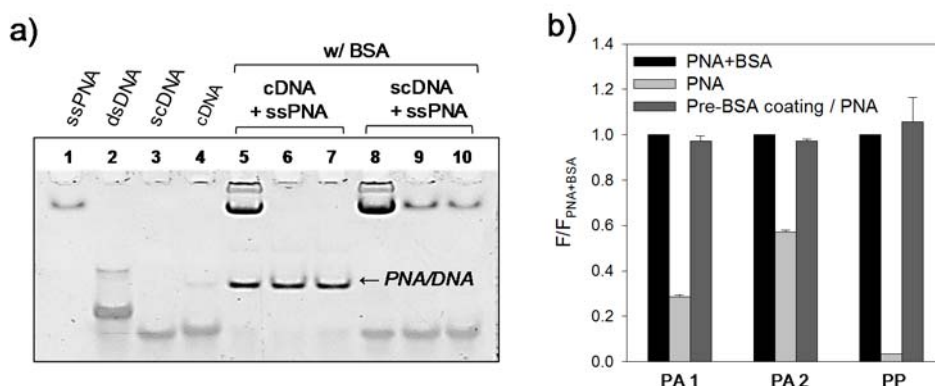
Figure 3.7 Effect of BSA on PNA functionality and other kinds of hydrophobic surface. a) Gel electrophoresis was performed on a 15% polyacrylamide gel. Lanes 1-4 show ssPNA, dsDNA, ssDNA (bottom strand) and ssDNA (upper strand). Lanes 5-7 show the hybridization of 10 pmol of PNA with equal molar amount of cDNA in the presence of various concentrations of BSA (1, 0.1, and 0.01 %). Lanes 8-10 show 10 pmol of PNA incubated with 10 pmol of scDNA in the presence of various concentrations of BSA (1, 0.1, and 0.01 %). b) Relative fluorescence intensity of F-PNA ($F_{PNA+BSA}$ = 1) on three different types of surfaces, PA 1: polystyrene surface, PA 2 : physically treated polystyrene surface for cell culture, PP: polypropylene surface. Pre-BSA coated surface was prepared by incubation of the corresponding surface with 1% BSA for 1hr, followed by washing with PBS 3 times.

We extended the application of BSA blocking to GO based sensing system using PNA. The fluorometric bioensing system was built on the preferential binding of GO to ssPNA over PNA/DNA duplex and the fluorescence quenching capability of GO.[6-9] In case of the duplex, the nucleobases are shielded within negatively-charged DNA backbone and thus, they existed preferentially apart from GO. However, unfavorable experimental conditions such as very high concentration of GO or presence of divalent metal ions can cause the nonspecific adsorption of the duplex on GO surface.[32-34] As a result, the target responsive fluorescence signal gets lower, resulting in poor performance as a sensor. Therefore, it is necessary to minimize the adsorption of the duplex on GO as well as adsorption of PNA on a hydrophobic support for better efficiency. Because GO is known to have affinity for various proteins including BSA due to its amphiphilicity,[35,36] we applied BSA in GO/PNA sensing system to prevent the adsorption of the PNA/DNA duplex on GO (Scheme 5.1b). The interaction of BSA on GO was first confirmed by using isothermal titration calorimetry (ITC) analysis (Figure 3.8).
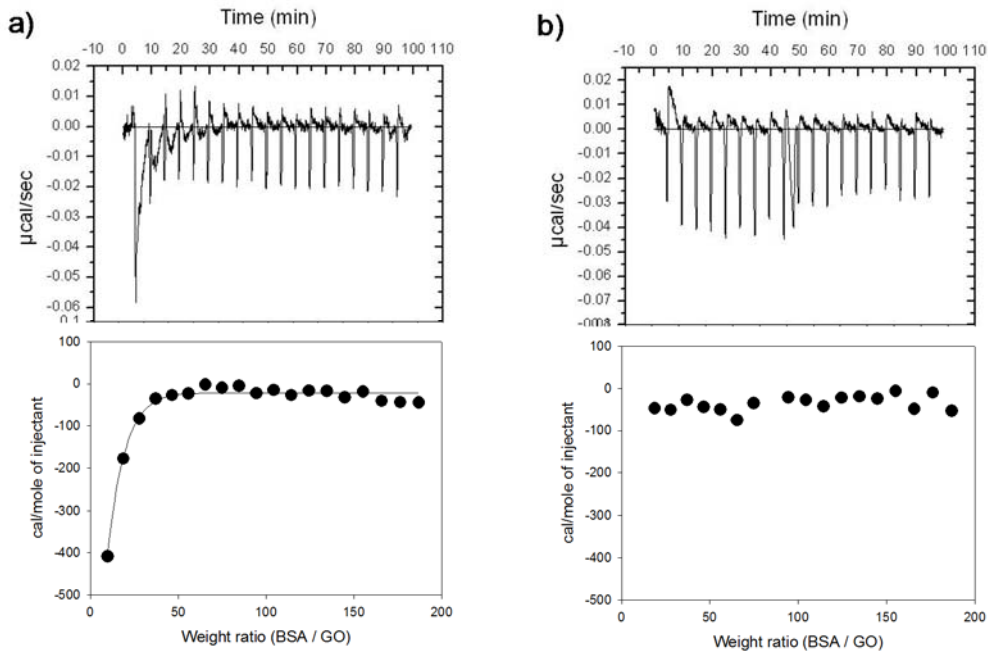
Figure 3.8 Isothermal titration calorimetry (ITC) analysis of GO (0.08 mg/ml) with a) BSA (each 15 μL of 1 mg/ml) and b) PBS as a negative control. The top panels show raw data of the heat pulses resulting from each titration, whereas the bottom panels show the integrated heat normalized per weight of injectant (BSA or 1X PBS) as a function of the weight ratio.

We then compared the adsorption of ssPNA and PNA/DNA duplex onto GO surface in the presence of BSA to verify the selective blocking of the adsorption of PNA/DNA duplex. We measured the degree of fluorescence quenching of F-PNA and F-PNA/DNA duplex with varying GO concentrations in the absence of and in the presence of 0.01% BSA. The concentration of BSA which maximized the FPNA/DNA/FPNA ratio was determined as 0.01% (Figure 3.9).
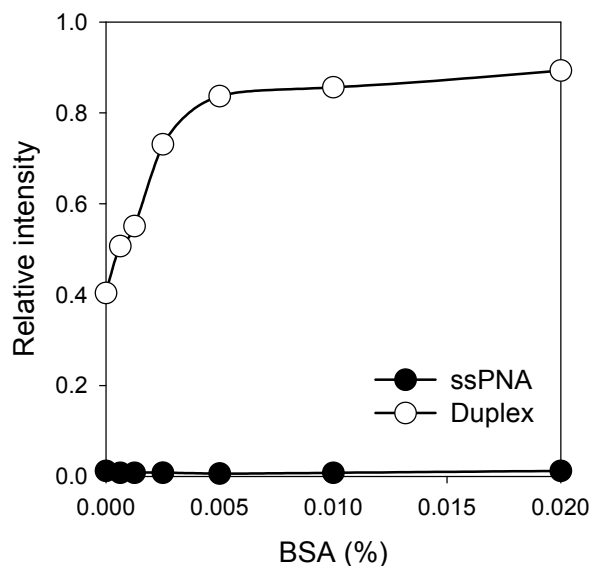
Figure 3.9 BSA dose-dependent relative fluorescence intensity of F-PNA and F-PNA/DNA duplex in the presence of GO.

In case of 10 pmol F-PNA, 0.10 and 0.13 μg of GO were required to quench the 50% fluorescence signal in a buffered solution without BSA and with BSA, respectively. However, F-PNA/DNA duplex (10 pmol) required 3.9 μg of GO for quenching the 50% fluorescence signal in a BSA containing buffered solution whereas 1.0 μg of GO was needed in a buffered solution omitting BSA (Figure 3.10a). It is notable that BSA in PNA/GO based sensor prevents the adsorption of PNA/DNA duplex on GO surface while it has little effect on the interaction

between ssPNA and GO surface. We then calculated the FPNA/DNA/FPNA at varying concentrations of GO to confirm the improved efficiency of the GO based sensor by BSA. When BSA was added in the PNA/GO mixture, the histogram of FPNA/DNA/FPNA shifted toward slightly higher GO concentration. However, meaningful values of FPNA/DNA/FPNA were obtained in much broader range of GO and a higher maximum value of FPNA/DNA/FPNA was observed in the presence of 0.01% BSA, indicating that BSA enabled the sensor to detect the target DNA with higher sensitivity in wider range of GO concentrations (Figure 3.10b).
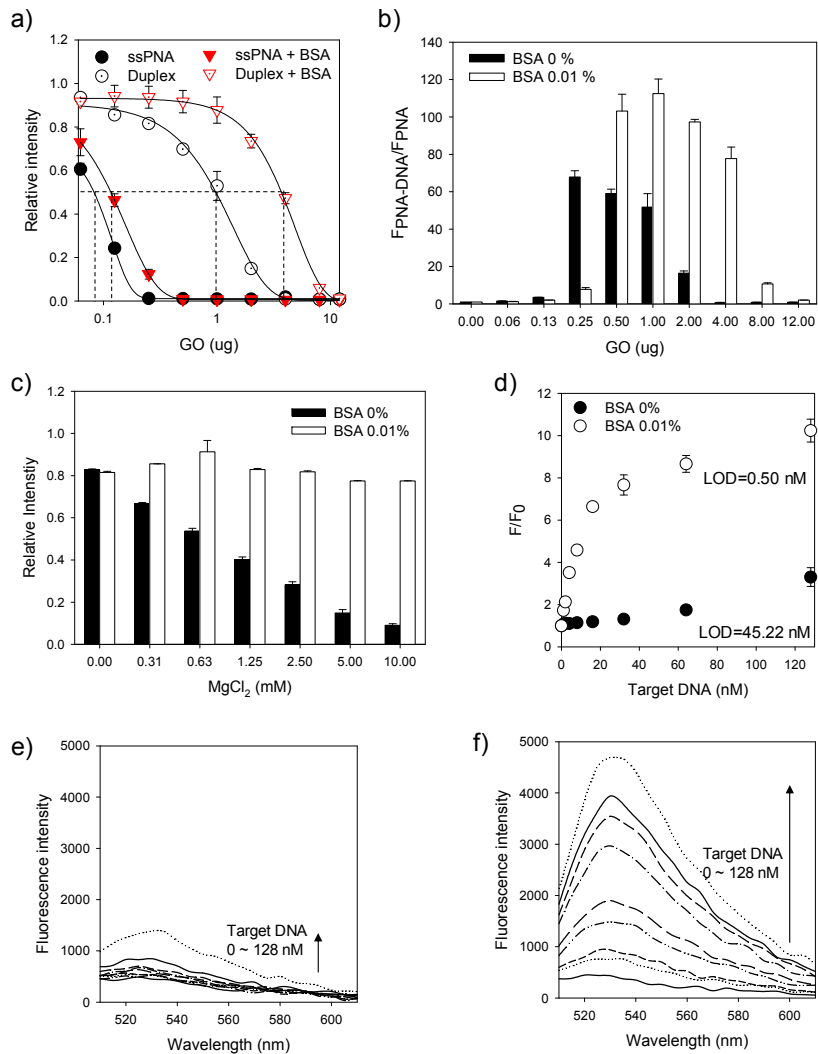
Figure 3.10   Signal enhancement by BSA in sensing platform using GO and PNA probe. a) GO concentration-dependent fluorescence intensity of F-PNA and F-PNA/DNA duplex in a buffered solution with or without 0.01% BSA. b) GO concentration-dependent FPNA-DNA/FPNA. c) Mg2+ concentration-dependent relative fluorescence intensity of F-PNA/DNA duplex in the presence of GO. d) Fluorescence recovery of F-PNA/GO upon addition of target DNA in a buffered solution containing 2.5 mM Mg2+ and BSA. Fluorescence spectra of PNA/GO upon addition of various concentration of target DNA in the presence of e) BSA 0%, GO 1 µg and f) BSA 0.01%, GO 1.5 µg in a buffered solution containing 2.5 mM Mg^{2+}.

The BSA effect for selective blocking of GO could also be verified by elevating the concentration of metal ions in sensing condition. Divalent cations such as Mg^{2+} and Ca^{2+} required for various biofunctions generally facilitate the ad-sorption of PNA/DNA duplex onto the GO surface by neutralizing the electrostatic repulsion between the duplexes and GO. However, addition of BSA to GO in a solution containing Mg^{2+} prevented the adsorption of the duplex on GO and thus, the fluorescence of the dye conjugated to PNA did not diminish over time even under high concentrations of Mg^{2+} (Figure 3.10c). Next, we carried out DNA detection in a buffered solution containing 2.5 mM $MgCl_2$ in the presence of BSA. Under the condition, the sensor with BSA exhibited a detection limit of 0.5 nM according to the equation, LOD = 3.3 (SD/S), which was 90-fold lower than that of the conventional PNA/GO based DNA sensing system omitting BSA of which detection limit was 45.2 nM (Figure 3.10 d,e,f).

3.3 Conclusion

In summary, BSA was employed in PNA application to enhance the stability of PNA in hydrophobic containers and improve the sensing performance of GO/PNA based DNA sensor. Although PNA has favorable properties such as higher chemical/biological stability, specificity and binding affinity for target nucleic acids compared to natural nucleic acid probes, its application has been limited due to nonspecific adsorption on hydrophobic surface. By incorporating 0.01% BSA in a PNA solution, the adsorption of PNA on hydrophobic surface was easily prevented and the portion of the effective PNA strands for target binding could be in-creased without any disturbance on hybridization with a complementary target. Moreover, high concentration of BSA in a PNA stock showed same effect in preventing the nonspecific adsorption during the usage of diluted PNA stock. Also, in the GO based biosensor using PNA, BSA interrupted the unfavorable adsorption of PNA/DNA duplex on GO surface, while allowing the adsorption of ssPNA. The selective blocking on GO can improve the performance of the system by reducing the detection limit by 90-folds. This work is the first to utilize BSA for high yield of available PNA in its application by preventing the nonspecific adsorption and for signal enhancement in GO/PNA based sensor sys-tem. We believe that the present study will provide great opportunity to widen PNA application as useful tools in basic life science and biomedical research as well as therapeutics in gene therapy.

3.4 Material and Methods

Materials. Bovine serum albumin (BSA) was purchased from Bovogen Biologicals (Victoria, Australia). DNA strands were purchased from Genotech (Daejeon, Korea). Dye labeled peptide nucleic acid (F-PNA) strand (5'- FAM-OO- TTT GAG GGA AGT TAC GCT TAT -3') was purchased from Panagene (Daejeon, Korea). Dye labeled DNA (F-DNA) strand (5'- FAM-TTT GAG GGA AGT TAC GCT TAT -3'), complementary DNA strand (5'- ATA AGC GTA ACT TCC CTC AAA -3') and scrambled sequenced DNA strand (5'- TAG CTT ATC AGA CTG ATG TTG A -3') were purchased from Genotech (Daejeon, Korea). Microtube was purchased from Axygen (Tewksbury, USA). 96 well black plate was purchased from SPL (Pocheon, Korea). 96 well cell culture plate with the physical surface treatment was purchase from Greiner Bio-One (Frickenhausen, Germany). Fluorescence intensity and fluorescence image were obtained by a fluorometer SynergyMx (Biotek, UK).

DNA detection using PNA and Graphene Oxide in the presence of BSA.

To prepare PNA/GO complex, 20 pmol of PNA strand was incubated with GO 1 µg in 30 µl of PBS (pH 7.2 buffer containing 137 mM NaCl, 2.7 mM KCl) containing 0 or 0.01% BSA for 30min. Then, 30 µl of various concentrations of DNA target in PBS were added to the mixture. After incubation at room temperature for 2 hr, fluorescence intensity was measured at 520 nm.

3.5 Reference

1. Hyrup, B., Nielsen, P. E., 1996, *Bioorg. Med. Chem.,* **4**, 5-23.

2. Ray, A., Norden, B., 2000, *FASEB j.,* **14**, 1041-1060.

3. Gaylord, B. S., Massie, M. R., Feinstein, S. C., Bazan, G. C., 2005, *Proc. Natl. Acad. Sci. U.S.A.,* **102**, 34-39.

4. Zhang, G. J., Zhang, G., Chua, J. H., Chee, R. E., Wong, E. H., Agarwal, A., Buddharaju, K. D., Singh, N., Gao, Z., Balasubramanian, N., 2008, *Nano Lett.,* **8**, 1066-1070.

5. Soleymani, L., Fang, Z., Sargent, E. H., Kelley, S. O., 2009, *Nat. Nanotechnol.,* **4**, 844-848.

6. Ryoo, S. R., Lee, J., Yeo, J., Na, H. K., Kim, Y. K., Jang, H., Lee, J. H., Han, S. W., Lee, Y., Kim, V. N., Min, D.-H., 2013, *ACS Nano,* **7**, 5882-5891.

7. Kotikam, V., Fernandes, M., Kumar, V. A., 2012, *Phys. Chem. Chem. Phys.,* **14**, 15003-15006.

8. Guo, S., Du, D., Tang, L., Ning, Y., Yao, Q., Zhang, G. J., 2013 *Analyst,* **138**, 3216-3220.

9. Park, J. S., Baek, A., Park, I. S., Jun, B. H., Kim, D. E., 2013, *Chem. Commun.,* **49**, 9203-9205.

10. Lee, J., Park, I.-S., Jung, E., Lee, Y., Min, D.-H., 2014, *Biosens. Bioelectron.,* **62**, 140-144.

11. Tackett, A. J., Corey, D. R., Raney, K. D., 2002, **30**, 950-957.

12. Efimov, V. A., Choob, M. V., Buryakova, A. A., Kalinkina, A. L., Chakhmakhcheva, O. G., 1998, *Nucleic Acids Res.,* **26**, 566-575.

13. Gildea, B. D., Casey, S., MacNeill, J., Perry-O'Keefe, H., Sorensen, D., Coull, J. M., 1998, *Tetrahedron Lett.,* **39**, 7255-7258.

14. Kuwahara, M., Arimitsu, M., Sisido, M., 1999, *J. Am. Chem. Soc.,* **121**, 256-257.

15. Sahu, B., Sacui, I., Rapireddy, S., Zanotti, K. J., Bahal, R., Armitage, B. A., Ly, D. H., 2011, *J. Org. Chem.,* **76**, 5614-5627.

16. Narita, M., Ishikawa, K., Chen,J. Y., Kim, Y., 1984, *Int. J. Peptide Protein Res.,* **24**, 580-587.

17. Uhlmann, E., Peyman, A., Breipohl, G., Will, D. W., 1998, *Angew. Chem. Int. Ed.,* **37**, 2796-2823.

18. Lateef, S. S., Gupta, S., Jayathilaka, L. P., Krishnanchettiar, S., Huang, J. S., Lee, B. S., 2007, *J. Biomol. Tech.,* **18**, 173-176.

19. Abibi, A., Protozanova, E., Demidov, V. V., Frank-Kamenetskii, M. D., *Biophys. J.,* **86**, 3070-3078.

20. Sen, A. Nielsen, P. E., 2006, *Biophys. J.,* **90**, 1329-1337.

21. Brorson, S. H., 1997, *Micron.,* **28**, 189-195.

22. Brown, J. R., 1975, *Fed. Proc.* **34**, 591-591.

23. Jeyachandran, Y. L., Mielezarski, E., Rai, B., Mielczarski,J. A., 2009, *Langmuir,* **25**, 11614-11620.

24. Sawasdikosol, S., 2010, *Curr. Protoc. Immunol.,* Chapter 11, Unit 11 3 1-11.

25. Xiao, Y., Isaacs, S. N., 2012, *J. Immunol. Methods,* **384**, 148-151.

26. Allen, M. J., Tung, V. C., Kaner, R. B., 2010, *Chem. Rev*., **110**, 132-145.

27. Cote, L. J., Kim, F., Huang, J., 2009, *J. Am. Chem. Soc*., **131**, 1043-1049.

28. Zhu, Y., Murali, S., Cai, W., Li, X., Suk, J. W. Potts, J. R., Ruoff, R. S., 2010, *Adv. Mater.* **22**, 3906.

29. Kim, F., Cote, L. J., Huang, J., 2010, *Adv. Mater*. **22**, 1954.

30. Lu, C. H., Yang, H. H., Zhu, C. L., Chen, X., Chen, G. N., 2009, *Angew. Chem. Int. Ed.,* **48**, 4785-4787.

31. Li, F., Pei, H., Wang, L. H., Lu, J. X., Gao, J. M., Jiang, B. W., Zhao, X. C., Fan, C.H., 2013, *Adv. Funct. Mater,* **23**, 4140-4148.

32. Lei, H. Z., Mi, L. J., Zhou, X. J., Chen, J. J., Hu, J., Guo, S. W., Zhang, Y., 2011, *Nanoscale,* **3**, 3888-3892.

33. Zhao, X. C., 2011, *J. Phys. Chem. C,* **115**, 6181-6189.

34. Yun, J. M., Kim, K. N., Kim, J. Y., Shin, D. O., Lee, W. J., Lee, S. H., Lieberman, M., Kim, S. O., 2012, *Angew. Chem. Int. Ed.,* **51**, 912-915.

35. Liu, J., Fu, S., Yuan, B., Li, Y., Deng, Z., 2010, *J. Am. Chem. Soc.*, **132**, 7279-7281.

36. Cote, L. J., Kim, J., Tung, V. C., Luo, J. Y., Kim, F., Huang, J. X., 2011, *Pure Appl. Chem.,* **83**, 1731-1740.

4. A New Strategy for Nucleic Acid Detection with High Sequence Specificity Using Graphene Oxide and Peptide Nucleic Acid

4.1 Introduction

Nucleic acid detection is a crucial tool in clinical diagnosis and monitoring of the viral infection,[1] cancer[2] and diseases associated with genetic alterations. [3] In general, most of the detection methods such as blotting methods, [4] fluorescence in situ hybridization (FISH),[5] polymerase chain reaction (PCR)[6] and DNA microarray[7] were based on the sequence specific recognition by using single stranded nucleic acid as a probe, through Watson-Crick base paring. Fundamentally, the hybridization of probe and target occurs with sequence specificity, but one or two nucleotide substitution in target is insufficient for discrimination of the mismatched target from corresponding perfect matched target. A single mismatched base pair (bp) within DNA duplex shows decreases of melting temperature (T_m) less than 3 ℃.[8]

Precise recognition of few base differences in sequences having very high sequence similarity is important because it provides information on genetic mutation,[9] DNA damage[10] and single-nucleotide polymorphism (SNP).[11] Recently, to cover the shortage of sequence specificity, structural modified

artificial probes were introduced in many sensor systems.[12] For examples, peptide nucleic acid (PNA) has neutral amide bond instead of phosphate backbone, which enables PNA to form highly stable duplexes with complementary target with high specificity in short time.[13] Locked nucleic acid (LNA) possessing a methylene bridge between the 2′-oxygen of ribose and the 4′-carbon also represents strong affinity to target as well as high sequence specificity.[14] Typically, a single mismatched bp in hybrid duplex of artificial probe and natural target causes greatly lower binding affinity, resulting in a wide decline of Tm upto 15 ℃.[8,15] The larger gap of Tm compared to natural probes allowed nucleic acid detection with high sequence specificity. In the modified probe used sensing systems, discrimination of one or more mismatches is commonly achieved by adjusting the hybridization condition such as temperature, ionic strength or formamide concentration, or dissociation conditions of the probe and target duplex.[16] However, most of these systems should be performed by careful design of probe and optimizing the complicated discriminating condition.

We therefore have suggested a new simple strategy for nucleic acid detection with extremely high sequence specificity using graphene oxide (GO) and PNA. GO,[17] a water-soluble derivative of graphene, has been recently harnessed in diverse biological applications such as drug delivery,[18] catalysis,[19] enzyme activity assay[20] and biosensor.[21] General strategy in these applications relies on the strong binding of single stranded nucleic acid and/or hydrophobic molecules

with GO through pi-pi stacking and/or hydrogen bonding interactions and the fluorescence-quenching capability of GO. As a probe, we chose PNA probe, one of the artificial nucleic acid for high sequence specificity. Addition to the widely known properties described above, PNA could also interact with negatively charged GO stronger than negatively charged nucleic acids and construct stable PNA/GO complex, thus the combination of PNA and GO has come into a spotlight in the field of biological application.[22]

In this study, the highly efficient discrimination of single nucleotide substitution was achieved by eliminating the false signal generated from pre-hybridized duplex of PNA and mismatched target. Upon incubation of fluorescent dye conjugated PNA with totally or partially complementary RNA in a solution, the PNA/RNA duplex was formed in a few minutes and the hybridization yield was inversely proportional to a number of mismatched pair and the site. By elevating the temperature of a hybridized PNA/RNA duplex in the presence of GO, the thermo-unstable duplex with mismatched target was relatively denatured and the temporarily dissociated ssPNA from mismatched target was adsorbed on GO. Finally, fluorescence signal for mismatched target was quenched by GO and only FAM-PNA maintaining the hybridization with perfect matched target showed fluoroescence emission (Scheme 4.1).
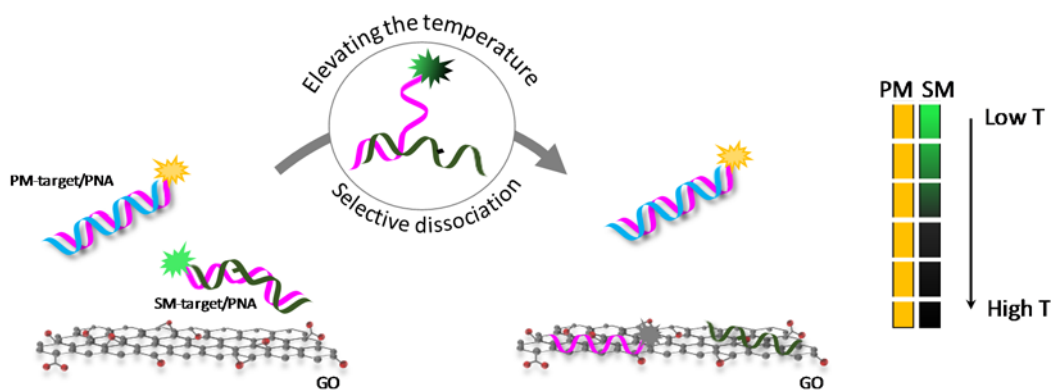
Scheme 4.1. A strategy for single mismatch discrimination in miRNA using PNA and GO.

4.2 Result

To demonstrate our strategy, we chose three RNA in let-7 miRNA family, let-7a, let-7c and let-7f RNA, as a perfect matched (PM) target and two types of single mismatched (SM) targets, respectively. let-7 miRNA family members are conserved across diverse animals in sequence and function, and its abnormal expression leads to a less differentiated cellular state and the development of cell-based diseases such as cancer.[24] let-7c RNA (5'- UGA GGU AGU AGG UUG UAU GGU U -3') and let-7f RNA (5'- UGA GGU AGU AGG UUG UAU GGU U -3') have each one nucleotide substitution from let-7a RNA (5'- UGA GGU AGU AGG UUG UAU AGU U -3') in different site, thus they are suitable model nucleic acid targets for evaluating the discrimination of single nucleotide substitution as well as interesting biomarkers for sensor system (Figure 4.1a). We then prepared carboxyfluorescein (FAM) labeled ssPNA probe of which sequence was fully complementary to let-7a RNA (FAM–-AAC TAT ACA ACC TAC TAC CTC A) and determined the optimal GO concentration for quenching the fluorescence of FAM-PNA probe. We found that the fluorescence of FAM-PNA probe (10 pmol) was quenched up to ~98% in the presence of GO (0.1 µg), giving maximum quenching efficiency under the experimental condition (Figure 4.1b,c).

a)   let-7 miRNA family   *let-7a* : UGA GGU AGU AGG UUG UAU AGU U
                          let-7C : UGA GGU AGU AGG UUG UAU **G**GU U
                          let-7f : UGA GGU AGU AG**A** UUG UAU AGU U

let-7a PNA probe : FAM−OO−AAC TAT ACA ACC TAC TAC CTC A
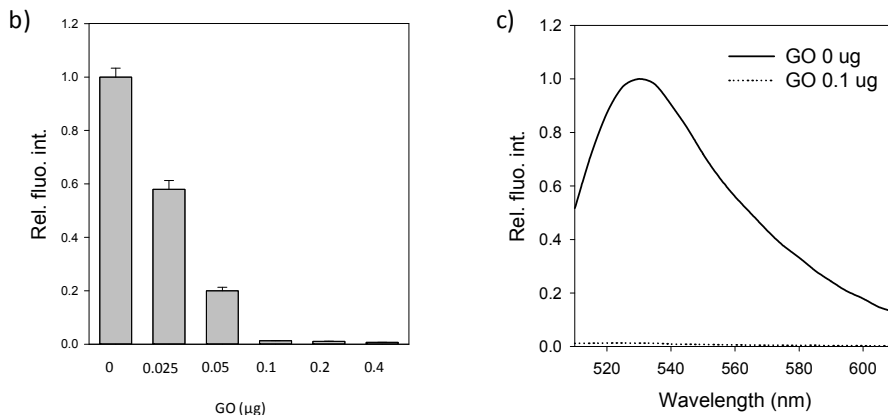
Figure 4.1   Fluorescence quenching of dye conjugated to PNA by GO. a) Sequences of target miRNA and FAM conjugated let-7a PNA probe. b) Relative fluorescence intensity and c) spectra of FAM conjugated to PNA in the presence of GO. The fluorescence signal of 10 pmol of FAM coujugated PNA was quenched by 0.1 ug of GO.

Before the introduction of the new strategy to GO based sensor system, we conducted nucleic acid detection using fluorescence quenched FAM-PNA by GO and synthetic RNAs to confirm the sequence specificity of conventional system. According to the protocol reported previously, the FAM-PNA probe was mixed with GO solution to construct PNA/GO complex, then each miRNA target was added. The fluorescence intensities of the mixtures were increased with all totally and partially complementary target (let-7a, let-7c and let-7f RNA), whereas which a mixture with scrambled RNA wasn't. Upon addition of let-7c and let-7f

64

RNA, the fluorescence of FAM-PNA probe showed 53% and 73% of fluorescence recovery compared to let-7a RNA, respectively (Figure 4.2). This results indicated that the established nucleic acid sensing system wasn't enough to use in the applications requiring extremely high sequence specificity such as miRNA profiling and SNP detection, unfortunately.
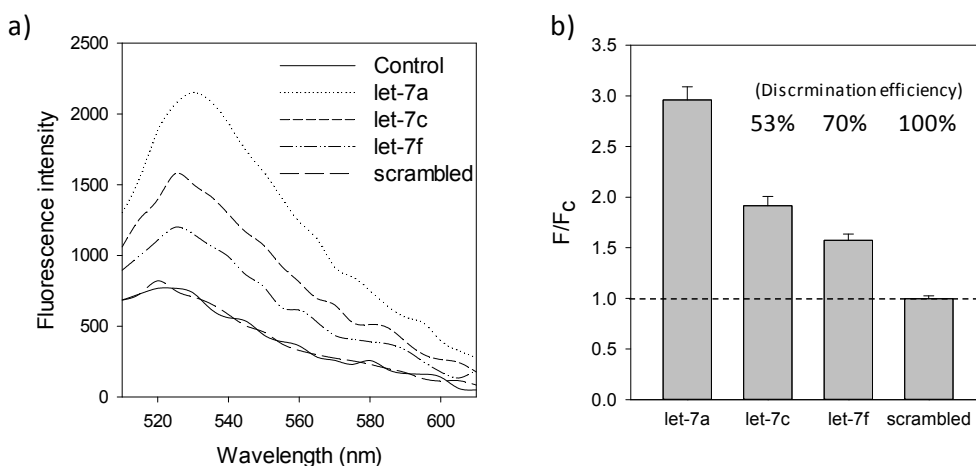
Figure 4.2 Single mismatch discrimination using conventional GO based sensing system. a) Fluorescence spectra and b) F/Fc of FAM labeled let-7a probe/GO complex in the presence of various kinds of target

Next, we carried out temperature dependent single mismatch discrimination test to optimize the temperature for dissociation of PNA from mismatched target. FAM-PNA was pre-incubated with three synthetic miRNAs in buffered solution for hybridization, and then GO was added to the duplex containing solution. The mixture was heated at high temperature (55 ℃ - 75 ℃) for 5 min to induce

dissociation of less stable PNA/RNA duplex and adsorption of ssPNA on GO. At room temperature without heating, let-7c and let-7f RNA were discriminated from let-7a RNA with only 80% and 69% efficiency. However, upon the heating at high temperature, the efficiency value was increased and it reached upto 96% at 70 ℃ (Figure 4.3a). Under the experimental condition, high sequence specificity was confirmed by showing almost overlapped fluorescence spectra of mixtures containing let-7c, let-7F RNA with scrambled RNA (Figure 4.3b).
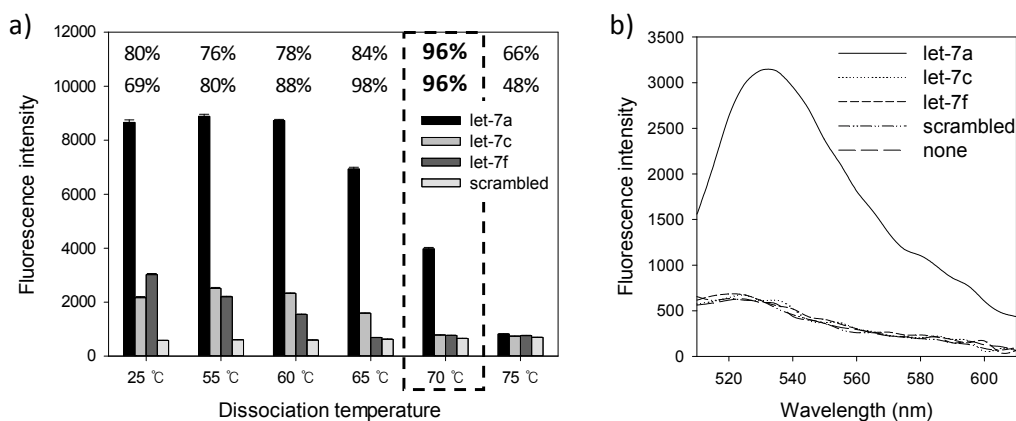
Figure 4.3 Temperature dependent discrimination (RNA target). a) Fluorescence intensity of FAM labeled PNA probe in the presence of each miRNA after thermal dissociation step in a broad range of temperature in the presence of 0.1 μg of GO. The discrimination efficiencies (discrimination efficiency (%) = 100 X (F - $F_{scrambled}$)/($F_{perfect\ matched}$-$F_{scrambled}$)) of let-7a PNA probe against let-7c RNA (upper) and let-7f RNA (bottom) were described above the bar graphs. b) fluorescence spectra of FAM conjugated PNA with target miRNA after thermal dissociation at 70 ℃ in the presence of 0.1 μg of GO.

We also repeated same experiment for temperature dependent discrimination using ssDNA targets possessing the same sequence with let-7a, let-7c, let-7f RNA but thymine in place of uracil. Screening of a wide range of dissociation temperature using DNA targets, optimized discrimination efficiency over 95% was obtained at 65 ℃, which is 5 ℃ lower than RNA targets (Figure 4.4). This shift of dissociation temperature was demonstrated by the previously reported result that Tm value of PNA/DNA duplex was 4 ℃ lower than PNA/RNA duplex.[15] The data suggested that the present GO based platform is highly sensitive to Tm of duplexes and attractive for discrimination of small difference of Tm caused by single mismatched bp.
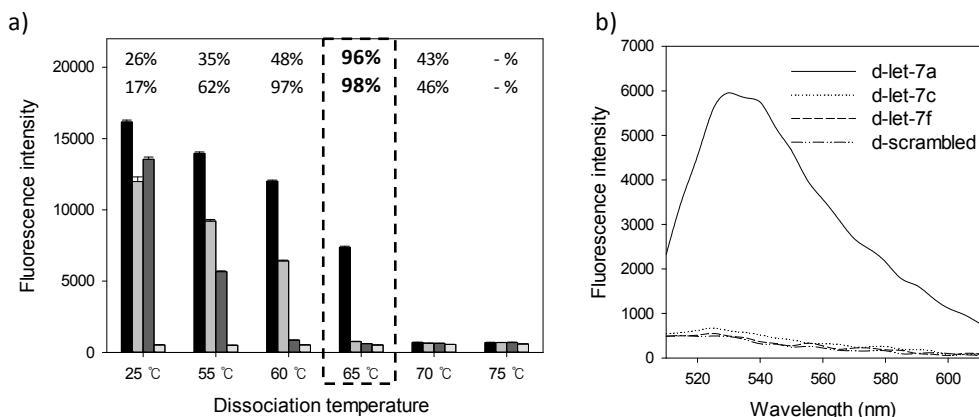
Figure 4.4 Temperature dependent discrimination (DNA target). a) Fluorescence intensity of FAM labeled let-7a PNA probe in the presence of each DNA target possessing let-7 miRNA family (d-let-7) after thermal dissociation step in a broad range of temperature in the presence of 0.1 μg of GO. The discrimination efficiencies of let-7a PNA probe against d-let-7c (upper) and d-let-7f (bottom) were discribed above the bar graphs. b) fluorescence specra of FAM conjugated PNA with target DNA after termal dissociation at 70 ℃ in the presence of GO.

Next, we performed quantitative fluorometric detection of target RNA with the procedure containing thermal treatment. Various concentrations of target let-7a RNA solutions ranging from 0 to 100 nM were mixed with FAM-PNA probe and then, GO solution was added. The mixed solutions of RNA, FAM-PNA and GO underwent the thermal treatment step for selective dissociation at 70 ℃ for 5 min. The fluorescence emission spectra of the mixture showed the RNA concentration dependent fluorescence enhancement (Figure 4.5a). This sensor

showed a linear fluorescence increase between 0 and 6.25 nM with the detection

limit of 230 pM according to the equation, LOD = 3.3 (SD / S) (LOD: limit of

detection, SD: standard deviation, S: slope of the calibration curve) (Figure 4.5b).
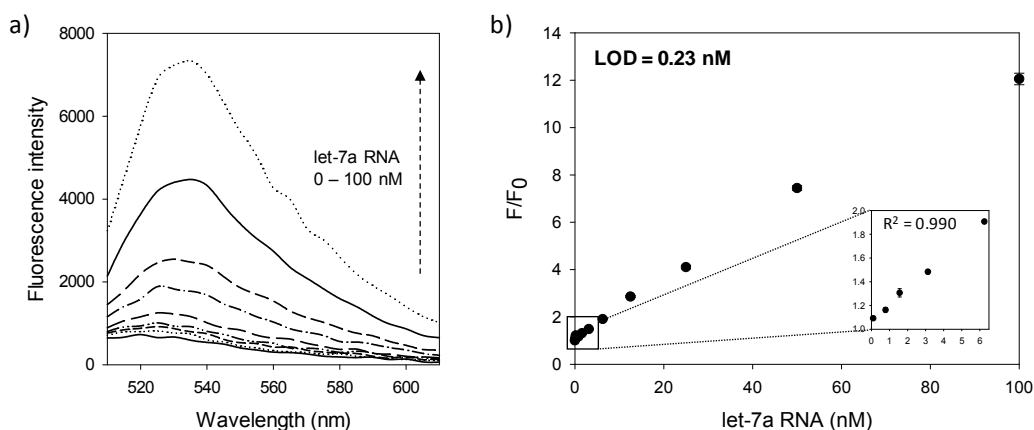
Figure 4.5 Limit of detection test in buffered solution. a) Fluorescence spectra of PNA probe in presence of various concentration of let-7 miRNA in buffered solution. b) Fluorescence intensity enhancement (F/F_0) with wide concentration range of target (F: fluorescence intensity of PNA probe with target, F0: fluorescence intensity of PNA probe without target).

To investigate the applicability for highly sequence specific nucleic acid

detection in serum containing biological samples, we carried out the same

experiment using RNA spiked cell lysate (10000 cells per a sample). Under the

established experimental condition, let-7a RNA couldn't be totally discriminated

against single mismatched target, let-7c, let-7f RNA in a whole range of dissociation temperature (Figure 4.6).
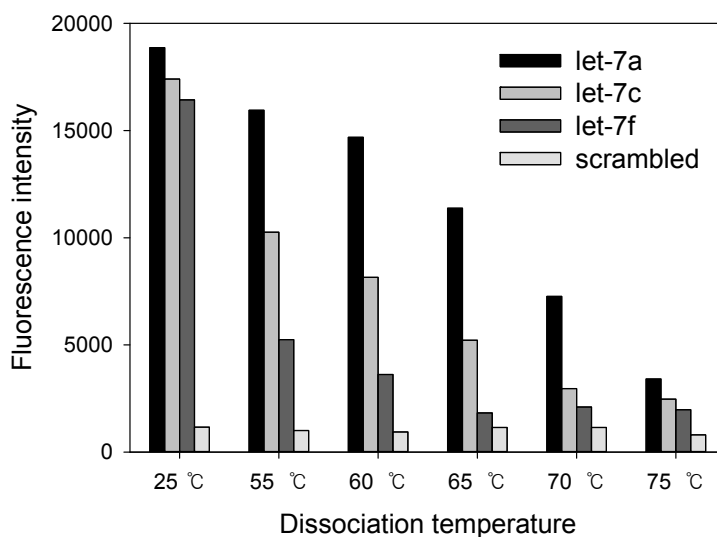
Figure 4.6 Temperature dependent discriminaiton of spiked miRNA in cell lysate. Fluorescence intensity of FAM labeled PNA probe in the presence of each spiked let-7 miRNA in HeLa cell lysate (10000 cells per well) after thermal dissociation step with broad range of temperature in the presence of 0.1 µg of GO. Although the signal of scrambled RNA was almost quenched, perfect matched target wasn't discriminated from mismatched target efficiently, even at high temperature.

Thus, we examined higher concentraiton of GO for overcoming the disturbance of proteins in lysate for adsorption of dissociated ssPNA. As expected,

mixtures of FAM-PNA and RNA including 0.5 μg of GO showed high efficiency

of discrimination over 95% (Figure 4.7a,b). The fluorescence emission spectra

showed slightly higher fluorescence intensity compared to that from solutions

prepared in 1XPBS with same conditions (Figure 4.7c). This finding agrees with

previously reported result that proteins in GO based sensor system can enhance

the target specific signal by blocking nonspecific adsroption of duplex selectively.

Under the condition, the sensor also exhibited a linear fluorescence increase in

the same concentration range of target RNA (0 ~ 6.25 nM) with a slightly higher

detection limit of 810 pM according to the equation, LOD = 3.3 (SD / S) (Figure

4.7d).
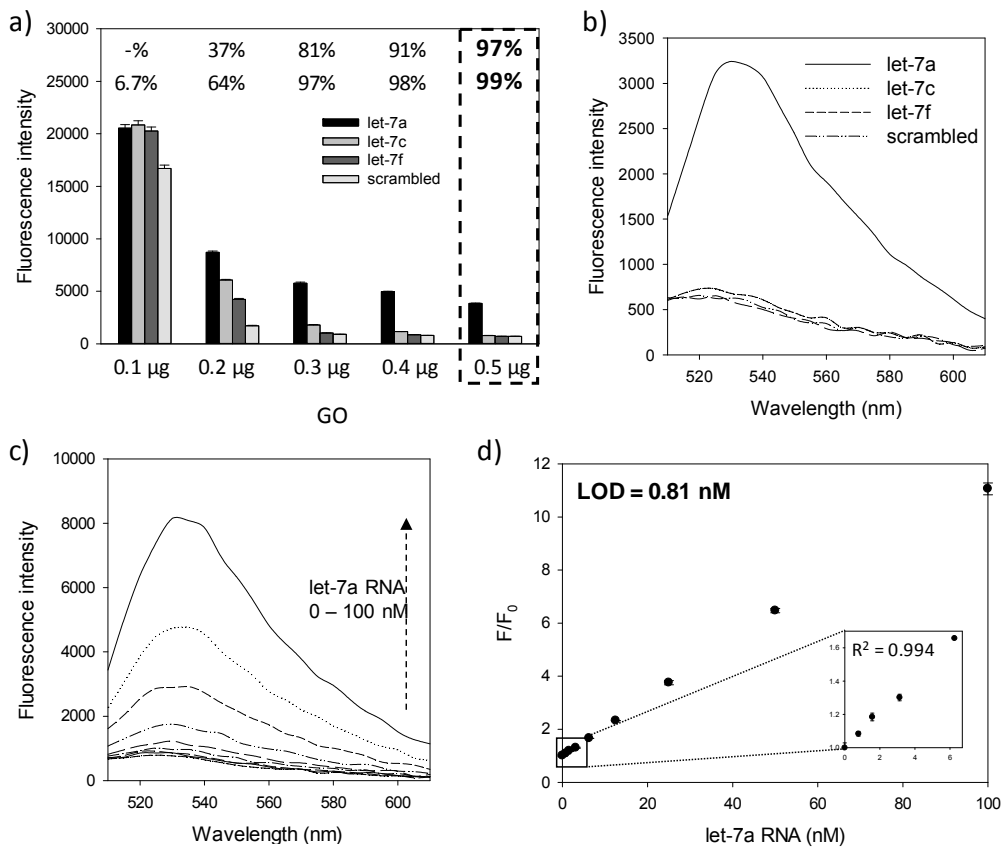
Figure 4.7 Single mismatch discrimination of spiked miRNA in cell lysates. a) Fluorescence intensity of FAM conjugated let-7a PNA probe in the presence of each spiked let-7 miRNA in HeLa cell lysate (10000 cells per well) after thermal dissociation at 70 ℃ in the presence of various amount of GO. Discrimination efficiencies of let-7a PNA probe against let-7c (upper) and let-7f (bottom) were described above the bar graphs. b) Fluorescence spectra of FAM conjugated PNA with target miRNA after thermal dissociation in the presence of 0.5 μg of GO. c) Fluorescence spectra and d) Fluorescence intensity enhancement (F/F_0) of PNA probe in presence of various concentration of spiked let-7a miRNA in HeLa cell lysate after thermal dissociation step in the presence of 0.5 μg of GO. (F: fluorescence intensity of PNA probe with target, F0: fluorescence intensity of PNA probe without target).

72

Finally, we demonstrated the capability of multiplexed detection in a solution using RNA targets possessing only one nucleotide difference each other. We chose two sets of RNA targets, let-7a/let-7c RNA and let-7a/let-7f RNA. Each complimentary sequenced PNA probe for let-7a, let-7c and let-7f RNA was conjugated with three different fluorescent dyes—FAM, ROX (6-carboxyl-X-rhodamine) and Cy5 (cyanine 5) which showed emission maxima of 518 (green), 608 (orange) and 670 nm (red) with excitation at 492, 587 and 650 nm, respectively. For two kinds of RNA detection in a solution, each target RNA or a combination of two RNAs (200 nM) were added to the mixture of the each corresponding dye labelled PNA probes (each concentration= 100 nM), followed by addition of optimized amount of GO (Figure 4.8).
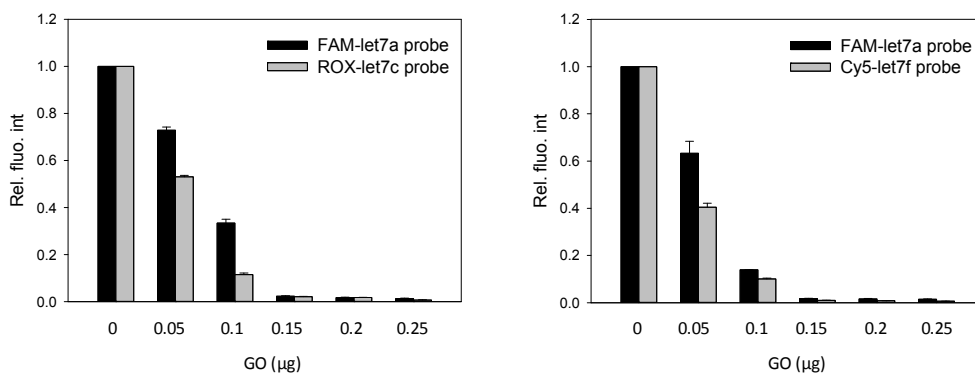
Figure 4.8   Multi-probe quenching test in a solution. Relative fluorescence intensity of a) FAM-let-7a PNA probe and ROX-let-7c PNA probe, b) FAM-let-7a PNA probe and Cy5-let-7f PNA probe in the presence of various amount of GO in a mixed solution.

Then, we screened the temperature from 65 ℃ to 75 ℃ with the interval of 2 ℃ for 5 min to optimize the temperature for effective dissociation of two different PNA probe from mismatched target in a solution (Figure 4.9).

a) Discrimination of let-7a and let-7c in a solution
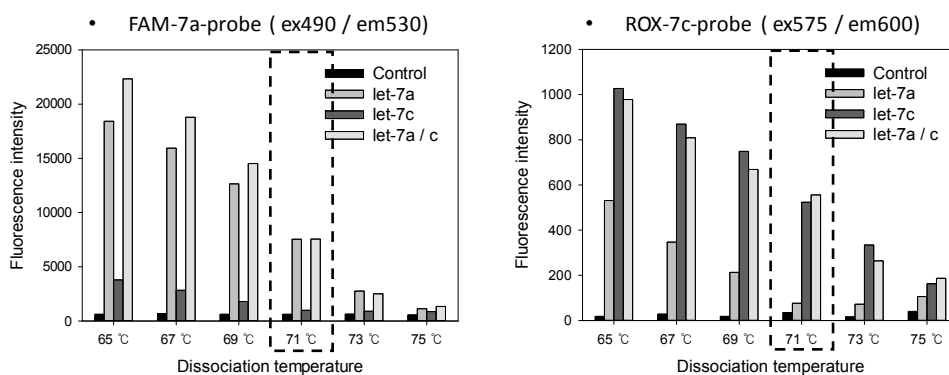
b) Discrimination of let-7a and let-7c in a solution
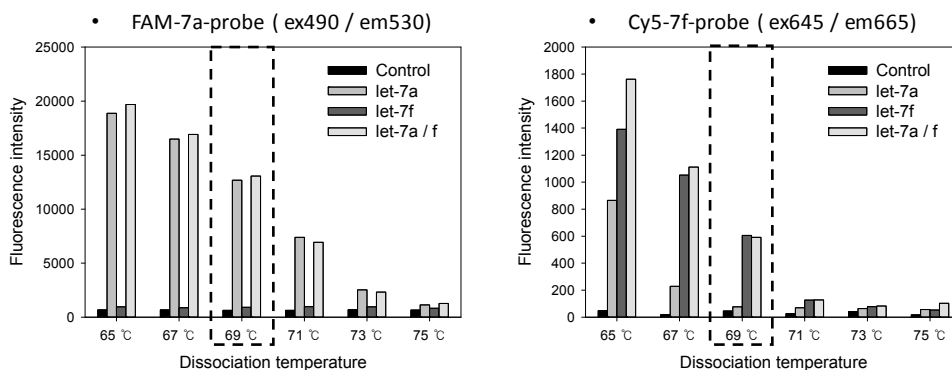
Figure 4.9 Temperature dependent multiplex detection of a) let-7a and let-7c , b) let-7a and let-7f with each corresponding PNA probe in a solution after thermal dissociation step from 65 ℃ to 75 ℃ in the presence of GO.

As a result, let-7a/let-7c RNA and let-7a/let-7f RNA were highly discriminated detection at 69 ℃ and 71 ℃, respectively. These tendency of optimized temperatures agrees with the order of Tm of each PNA probe with perfect matched target (82 ℃ for let-7c pair > 79 ℃ for let-7a pair > 76 ℃ for let-7f pair). At each optimized temperature, green, orange and red fluorescence emission spectra and images were obtained only in the sample containing each corresponding RNA target and PNA probe (Figure 4.10).
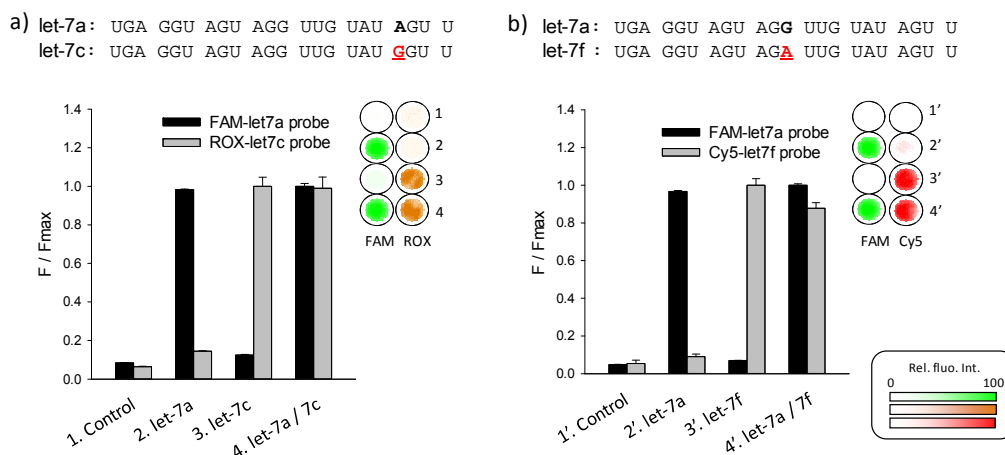
Figure 4.10 Multiplex miRNA detection at each optimal temperature. A bar graph and fluorescence images showing relative fluorescence intensity of a) FAM-let-7a probe / ROX-let-7c probe, b) FAM-let-7a probe / Cy5-let-7f probe in the presence of each target miRNA (200 nM). (F: fluorescence intensity of PNA probe with target, F_{max}: Maximum fluorescence intensity of each PNA probe observed in the presence of perfect matched target).

75

4.3 Conclusion

In conclusion, we developed a new strategy for discrimination of single mismatched target using GO and PNA probe. To the best of our knowledge, this work provides the first example of highly effective single mismatch discrimination among a lot of GO based sensors. The present system utilized each remarkable properties of PNA probe and GO. First, PNA probe provides high binding affinity and sequence specificity to target due to its neutral backbone. The duplex of PNA probe with a single mismatched target was less stable than with perfect matched target, resulting in selective denaturation upon elevating the temperature. Second, GO acts as a scavenger for adsorption of ssPNA dissociated from mismatched target as well as a superquencher for the dye conjugated to the PNA. In addition, owing to the strong interaction between PNA and GO, quantitative miRNA detection with high sequence specificity was enabled even in the serum containing samples without a wide variation of LOD. The present sensor is technically straightforward and compatible with multiplexed sensing formats using sequentially similar targets. Many samples can be simultaneously prepared, and the quantitative multiplex detection with high specificity can be carried out by simply obtaining a fluorescence image of the samples after mixing and incubation at each optimized temperature without separation of mismatched RNA. Finally, this sensing platform can be applied to detection of point-mutations and single nucleotide polymorphisms (SNPs) of DNA as well as

discrimination in other miRNA family by simply changing the sequence of PNA probe and optimizing the dissociation temperature. We believe that this new strategy for highly discriminating of single mismatch using PNA probe and GO will become an important tool in the basic research of nucleic acid and the field of personalized diagnostics of diseases.

4.4 Material and Methods

Materials.   RNA strands were purchased from Bioneer (Daejeon, Korea). DNA strands were purchased from Genotech (Daejeon, Korea). PNA probes were purchased from Panagene (Daejeon, Korea). Temperature control was performed by using thermocycler (BioRad, USA). Fluorescence intensity and fluorescence image were obtained by fluorometer SynergyMx (Biotek, UK).

Temperature dependent mismatch discrimination using peptide nucleic acid and graphene oxide.   Firstly, to prepare target/PNA probe duplex, 1 μL of 5 μM RNA target strand was mixed with 10 pmol of dye labeled PNA probe in pH 7.2 1XPBS buffer containing NaCl 137 mM, KCl 2.7 mM, followed by incubation at room temperature for 10min. Then, 0.1 μg of GO was added to the mixture, followed by heating at high temperature (55 ℃ - 75 ℃) for 5 min to induce selective dissociation of relatively unstable duplex. After cooling down, fluorescence intensity of the mixture was measured.

Multiplex detection of let-7a and let-7c possessing only one base difference between them.   For preparation of probe/target duplex, two RNA target strands (20 pmol) was incubated with FAM labeled let-7a probe and ROX labeled let-7c probe (each 10 pmol) in a 1XPBS solution for 10 min. Then, 0.3 μg of GO was added to the mixture, followed by heating at 71 ℃ for 5 min to induce selective

dissociation of two kinds of relatively unstable duplex. After cooling down, fluorescence intensity of the mixture was measured at ex 492 nm/em 518 nm for FAM-let7a probe and 587 nm/608 nm for ROX-let7c probe.

4.5 Reference

1. a) Chu, J. S., Chen, C. C., Chang, K. J., 1998, *Cancer lett.* **124**, 53. b) Dejean, A., Lugassy, C., Zafrani, S., Tiollais, P., Brechot, C., 1984, *J. Gen.Virol.* **65**, 651-655.

2. Mitchell, P. S., Parkin, R. K., Kroh, E. M., Fritz, B. R., Wy-man, S. K., Pogosova-Agadjanyan, E. L., Peterson, A., Note-boom, J., O'Briant, K. C., Allen, A., Lin, D. W., Urban, N., Drescher, C. W., Knudsen, B. S., Stirewalt, D. L., Gentleman, R., Vessella, R. L., Nelson, P. S., Martin, D. B., Tewari, M., 2008, *Proc. Natl. Acad. Sci. U.S.A.* **105**, 10513-10518.

3. Barany, F., 1991, *Proc. Natl. Acad. Sci. U.S.A.* **88**, 189-193.

4. Wahl, G. M., Meinkoth, J. L., Kimmel, A. R., 1987, *Methods Enzymol.* **152**, 572-581.

5. Levsky, J. M., Singer, R. H., 2003, *J. Cell Sci.* **116**, 2833-2838.

6. Chen, S. C., Halliday, C. L., Meyer, W., 2002, *Med. Mycol.* **40**, 333-357.

7. Heller, M. J., 2002, *Annu. Rev. Biomed. Eng.* **4**, 129-153.

8. You, Y., Moreira, B. G., Behlke, M. A., Owczarzy, R., 2006, *Nucleic Acids Res.* **34**, e60.

9. Fedier, A., Fink, D., 2004, *Int. J. Oncol.* **24**, 1039-1047.

10. Collins, A. R., Duthie, S. J., Dobson, V. L., 1993, *Carcinogenesis* **14**, 1733-1735.

11. Barreiro, L. B., Laval, G., Quach, H., Patin, E., Quintana-Murci, L., 2008, *Nat. Genet.* **40**, 340-345.

12. a) Gaylord, B. S., Heeger, A. J., Bazan, G. C., 2002, *Proc. Natl. Acad. Sci. U.S.A.* **99**, 10954-10957. b) Fabris, L., Dante, M., Braun, G., Lee, S. J., Reich, N. O., Moskovits, M., Nguyen, T. Q., Bazan, G. C., 2007, *J. Am. Chem. Soc.* **129**, 6086-6087. c) Obernosterer, G., Martinez, J., Alenius, M., 2007, *Nat. Protoc.* **2**, 1508-1514.

13. Hyrup, B., Nielsen, P. E., 1996, *Bioorg. Med. Chem.* **4**, 5-23.

14. Braasch, D. A., Corey, D. R., 2001, *Chem.Biol*. **8**, 1-7.

15. Jensen, K. K., Orum, H., Nielsen, P. E., Norden, B., 1997, *Biochemistry* **36**, 5072-5077.

16. Urakawa, H., El Fantroussi, S., Smidt, H., Smoot, J. C., Tri-bou, E. H., Kelly, J. J., Noble, P. A., Stahl, D. A., 2003, *Appl. Environ. Microbiol*. **69**, 2848-2856.

17. a) Allen, M. J., Tung, V. C., Kaner, R. B., 2010, *Chem Rev*., **110**, 132-145. b) Loh, K. P., Bao, Q., Eda, G., Chhowalla, M., 2010, *Nat. Chem*. **2**, 1015-1024. c) Zhu, Y., Murali, S., Cai, W., Li, X., Suk, J. W., Potts, J. R., Ruoff, R. S., 2010, *Adv. Mater*. **22**, 3906-3924.

18. Liu, Z., Robinson, J. T., Sun, X., Dai, H., 2008, *J. Am. Chem. Soc*. **130**, 10876-10877.

19. Pyun, J., 2011, *Angew. Chem. Int. Ed*. **50**, 46-48.

20. a) Jang, H., Kim, Y.-K., Kwon, H.-M., Yeo, W.-S., Kim, D.-E., Min, D.-H., 2010, *Angew. Chem. Int. Ed*. **49**, 5703-5707. b) Lee, J., Kim, Y.-K., Min, D.-H., 2010, *J. Am. Chem. Soc*. **132**, 14714-14717.

21. a) Lu, C. H., Yang, H. H., Zhu, C. L., Chen, X., Chen, G. N., 2009, *Angew. Chem. Int. Ed*. **48**, 4785-4787. b) He, S. J., Song, B., Li, D., Zhu, C. F., Qi, W. P., Wen, Y. Q., Wang, L. H., Song, S. P., Fang, H. P., Fan, C. H., 2010, *Adv. Func. Mat*. **20**, 453-459.

22. a) Guo, S., Du, D. X., Tang, L. N., Ning, Y., Yao, Q. F., Zhang, G., 2013, *Analyst* **138**, 3216-3220. b) Ryoo, S.-R., Lee, J., Yeo, J., Na, H.-K., Kim, Y.-K., Jang, H., Lee, J. H., Han, S. W., Lee, Y., Kim, V. N., Min, D.-H. 2013, *ACS Nano* **7**, 5882-5891. c) Park, J. S., Baek, A., Park, I.-S., Jun, B.-H., Kim, D.-E., 2013, *Chem. Commun*. **49**, 9203-9205. d) Lee, J., Park, I.-S., Jung, E., Lee, Y., Min, D.-H., 2014, *Biosens. Bioelecron*. **62**, 140-144.

23. Luo, J., Cote, L. J., Tung, V. C., Tan, A. T., Goins, P. E., Wu, J., Huang, 2010, *J. Am. Chem. Soc*. **132**, 17667-17669.

24. a) Pasquinelli, A. E., Reinhart, B. J., Slack, F., Martindale, M. Q., Kuroda, M. I., Maller, B., Hayward, D. C., Ball, E. E., Degnan, B., Muller, P., Spring, J., Srinivasan, A., Fishman, M., Finnerty, J., Corbo, J., Levine, M., Leahy, P., Davidson, E., Ruvkun, G., 2000, *Nature* **408**, 86-89. b) Johnson, S. M., Grosshans, H., Shingara, J., Byrom, M., Jarvis, R., Cheng, A., Labourier, E., Reinert, K. L., Brown, D., Slack, F. J., 2000, *Cell* **120**, 635-647.

5. A Simple DNA Exonuclease Activity Assay Based on Graphene Oxide

5.1 Introduction

Exonucleases are DNA degrading enzymes by catalyzing hydrolysis of phosphodiester bonds from the 3' or the 5' end.[1] They play pivotal roles in a variety of physiological and cellular processes. For example, DNA polymerases which catalyze the synthesis of nucleic acids on pre-existing nucleic acid templates have the exonuclease activity to mediate proofreading and DNA repair during DNA replication process.[2] 3'→5' exonucleases are a class of this enzyme family, which remove nucleotides at the 3' termini from DNA strands to prevent the formation of aberrant double stranded structure.[3] They are directly involved in maintaining genome stability through the proofreading function during DNA replication. For example, TREX 1 which is the major 3'→5' exonuclease in mammalian cells shows a proofreading role during lagging strand DNA synthesis or a gap filling role during DNA repair.[4] Mutations in this gene cause serious diseases including chilblain lupus, retinal vasculopathy cerebral dystrophy (RVCL), Aicardi-Goutieres syndrome and Cree encephalitis.[5-9] Therefore, it is important to measure the enzyme activities for drug development and mechanistic study. Traditionally, gel electrophoresis and/or ^{32}P labelled substrates are popularly chosen to measure the activity of exonucleases.[10,11]

However, these assay methods are laborious, time/cost-consuming, and not suitable for high throughput assay. Recently, alternative approaches have been developed such as colorimetric and fluorescence methods based on nanomaterials for monitoring of exonuclease activity.[12-14]

Here, we report a new 3'→5' DNA exonuclease activity assay method based on graphene oxide (GO) (Scheme 1). Graphene, a single atomic layer carbon nanosheet, is an attractive material with extraordinary electronic, thermal, and mechanical properties.[15] GO, a water-soluble derivative of graphene, has a great potential for biological applications, such as biosensors, and enzyme activity assays.[16,17] Previously, GO was shown to interact with ssDNA through pi-stacking interactions, whereas dsDNA cannot be effectively bound to the GO surface.[18] Our strategy for exonuclease assay relies on the binding of fluorescently labeled ssDNA with GO and quenching of fluorescence by GO. To demonstrate our strategy, we use a hairpin-structured DNA substrate labeled with a fluorescent dye at 5' end and exonuclease III (Exo III) which digests dsDNA, not ssDNA, specifically from the 3' terminus until dsDNA is depleted.[19] This enzyme affords the dye-conjugated ssDNA from the hairpin-substrate, resulting in the quenching of fluorescence of the dye by adsorption to GO (Scheme 5.1).
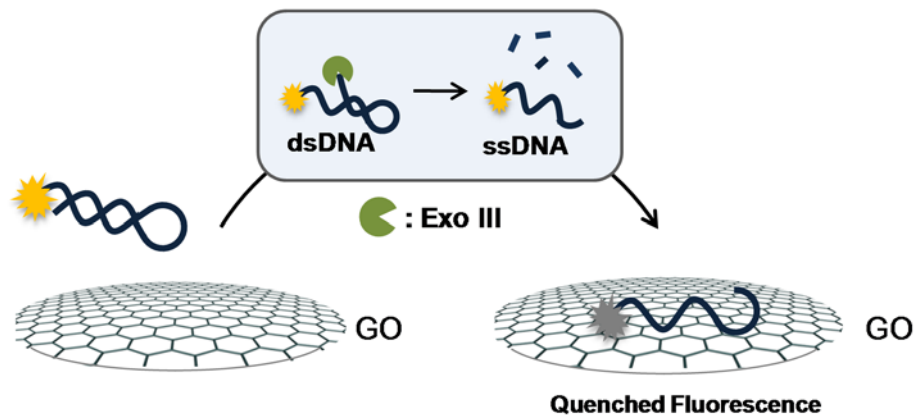
Scheme 5.1 A strategy for 3'→5' DNA exonuclease activity assay based on GO.

5.2 Result

First, we prepared an aqueous suspension of GO according to a modified Hummers method.[20] The formation of the single layered GO sheet with ~ 1.4 nm thickness was confirmed by atomic force microscopy (AFM) image and the height profile (Figure 5.1a,b). Next, we characterized the GO using FT-IR and Raman spectroscopy. The FT-IR spectrum showed several characteristic peaks which suggest successful formation of GO, including peaks at 1625 and 1087 cm-1 from C=C skeletal vibrations and C–O stretching, respectively (Figure 5.1c). The Raman spectrum of GO showed G band at 1598 cm^{-1} from the ordered sp2 carbon domain, and D band at 1359 cm^{-1} which indicates the structural disorder of the sp2 carbon domain, induced by oxidation and exfoliation (Figure 5.1d). Collectively, the data suggest the successful preparation of GO.
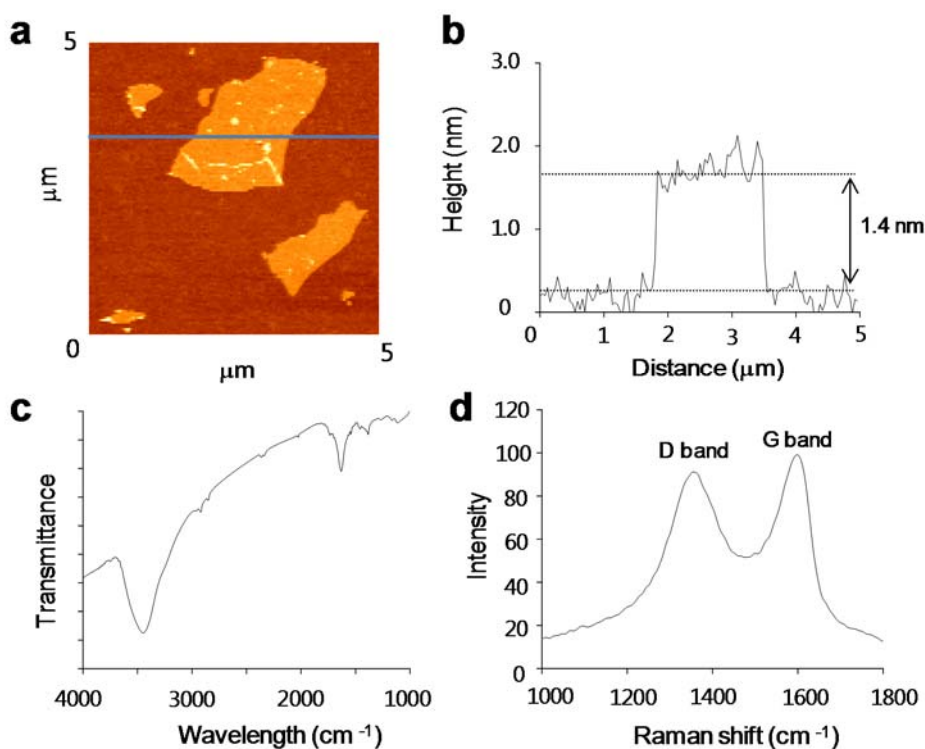
Figure 5.1 GO characterization. a) AFM image and b) height profile of GO c) FT-IR and d) Raman spectra of GO, which present characteristic peaks corresponding to functional groups and disordered sp^2 structures in GO.

Next, a substrate DNA of Exo III was prepared by self-annealing the fluorescein amidite (FAM) labeled hairpin DNA sequence (5' FAM— GGCCGAGC TTTTTT GCTCGGCC – 3') (Figure 5.2a). The substrate DNA was prepared in a buffer solution containing 10 mM Bis-Tris Propane, 10 mM MgCl$_2$,

and 1 mM dithiothreitol (Exo III reaction buffer, pH 7.0). Optimal GO concentration was determined by comparing the fluorescence intensity between the hairpin substrate DNA and the DNA product (ssDNA) generated by Exo III-mediated hydrolysis, in the presence of the various concentrations of GO. We found that 5.5 μg/mL GO showed ca. 91% quenching efficiency, giving a maximum difference in fluorescence intensities between intact hairpin substrate DNA and product ssDNA produced by Exo III (Figure 5.2b)

Figure 5.2 Fluorescence quenching of the FAM that is conjugated to ssDNA by GO. a) DNA sequence prepared for Exo III reaction is shown. DNA shows the hairpin structure consisting of 8-bp sequence at 5'-terminus and its complementary sequence at the 3'-terminus connected by a 6-bp flexible thymine-rich linker. b) Fluorescence spectra of hairpin DNA substrate and ssDNA product generated from Exo III-mediated digestion were obtained in the presence of GO (5.5 mg/ml).

We then performed the time-dependent digestion of the hairpin DNA substrate catalyzed by Exo III. Reaction mixtures were prepared by adding 1 or 0.125 U of Exo III to 30 μL of hairpin substrate solution in Exo III reaction buffer. Then, GO solution was added to the Exo III reaction mixture to make final concentration 5.5 μg/mL in a 96-well plate at 10 min intervals (Figure 5.3a). The fluorescence spectrum was then obtained from each well using a fluorometer. Enzyme concentration-dependent DNA hydrolysis assay was next performed using various concentrations of Exo III (Figure 5.3b). As expected, the DNA digestion proceeded faster with higher concentrations of Exo III. We next performed inhibition assays of Exo III using two known inhibitors to demonstrate that the present method was quantitative and applicable to the evaluation of inhibitors. Aurintricarboxylic acid (ATA) and ethylenediaminetetraacetic acid (EDTA) were chosen as Exo III inhibitors.[21] Exo III (1 U) was added to hairpin substrate solution in the presence of various concentrations of the inhibitors, and incubated at room temperature for 30 min. Fluorescence spectra were obtained after mixing the reaction mixtures with GO solution. Dose-dependent inhibition curves were plotted based on fluorescence intensities. The IC50 values of ATA and EDTA were estimated to be 10.2 μM and 36.6 mM, respectively (Figure 5.3c, d).
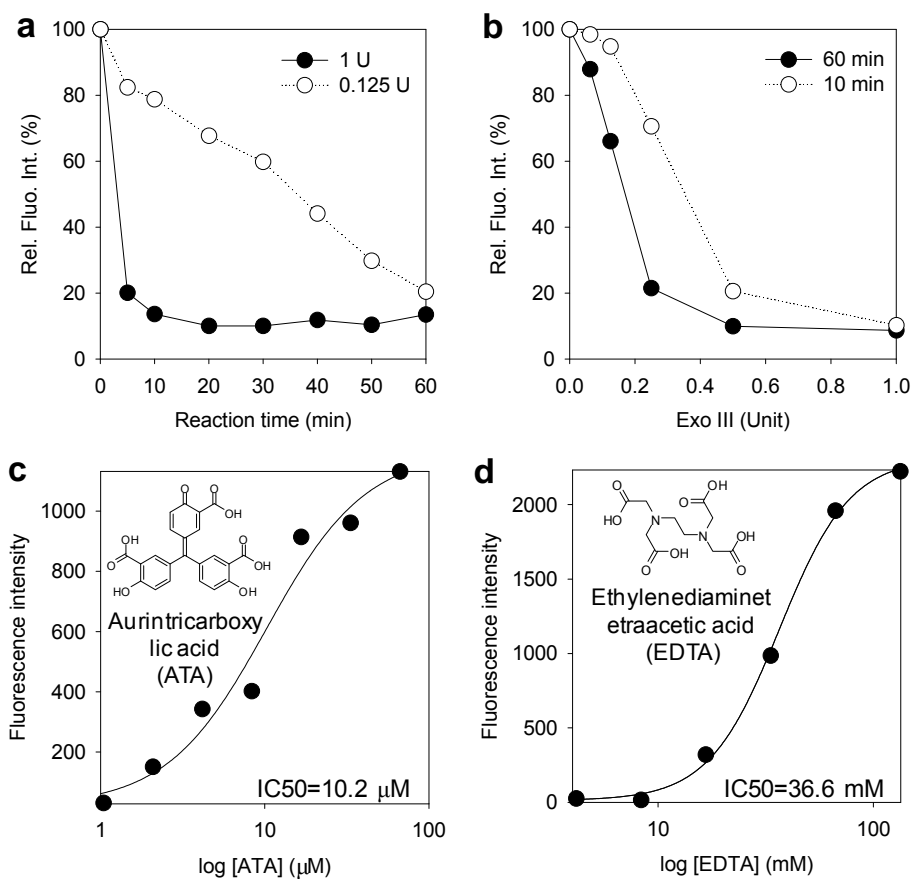
Figure 5.3 ExoIII activity assay. a) The time–dependent and b) enzyme concentration–dependent digestions of hairpin DNA substrate by Exo III were measured by obtaining fluorescence of the reaction mixtures. Dose-dependent inhibition of Exo III by c) ATA and d) EDTA were examined, and IC50 values were obtained.

Next, we carried out an experiment to compare a conventional method (gel electrophoresis) with the present GO-based method. In a typical method, the digested ssDNA and hairpin DNA are resolved using a urea-polyacrylamide gel

electrophoresis (Urea-PAGE). Exo III concentration-dependent DNA digestion was observed in both experiments (Figure 5.4a). In our GO-based assay, addition of GO led to the quenching of nuclease activity and allowed the simple and rapid detection of changes in fluorescence intensities. In contrast, the conventional gel-based assay required two steps involving the quenching of enzymatic activities by adding EDTA and subsequently, running a gel to resolve the hairpin substrate and the digested ssDNA.

Finally, we demonstrated the feasibility of conducting parallel assays using our GO based platform by obtaining fluorescence images of multiple reaction mixtures. The samples were prepared by mixing the hairpin substrate solution with or without inhibitors and Exo III in a 96-well plate. As expected, the enzyme-treated samples without the addition of any inhibitor showed the lowest fluorescence, compared with the other samples (Figure 5.4b). Next, various concentrations of inhibitors were mixed with the hairpin DNA substrate followed by addition of Exo III stock solution. The fluorescence images obtained after addition of GO showed increasing fluorescence intensity as the concentration of inhibitors was raised. It was clear that our GO-based exonuclease activity assay method was compatible with parallel enzyme activity measurements, such as inhibitor screening, unlike the conventional gel-based assay.
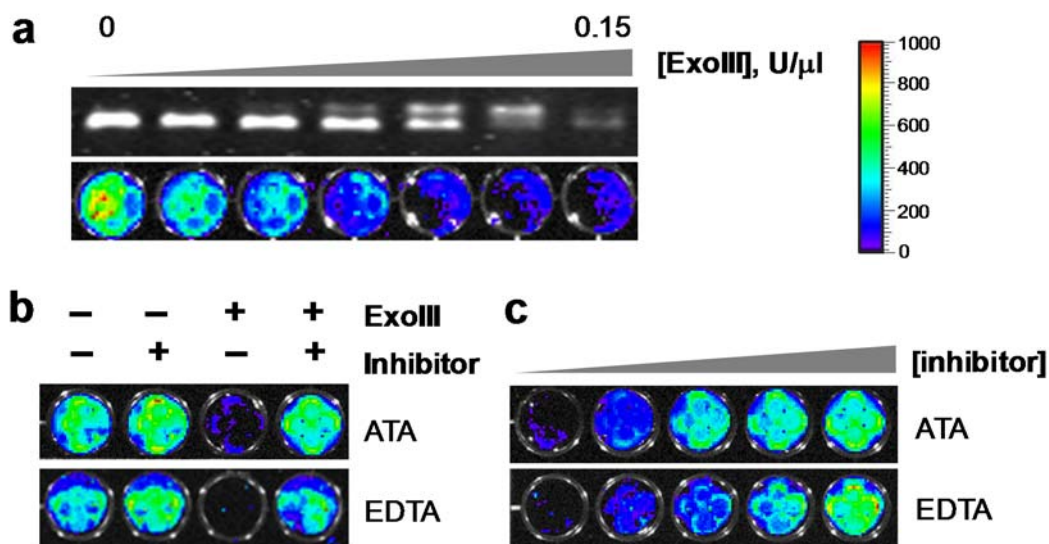
Figure 5.4 Fluorescence images for Exo III assay. a) Comparison between a conventional exonuclease assay method and the new method based on GO. Gel electrophoresis was performed as a conventional method to resolve DNAs according to the differences in length. Fluorometric assay based on GO showed the fluorescent images depending on the concentration of Exo III. b) Fluorescent images obtained from the inhibition assay of Exo III. Row 1: ATA inhibition, Row 2: EDTA inhibition of Exo III activity; c) Fluorescent images obtained from concentration-dependent inhibition assay. Row 1: ATA inhibition; Row 2: EDTA inhibition of Exo III activity.

5.3 Conclusion

In conclusion, we developed the new GO based assay for 3'→5' DNA exonuclease activity. This method utilized a DNA substrate with hairpin structure to prevent adsorption to GO before digestion. Degradation of the substrate by Exo III yielded ssDNA resulting in binding of ssDNA with GO and therefore, quenching of fluorescence. The present platform for exonuclease activity assay is more cost- and time-efficient compared to the conventional assay such as a gel based assay. In addition, this method is technically simple and compatible with parallel assay formats. Many samples can be prepared, and the quantitative analysis of their activity can be performed by simply obtaining a fluorescence image of the samples. Finally, this platform, based on GO, is versatile and can be applied to measure the activity of other classes of exonucleases by adjusting the structure of substrate DNA to corresponding enzymes. We expect that this assay platform will become an important assay tool in drug development and basic research related to exonucleases.

5.4 Material and Methods

Materials.   Arintricarboxylic acid (ATA) were purchased from Sigma-Aldrich (MO, USA). Fluorescent dye labelled hairpin DNAs for Exo III substrate (5' FAM— GGCCGAGC TTTTT GCTCGGCC – 3') was purchased from Genotech (Daejeon, Korea). Exonuclease III (Exo III) was purchased from New England BioLabs (MA, UK). Ethylenediamine tetraacetic acid (EDTA) was purchased from BIO-RAD (CA, USA). Fluorescence intensity was measured by fluorometer SynergyMx (Biotek, UK)

Exo III activity assay by GO based platform.   To prepare hairpin structured DNA substrate of Exo III, 2.5 µL of 100 µM fluorescent dye labeled DNA in pH 8.0 buffer containing 50 mM Tris-HCl and 50 mM NaCl was self-annealed by heating to 90oC for 5 min and followed by slow cooling at room temperature for 1 hr. For Exo III activity assay, reaction mixture was prepared by mixing Exo III enzyme stock with 200 nM annealed DNA in 1X Exo III reaction buffer (pH 7.0, 10 mM Bis-Tris Propane, 10 mM $MgCl_2$, and 1 mM dithiothreitol). After incubation at room temperature for designated time, 30 µL of reaction mixture and 30 µL of 11 µg/ml GO solution were mixed in a 96-well plate. Fluorescence intensity was measured at 520 nm.

Exo III inhibition assay by GO based plarform.   For EDTA-Exo III inhibition assay, EDTA solutions with various concentrations were mixed with 200 nM DNA in 1X Exo III reaction buffer followed by addition of 1 Unit of Exo III. After incubation at room temperature for 30min, each 30 μL of reaction mixtures were mixed with 30 μL of 11 μg/ml GO solutions in a 96-well plate. In case of ATA-Exo III, ATA solutions with various concentrations were mixed with 200 nM DNA in 1X Exo III reaction buffer and followed by addition of 1 Unit of Exo III. After incubation at room temperature for 1hr, each 30 μL of reaction mixtures were mixed with 30 μL of 11 μg/ml GO solutions in a 96-well plate. Fluorescence intensity was measured at 520 nm.

5.5 Reference

1. Fraser, M. J., 1994, *Bioessays*, **16**, 761-766.; Zuo, Y., Deutscher, M.. P., 2001, *Nucleic Acids Res.*, **29**, 1017-1026.

2. Joyce, C. M., Steitz, T. A., 1994, *Annu. Rev. Biochem.*, **63**, 777-822.; Khare, V., Eckert, K. A., 2002, *Mutat. Res.*, **510**, 45-54.

3. Shevelev,I. V., Hubscher, U., 2002, *Nat. Rev. Mol. Cell Biol.*, **3**, 364-376.

4. Yang, Y. G., Lindahl, T., Barnes, D. E., 2007, *Cell*, **131**, 873-886.

5. Crow, Y. J., Hayward,B. E., Parmar, R., Robins, P., Leitch, A., Ali, M.., Black, D. N., van Bokhoven, H., Brunner, H. G., Hamel, B. C., Corry, P. C., Cowan, F. M., Frints, S. G., Klepper, J., Livingston, J. H., Lynch, S. A., Massey, R. F., Meritet, J. F., Michaud, J. L., Ponsot, G., Voit, T., Lebon, P., Bonthron, D. T., Jackson, A. P., Barnes, D. E., Lindahl, T., 2006, *Nat. Genet.*, **38**, 917-920.

6. Richards, A., van den Maagdenberg, A. M., Jen, J. C., Kavanagh, D., Bertram, P., Spitzer, D., Liszewski, M. K., Barilla-Labarca, M. L., Terwindt, G. M., Kasai, Y., McLellan, M., Grand, M. G., Vanmolkot, K. R., de Vries, B., Wan, J., Kane, M. J., Mamsa, H., Schafer, R., Stam, A. H., Haan, J., de Jong, P. T., Storimans, C. W., van Schooneveld, M. J., Oosterhuis, J. A., Gschwendter, A., Dichgans, M., Kotschet, K. E., Hodgkinson, S., Hardy, T. A., Delatycki, M. B., Hajj-Ali, R. A., Kothari, P. H., Nelson, S. F., Frants, R. R., Baloh, R. W., Ferrari,M. D., Atkinson, J. P., 2007, *Nat. Genet.*, **39**, 1068-1070.

7. Kavanagh, D., Spitzer, D., Kothari, P. H., Shaikh, A., Liszewski, M. K., Richards, A., Atkinson, J. P., 2008, *Cell Cycle*, **7**, 1718-1725.

8. Lehtinen, D. A., Harvey, S., Mulcahy, M. J., Hollis, T., Perrino, F. W., 2008, *J. Biol. Chem.*, **283**, 31649-31656.

9. de Vries, B., Steup-Beekman, G. M., Haan, J., Bollen, E. L., Luyendijk, J., Frants, R. R., Terwindt, G. M., van Buchem, M. A., Huizinga, T. W., van den Maagdenberg, A. M., Ferrari, M. D. *Ann. Rheum. Dis.*, **69**, 1886-1887.

10. Nimonkar, A. V., Ozsoy, A. Z., Genschel, J., Modrich, P., Kowalczykowski, S. C., 2008, *Proc. Natl. Acad. Sci. U S A*, **105**, 16906-16911.

11. Lehtinen, D. A., Harvey, S., Mulcahy, M. J., Hollis, T., Perrino, F. W., 2008, *J. Biol. Chem.*, **283**, 31649-31656.

12. Ou, L. J., Jin, P. Y., Chu, X., Jiang,J. H., Yu,,R. Q., 2010, *Anal. Chem.*, **82**, 6015-6024.

13. Guhrs, K. H., Groth, M., Grosse, F., 2010, *Anal. Biochem.*, **405**, 11-18.

14. Leung, C. H., Chan, D. S., Man, B. Y., Wang, C. J., Lam, W., Cheng, Y. C., Fong, W. F., Hsiao, W. L., Ma, D. L., 2011, *Anal. Chem.*, **83**, 463-466.

15. Novoselov, K. S., Geim, A. K., Morozov, S. V., Jiang, D., Zhang, Y., Dubonos, S. V., Grigorieva, I. V., Firsov, A. A. *Science*, 2004, **306**, 666-669.

16. Lu, C. H., Yang, H. H., Zhu, C. L., Chen, X., Chen, G. N., 2009, *Angew. Chem. Int. Ed.*, **48**, 4785-4787.

17. Jang, H., Kim, Y. -K., Kwon, H. M., Yeo, W. -S., Kim, D. E., Min, D. -H., 2010, *Angew. Chem. Int. Ed.*, **49**, 5703-5707; Lee, J., Kim, Y. -K., Min, D. -H., 2010, *J. Am. Chem. Soc.*, **132**, 14714-14717; Zhang, M., Yin,B. C., Wang, X. F., Ye, B. C., 2010, *Chem. Commun. (Camb)*, **47**, 2399-2401; Gu,X., Yang, G., Zhang, G., Zhang, D., Zhu, D., 2011, *ACS Appl. Mater. Interfaces.*, **3**, 1175.

18. Swathi; R. S., Sebastian, K. L. *J Chem Phys*, 2008, **129**, 054703; Swathi, R. S., Sebastian, K. L., 2009, *J Chem Phys*, **130**, 086101.

19. Kuo, C. F., Mol, C. D., Thayer, M. M., Cunningham, R. P., Tainer, J. A., 1994, *Ann. N. Y. Acad. Sci.*, **726**, 223-234.

20. Cote, L. J., Kim, F., Huang, J., 2009, *J. Am. Chem. Soc.*, **131**, 1043-1049.

21. Hallick, R. B., Chelm, B. K., Gray, P. W., Orozco, E. M. Jr., 1977, *Nucleic Acids Res.*, **4**, 3055-3064; Mouratou, B., Rouyre, S., Pauillac, S., Guesdon, J. L. 2002, *Anal. Biochem.*, **309**, 40-47.

6. Robust and Quantitative Platform for Multiplexed Protein Kinase Inhibitor Screening

6.1 Introduction

Protein kinases are a family of enzymes that modifies proteins by transferring a phosphate group from ATP to serine, threonine or tyrosine residues in protein substrates.[1] These kinase are involved in many important biological processes including cell growth, differentiation and apoptosis.[2] Aberrations in protein kinase activity generally cause the development of severe diseases such as cancers, inflammations and diabetes. Therefore, evaluating the kinase activity and discovering its inhibitors are very important in the fields of clinical diagnosis and targeted therapy of related diseases.

Generally, there are two typical methods for measuring the activity of protein kinase, radiometric assay[3] using radioactive ATP with γ-^{32}P, and immunoassay[4] using phosphospecific antibody for specific recognition of transferred phosphate groups. Although these assay methods are utilized routinely for analyzing protein kinase activity in most laboratories, these methods require labor-intensive procedures, expensive reagents or instrumentations. Recently, various techniques based on fluorescence,[5] luminescence,[6] electrochemistry[7] or mass spectrometry [8] have been utilized to overcome the drawbacks of the traditional methods.

Nanomaterial based approaches, based on above techniques, have been actively developed for simple and multiplexed monitoring of protein kinase activities.[9]

Here, we report a robust protein kinase activity assay platform based on an affinity of phosphate group against TiO_2[10] and fluorescence super-quenching ability of graphene oxide (GO) by energy transfer.[11] Also, to demonstrate of the feasibility in drug discovery processes, the platform was utilized for protein kinase inhibitor screening. GO, a water soluble derivative of graphene, has been used in various bioapplications due to its unique mechanical, electronic, and optical properties as well as high biocompatibility.[12] Especially, it has come into spotlight in the field of bioanalytical application due to high affinity to various biomolecules and selective quenching phenomena of fluorescent molecules which was in close proximity with GO surface.[13] Various GO based analytical systems to detect various biomolecules such as DNA, protein and peptide have been reported since 2009.[14]

In this study, we employed the super-quenching ability of GO to simple and robust kinase activity assay. To supply the lack of difference of binding affinity on GO between substrate and phosphorylated substrate, new hybrid material based GO was required to run the phosphorylation specific adsorption and fluorescence quenching. Titanium dioxide (TiO_2) has been broadly used in metal oxide affinity chromatography (MOAC) in which phosphopeptide were bound selectively.[15] To combine the each property of GO and TiO_2, nano-sized TiO_2

particles was grown on the both side of GO sheets, resulting in TiO2 decorated GO sheet (TiO$_2$-GO). Upon the phosphorylation of dye labeled substrate peptide by protein kinase, the phosphorylated product can be adsorbed on TiO$_2$ GO and the fluorescence of dye conjugated on the peptide was quenched by nearest GO. Therefore, by measuring the change of fluorescence intensity, protein kinase activity can be analyzed simply and quantitatively. In this study, two protein kinase A (PKA) and extracellular signal regulated kinase 2 (ERK2) were used as representatives of protein kinase family (Scheme 6.1).
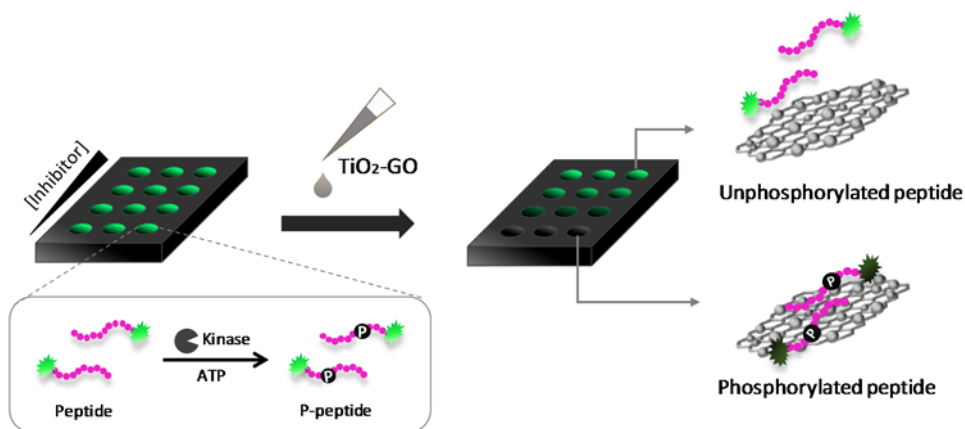
Scheme 6.1 A strategy for protein kinase activity assay using TiO$_2$ decorated GO.

6.2 Result

First, we achieved TiO$_2$-GO hybrid structure by growth of Ti(BuO)$_4$ nanoparticles on GO sheets. GO prepared by modified Hummers method[16] provided functional groups for anchoring sites for nucleation and growth of TiO$_2$. By slowing down the rate of hydrolysis, the growth of TiO$_2$ can be facilitated selectively on GO surface without formation of free TiO$_2$ in solution. [17] The growth of TiO$_2$ on GO was confirmed by atomic force microscopy (AFM) and the height profile showed that size of TiO$_2$ particle was below 9 nm (Figure 6.1a). Next, the Raman spectrum showed peaks at 1352 and 1601 cm^{-1}, which correspond respectively to the D band and G band of GO (Figure 6.1b). We further characterized the TiO$_2$-GO using transmission electron microscope (TEM) and scanning transmission electron microscope (STEM), of which images confirmed TiO$_2$ particles on GO (Figure 6.1c,d). Collectively, we confirmed that TiO2 uniformly coated GO was successfully prepared.
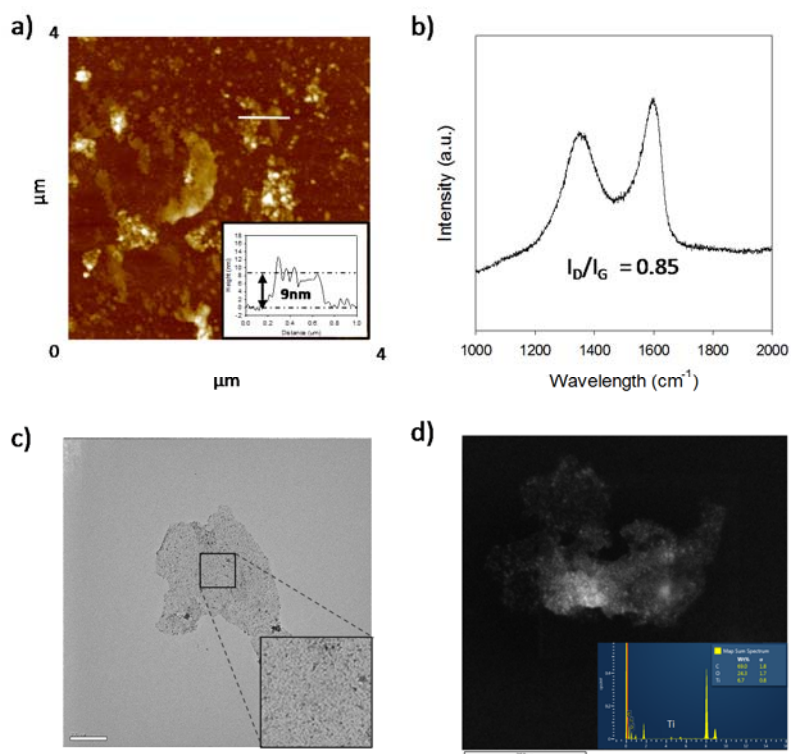
Figure 6.1 Characterization of TiO$_2$-GO. a) AFM image and height profile of TiO$_2$-GO. b) Raman spectrum of TiO$_2$-GO with identified peaks with GO. c) TEM and d) STEM images and EDS spectrum of TiO$_2$-GO.

The present strategy started with preparation of hydroxycoumarin labeled PKA substrate peptide (peptide 1: hydroxycoumarin-Leu-Arg-Arg-Ala-Ser-Leu-Gly) and TAMRA labeled ERK2 substrate peptide (peptide 2: TAMRA-Gly-Gly-Ala-Pro-Arg-Thr-Pro-Gly-Gly-Arg-Arg) by solid phase synthesis method.[18] Both of peptide 1 and 2 were successfully phosphorylated by PKA and ERK2 in Tris-HCl buffer solution (pH 7.4) containing MgCl2, and ATP, which were confirmed by MALDI-TOF analysis (Figure 6.2a,b).
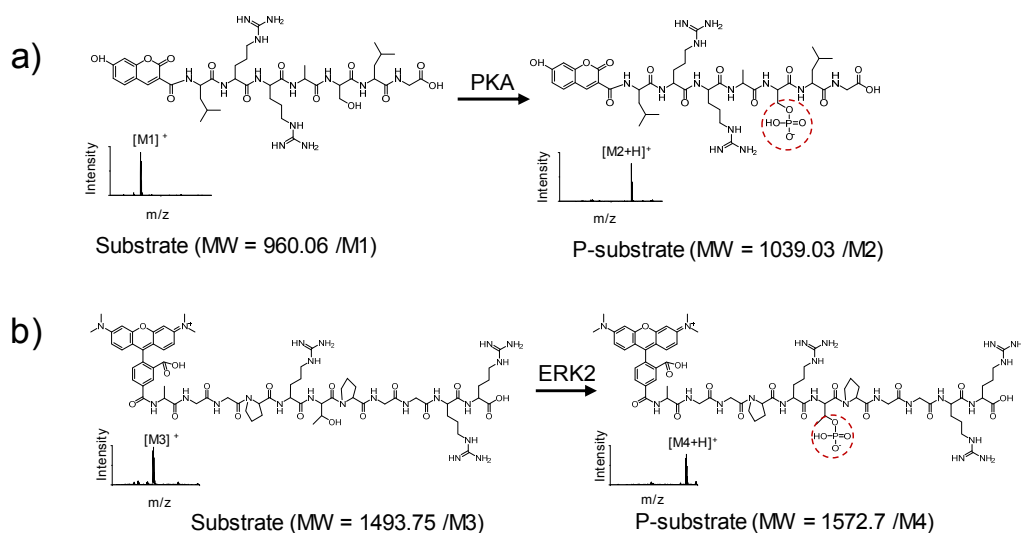
Figure 6.2 Chemical structures of a) 7-hydroxycoumarin conjugated PKA substrate peptide before and after PKA reaction, b) TAMRA conjugated ERK2 substrate peptide before and after ERK2 reaction. The each mass spectrum represented the successful phosphorylation of substrate peptide by PKA.

Then, we investigated the adsorption of phosphorylated peptide on TiO_2-GO, followed by selective fluorescence quenching of dye conjugated to the product. To complement the specificity of phosphorylated peptide for selective adsorption on TiO_2-GO, we utilized trifluoroacetic acid (TFA) and acetonitrile (ACN), which were known as interrupting the nonspecific adsorption of nonphosphorylated peptide on MOAC.[15] As a result, the combination of TFA and ACN showed the best discrimination between substrate and phosphorylated peptide (Figure 6.3).
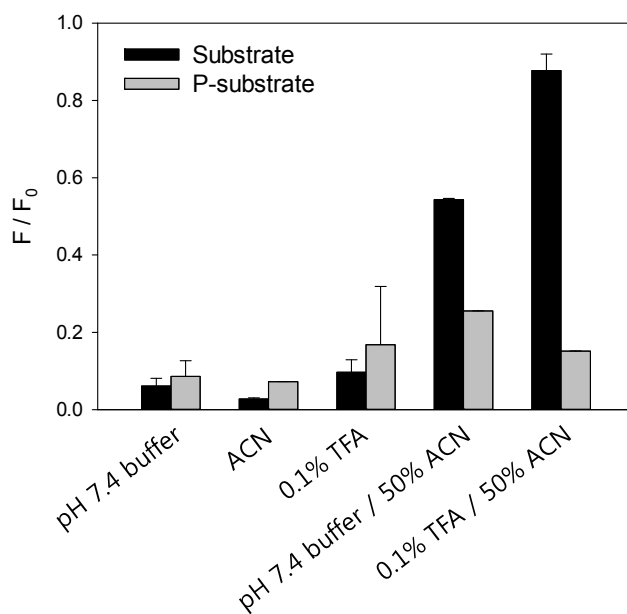
Figure 6.3 Optimal condition for perfect discrimination between substrate and product. Relative fluorescence intensity of dye conjugated peptides in various combination of solvent. The maximum intensities were measured at ex 390 / em 450 nm except for 0.1% TFA and TFA/ACN. In case of TFA containing solvent, the maximum signal was measured at ex 360 /em 450 nm (F_0 : fluorescence of peptide with TiO_2-GO 0 µg, F : florescence of peptides with TiO_2-GO 0.5 µg).

Upon mixing reaction mixture containing 20 pmol of each peptide with 0.5 μg of TiO$_2$-GO in 0.1 % TFA / 50% ACN, phosphorylate peptides immediately showed remarkable fluorescence decrease, whereas the substrate peptide maintained the strong fluorescence signal (Figure 6.4a,b).

We then performed time-dependent and kinase concentration dependent phosphorylation using PKA and peptide 1. Reaction mixtures were prepared by adding various concentration of PKA to substrate peptide solution containing 20 pmol of peptide and 200 pmol of ATP as phosphate group donor. Then, 2 μL of the PKA reaction mixture was removed at 10 min intervals and mixed immediately with 100 μL of 5 μg/mL TiO$_2$-GO in 0.1 % TFA/50% ACN in a 96-well plate. The fluorescence intensity was collected for each well using a fluorometer. As a result, the fluorescence signal was decreased according to reaction time and PKA concentration. It indicated that the phosphorylation ratio was increased depending on reaction time and enzyme concentration (Figure 6.4c,d).

Next, we carried out inhibition assays using two kinases and each corresponding inhibitors to confirm that the present method was quantitative and applicable to the evaluation of inhibitors. H-89[19] and 5-iodotubercidin[20] were well known as PKA and ERK2 inhibitors, respectively. For PKA inhibition, various concentrations of H-89 were incubated with PKA reaction mixture containing 20 U/ml PKA and incubated at room temperature for 30 min. Fluorescence spectra

were obtained after mixing reaction mixtures with TiO_2-GO in TFA/ACN. Dose-dependent inhibition curves were plotted based on fluorescence intensities and the IC50 value was estimated to be 1.5 µM (Figure 6.4e). Similarly, 1 uM ERK2 with 5-iodotubercidin also showed dose-dependent inhibition curve and 0.94 µM as IC50 value (Figure 6.4f).
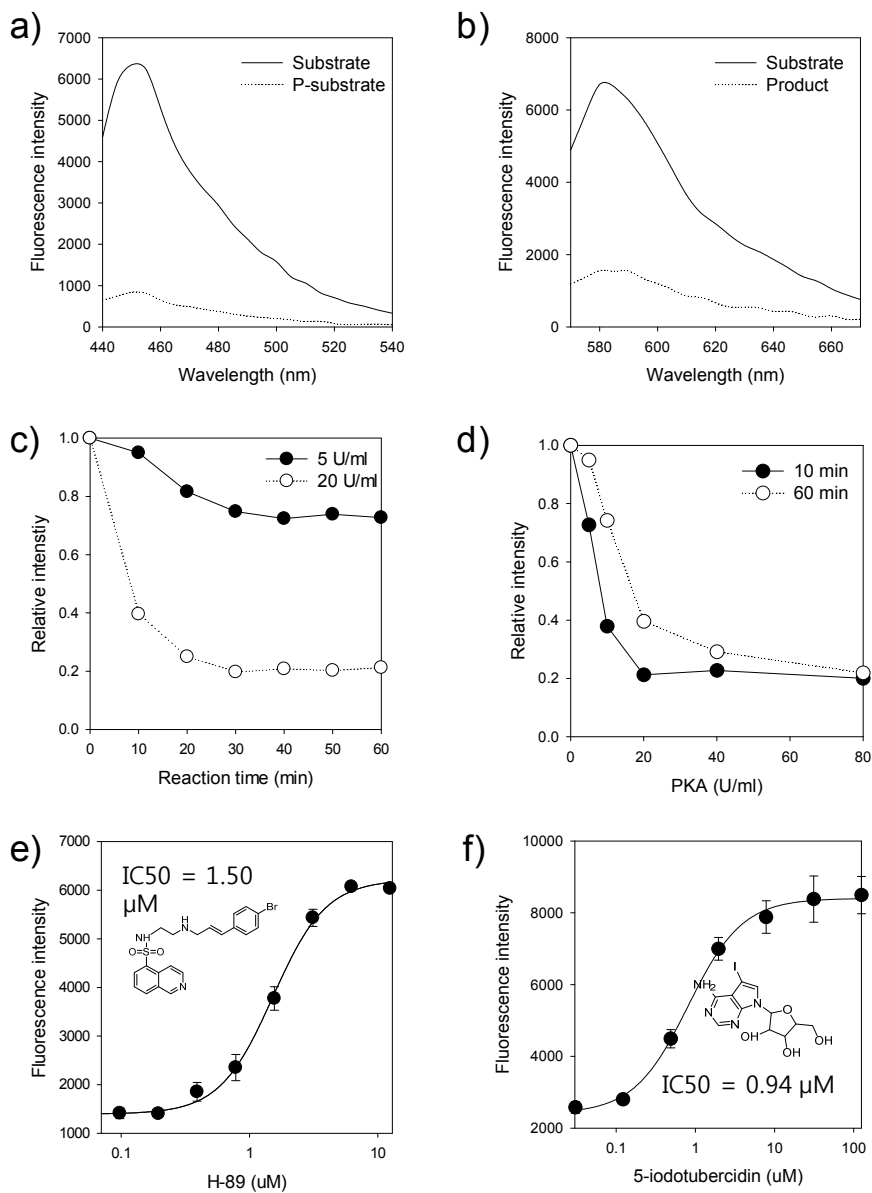
Figure 6.4   Protein kinase activity assay using TiO_2-GO. Selective fluorescence quenching of corresponding dye conjugated to phosphorylated peptide by a) PKA and b) ERK2. c) Time-dependent and d) kinase concentration dependent fluorescence analysis for phosphorylation of substrate peptide by PKA. e) PKA inhibition curve and IC50 using H-89. f) ERK2 inhibition curve and IC50 using 5-iodotubercidin.

To investigate capability of multiplexed kinase assay in a mixed solution, we conducted phosphorylation reaction of peptide 1 and 2 in the presence of both PKA and ERK2 in a solution, followed by mixing with TiO_2-GO in TFA/ACN. We first optimized TiO_2-GO concentration for multi-peptide analysis using phosphorylated or nonphosphorylated peptides mixture. 15 μg/mL TiO_2-GO was required for quenching of both phosphorylated peptides, and additional 0.0025% BSA was utilized to recover the selectivity under the high concentration of TiO_2-GO (Figure 6.5).

a) Coumarin-PKA substrate
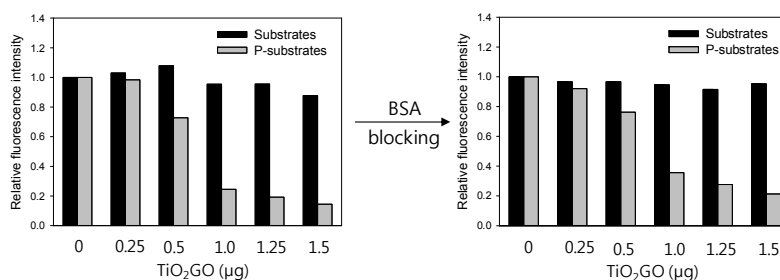
b) TAMRA-ERK2 substrate

Figure 6.5 Enhancement of discrimination between substrate and product in multiplex assay. Relative fluorescence intensity of a) Coumarin-PKA substrate and b) TAMRA-ERK2 substrate with various concentration of TiO_2-GO and/or BSA in TFA/ACN. BSA was a great help to prevent adsorption of substrate peptide in the presence of high concentration of TiO_2-GO.

108

On the basis of the results, kinase specific phosphorylation was examined by mixing each kinase or combination of kinases with peptide solution containing substrate 1 and peptide 2 and ATP. The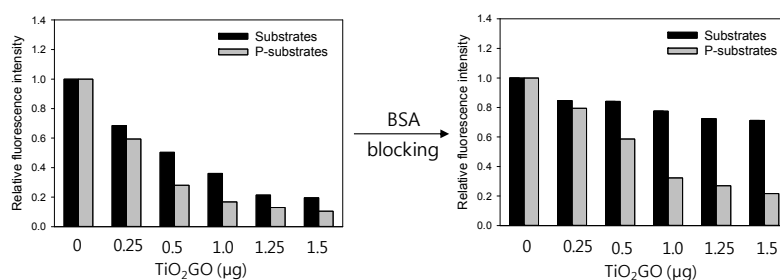 reaction mixtures were added to newly optimized TiO$_2$-GO in TFA/ACN, followed by measuring the fluorescence signal. As expected, each emission of coumarin (blue, ex 360 / em 450 nm) and TAMRA (yellow, ex 550 / em 585nm) were decreased only in the sample containing each corresponding target kinase (Figure 6.6a). Furthermore, we carried out each inhibitor specific nonphosphorylation test using H-89 and 5-iodotubercidin, as PKA inhibition and ERK2 inhibitor, respectively (Figure 6.6b). Reaction mixture was prepared by pre-incubation of inhibitors with kinases, followed by adding to peptides solution containing peptide1, peptide2 and ATP. After incubation for 1hr, the reaction mixtures were added to TiO$_2$-GO in TFA/ACN, followed by measuring the fluorescence intensity. As a result, blue and yellow emission were obtained only in the sample containing each corresponding inhibitor. These results are in good accordance with MS based analysis of peptides (Figure 6.6c,d). It appears that the present protein kinase activity assay platform can be applicable for high throuput multiplex assay.

a)

PKA	X	O	X	O
ERK2	X	X	O	O

■ Coumarin-PKA substrate
□ TAMRA-ERK2 substrate

b)

PKA/ERK2	X	O	O	O	O
Inhibitor 1	X	X	O	X	O
Inhibitor 2	X	X	X	O	O

c)

[M1+H] [M2+H] [M3+H] [M4+H]

Negative control

ERK2

PKA

ERK2, PKA

M1 : hydroxycoumarin-PKA substrate
M2 : phosphorylated 7-coumarin-PKA substrate
M3 : TAMRA-ERK2 substrate
M4 : phosphorylated TAMRA-ERK2 substrate

d)

[M1+H] [M2+H] [M3+H] [M4+H]

Negative control

Positive control

Inhibitor 1

Inhibitor 2

Inhibitor 1+2

Figure 6.6 Multiplex inhibition assay of PKA and ERK2 in a homogeneous solution using TiO_2-GO based fluorescence analysis. a) Peptide sequence specific phosphorylation: Relative fluorescence intensity ($F_{Substrate} = 1$) of two kinase substrate mixture with kinases. b) Inhibitor specific unphosphorylation : Relative fluorescence intensity ($F_{Substrate} = 1$) kinase reaction mixtures with each specific inhibitor. Inhibitor 1 : H-89/ PKA inhibitor, Inhibitor 2 : 5-iodotubercidin/ERK2 inhibitor. MALDI-TOF mass spectra of two kinds of peptides in a solution for c) phosphorylation with corresponding protein kinase, d) inhibition of phosphorylation by specific inhibitors in the presence of both PKA and ERK2.

110

Finally, to demonstrate the practical utility of this platform, we performed multiplexed, high-throughput screen for protein kinase inhibitors. Before the full scale study of screening of protein kinase inhibitor using the present platform, simple statistic parameter called "Z'-factor" was calculated to access the quality of the screening assay (Figure 6.7).[21] Generally, when Z' factor reaches 0.75 or higher, the corresponding system can be judged to be high performance assay.[22] To obtain the Z'-factor, we analyzed 20 positive and 20 negative control reactions using the present platform, followed by calculation of the each mean (σ) and each standard deviation (STD, μ). The Z'-factor obtained by using the equation (Z' factor = $1 - (3\sigma_{c+} + 3\sigma_{c-}) / |\mu_{c+} - \mu_{c-}|$) was 0.90 for PKA and 0.84 for ERK2, suggesting that the present platform was suitable for high throughput screening assay.
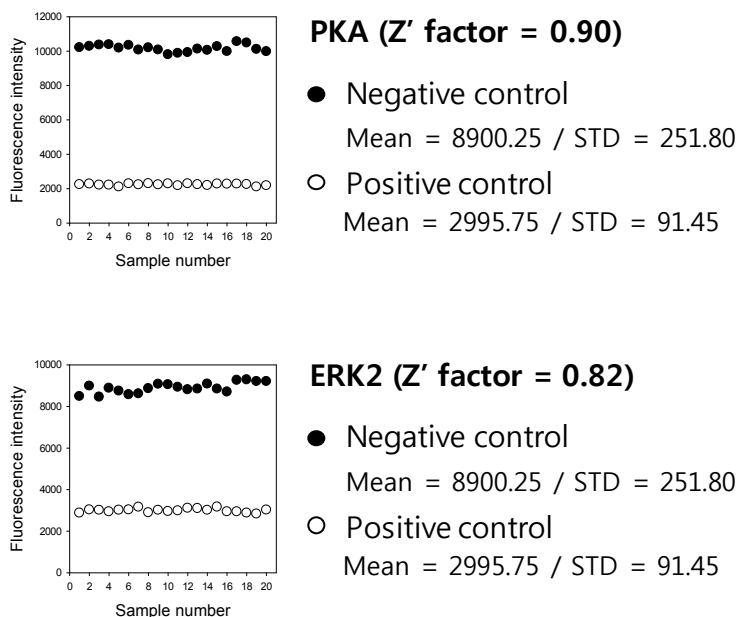
Figure 6.7 The Z'-factor was calculated for TiO_2-GO based platform from each control assay (20 samples). STD=standard deviation.

Then, we screened a library of structurally diverse and medicinally active 707 compounds for discovery of protein kinase inhibitor. Each bioactive compound was mixed with protein kinase cocktail composed of PKA and ERK2 in 96 well plates. After that, peptides and ATP solution were added to the mixture for beginning the kinase reaction. Positive and negative control reactions was run with every 88 compound screening. After 1hr of reactions, the mixtures was

112

added to TiO_2-GO in TFA/ACN, which induced the fluorescence quenching of dye of phosphorylated peptides without kinase inhibition, selectively.

Among the compounds of the library, 2 compounds (PIK-75 Hydrochloride, AT7867) showed strong blue emission over 50% of negative control and other 2 compounds (PHA-793887, Fisetin) showed strong yellow emission over 50% of negative control (Figure 6.8a, for the clear contrast of color, yellow emission was visualized as red in the 1st screening). The inhibition of phosphorylation by the 4 selected compounds was quantitatively analyzed by secondary inhibition assay (n=3) (Figure 6.8b), and the inhibition was confirmed by measuring molecular weight of peptides in reaction mixtures using MS based system (Figure 6.8c). Through the screening of compound library using the present platform, we identified PIK-75 Hydrochloride and PHA-793887, widely known inhibitors of PI3 kinase[23] and cyclin-dependent kinase,[24] as a potent PKA and ERK2 inhibitor, respectively. Also, the corresponding kinase inhibition by AT7867[25] and fisetin[26] agreed with previous studies.
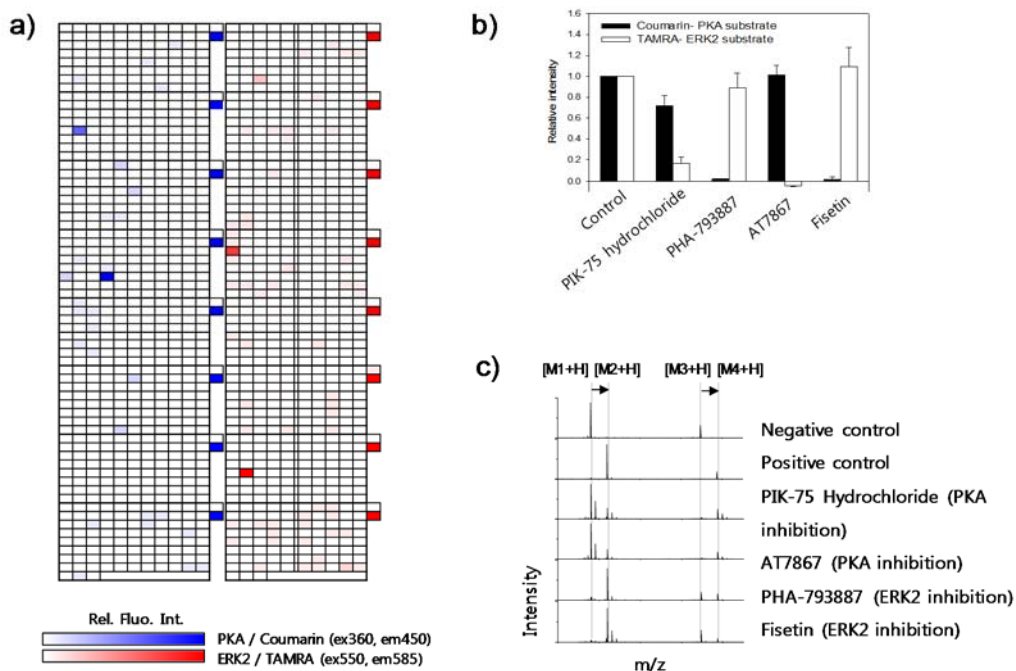
Figure 6.8   Multiplex protein kinase (PKA and ERK2) inhibitor screening using a set of bio-active molecules. a) At first, 703 compounds were screened for PKA and ERK2 in a homogeneous solution using TiO_2-GO based fluorescence analysis. b) Next, the selected molecules (relative fluorescence intensity > 0.5) were screened again using TiO_2-GO based fluorescence analysis and MALDI-TOF based analysis. d) MALDI-TOF mass spectra for inhibition of phosphorylation of each peptides by selected compounds from multiplexed screening assay.

We further characterized the discovered inhibitors by using the present platform to evaluate their quantitative inhibitory effect toward the respective protein kinase. PKA with PIK-75 hydrochloride or AT7867 showed dose dependent inhibition curve and 4.5 μM and 2.3 μM as IC50 value, respectively (Figure 6.9a,b). Similarly, ERK2 with PHA-793887 or Fisetin showed dose

114

dependent inhibition curve and 10 µM and 8.9 µM as IC50 value, respectively (Figure 6.9c,d). Consequently, we could screen a set of bioactive small molecules using multiplex assay method and successfully discover the specific inhibitors of each kinase.
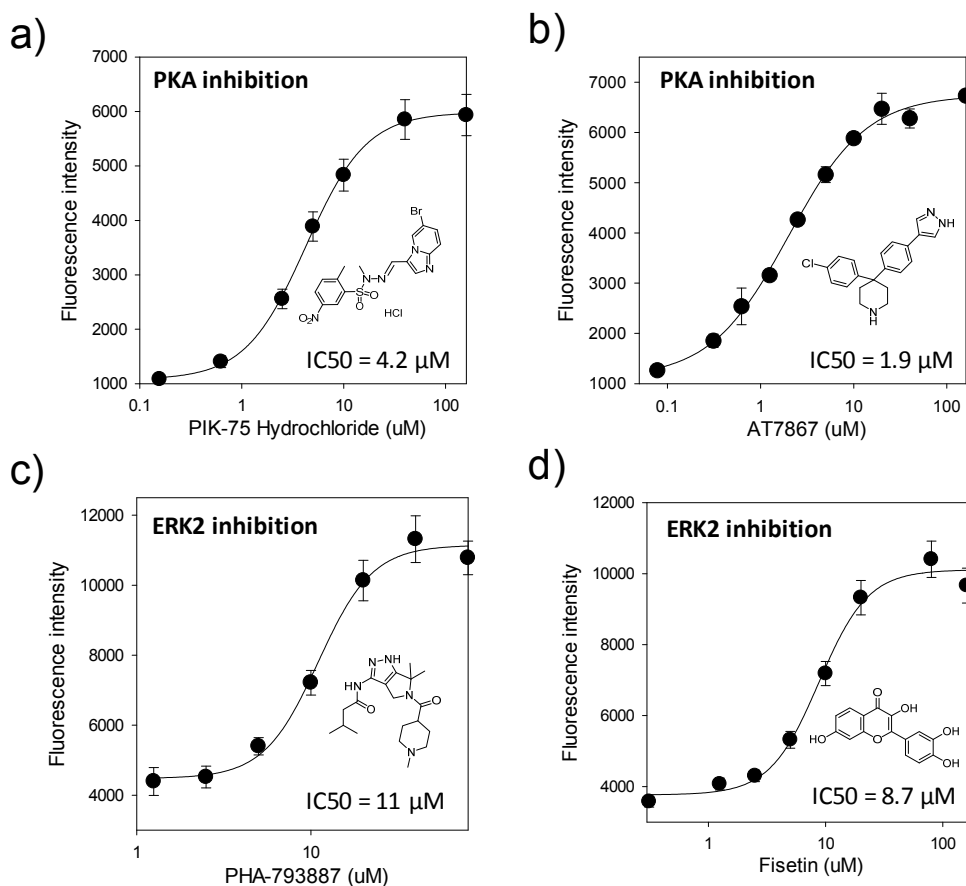

Figure 6.9 Protein kinase inhibition assay using 4 compounds discovered from three screens. PKA inhibition curve and IC50 using a) PIK-75 hydrochloride and b) AT7867. ERK2 inhibition curve and IC50 using c) PHA-793887 and d) Fisetin.

6.3 Conclusion

In conclusion, we developed a robust and quantitative protein kinase activity assay platform using TiO$_2$-GO hybrid nanomaterial and applied to screen the hundreds of small molecules for target specific inhibitor discovery. The analysis of protein kinase activity was performed by two steps, 1) protein kinase reaction with dye labelled substrate peptide in a reaction buffer, 2) selective fluorescence quenching of phosphorylated peptide by TiO$_2$-GO in TFA/ACN. Each TiO$_2$ and GO plays important roles, adsorbing phosphorylated peptide and quenching the fluorescence of dye conjugated to peptide, respectively. The sequential event can occur in a few seconds that allows robust and time-efficient analysis of protein kinase activity. In addition, the hybrid nanomaterial makes the present method more inexpensive because unlike typical assays, expensive reagents such as isotopes and fluorescent antibodies are not required. Furthermore, the combination of acidic condition (TFA), organic solvent (ACN) and BSA showed a synergetic effect for preventing the nonspecific adsorption of non-phosphorylated peptide on TiO$_2$-GO, resulting in high sensitivity and selectivity. This method is technically straightforward and compatible with multiplexd assay formats. The utility of the present platform has been demonstrated by discovering the inhibitors through multiplexed inhibitor screening for two protein kinase using hundreds of bioactive compounds. Finally, this platform, based on TiO$_2$-GO, is versatile and can be applied to other protein kinase assays regardless of a

sequence of peptide substrate because the selective fluorescence quenching only depends on an additional phosphate group transferred by protein kinase. We believe that this new TiO$_2$-GO based fluorescent platform for protein kinase activity assay will become an important assay tool in the field of protein kinase related basic research and drug development.

6.4 Material and Methods

Materials.   Sulfuric acid (H_2SO_4) was purchased from Samchun chemical (Seoul, Korea). Titanium(IV) butoxide ($Ti(BuO)_4$) was purchased from Sigma-Aldrich (MO, USA). 7-Hydroxycoumarin-3-carboxylic acid was purchased from Anaspec (California, USA). 5-(and-6)-Carboxytetramethylrhodamine was purchased from Invitrogen (Massachusetts, USA).

Preparation of TiO$_2$ decorated GO.   3ml of 1 mg/ml of GO was dissolved in 150 ml EtOH and the suspension was heated to 80 °C with stirring. 28 μL of $Ti(BuO)_4$ and 16 μL of H_2SO_4 was prepared in 4 mL of EtOH, which was injected in the mixture. The final solution was stirred at 80 °C for 12 h. Then, the reaction mixture was cooled down and the TiO_2-GO was collected by centrifugation, followed by washing with EtOH and water.

Protein kinase A assay using TiO$_2$-GO.   For phosphorylation by kinase, 20 pmol of dye conjugated substrate peptide and 200 pmol of ATP was mixed with corresponding kinase in Tris-HCl buffer (pH 7.4 buffer containing 40 mM Tris and 20 mM $MgCl_2$). After incubation at 30 ℃, 0.5 μg of TiO_2-GO pre-dispersed in 50% ACN and 0.1% TFA was added to the reaction mixture. Fluorescence intensity was measured at 450 nm.

118

Multiplex Protein kinase inhibition assay.   For multiplex inhibition assay using H-89 and 5-iodotubercidin, each 40 μM of inhibitors was prepared in kinase mixture containing 20 U/ml of PKA and 1 μM of ERK2. Then, each 20 pmol of coumarin-PKA substrate and TAMRA-ERK2 substrate was mixed with 400 pmol of ATP in Tris-HCl buffer (pH 7.4 buffer containing 40 mM Tris and 20 mM $MgCl_2$), which was added to kinase/inhibitor mixture. After incubation at 30 ℃, for 1 hr, 1.5 μg of TiO_2-GO pre-dispersed in 50% ACN and 0.1% TFA was added to the reaction mixture. Fluorescence intensity was measured at ex360/em450 nm and ex550 nm/em585nm for coumarin and TAMRA, respectively.

6.5 Reference

1. a) Noble, M. E. M., Endicott, J. A., Johnson, L. N., 2004, *Science* **303**, 1800-1805; b) B. Nolen, S. Taylor, G. Ghosh, 2004, *Mol. Cell* **15**, 661-675.

2. a) Derubertis, F. R., Craven, P. A., 1994, Diabetes **43**, 1-8; b) Kyriakis, J. M., Avruch, J., 2001, *Physiol. Rev.* **81**, 807-869; c) Griner, E. M., Kazanietz, M. G., 2007, *Nat. Rev. Cancer* **7**, 281-294; d) Gaestel, M., Kotlyarov, A., Kracht, M., 2009, N*at. Rev. Drug Discov.* **8**, 480-499.

3. Hutti, J. E., Jarrell, E. T., Chang, J. D., Abbott, D. W., Storz, P., Toker, A., Cantley, L. C., Turk, B. E., 2004, *Nat. methods* **1**, 27-29.

4. a) Gast, R., Glokler, J., Hoxter, M., Kiess, M., Frank, R., Tegge, W., 1999, *Anal. Biochem.* **276**, 227-241; b) Inagaki, N., Tsujimura, K., Tanaka, J., Sekimata, M., Kamei, Y., Inagaki, M., 1996, *Neurochem. Res.* **21**, 795-800.

5. Li, Y. J., Xie, W. H., Fang, G. J., 2008, *Anal. Bioanal. Chem.* **390**, 2049-2057.

6. Kasari, M., Padrik, P., Vaasa, A., Saar, K., Leppik, K., Soplepmann, J., Uri, A., 2012, *Anal. Biochem.* **422**, 79-88.

7. Wang, C. L., Wei, L. Y., Yuan, C. J., Hwang, K. C., 2012, *Anal. Chem.* **84**, 971-977.

8. Min, D.-H., Su, J., Mrksich, M., 2004, *Angew. Chem. Int. ed.* **43**, 5973-5977.

9. a) Ghadiali, J. E., Cohen, B. E., Stevens, M. M., 2010, *ACS Nano* **4**, 4915-4919; b) Bai, J., Zhao, Y. J., Wang, Z. B., Liu, C. H., Wang, Y. C., Li, Z. P., 2013, *Anal. Chem.* **85**, 4813-4821; c) Zhou, J., Xu, X., Liu, W., Liu, X., Nie, Z., Qing, M., Nie, L., Yao, S., 2013, *Anal. Chem.* **85**, 5746-5754; d) Zhou, J., Xu, X., Liu, X., Li, H., Nie, Z., Qing, M., Huang, Y., Yao, S., 2014, *Biosens. Bioelectorn.* **53**, 295-300.

10. a) Ji, J., Yang, H., Liu, Y., Chen, H., Kong, J. L., Liu, B. H., 2009, *Chem. Commun.* 1508-1510; b) Leitner, A., Sturm, M., Lindner, W., 2011, *Anal. Chim. Acta* **703**, 19-30.

11. a) Swathi, R. S., Sebastian, K. L., 2008, *J. Chem. Phys*. 129, 054703; b) Swathi, R. S., Sebastian, K. L., 2009, *J. Chem. Phys*. **129**, 086101.

12. a) Allen, M. J., Tung, V. C., Kaner, R. B., 2010, *Chem. Rev*. **110**, 132–145; b) Loh, K. P., Bao, Q., Eda, G., Chhowalla, M., 2010, *Nat. Chem*. **2**, 1015-1024

13. He, S., Song, B., Li, D., Zhu, C., Qi, W., Wen, Y., Wang, L., Song, S., Fang, H., Fan, C., 2010, *Adv. Func. Mat*. **20**, 453-459.

14. a) Lu, C. H., Yang, H. H., Zhu, C. L., Chen, X., Chen, G. N., 2009, *Angew. Chem. Int. ed*. **48**, 4785-4787; b) Jang, H., Kim, Y.-K., Kwon, H.-M., Yeo, W.-S., Kim, D.-E., Min, D.-H., 2010, *Angew. Chem. Int. ed*. **49**, 5703-5707; c) Lee, J., Kim, Y.-K., Min, D.-H., 2010, *J. Am. Chem. Soc*. **132**, 14714-14717; d) Lee, J., Kim, Y.-K., Min, D.-H., 2011, *Anal. Chem*. **83**, 8906-8912; e) Lee, J., Park, I.-S., Jung, E., Lee, Y., Min, D.-H., 2014, *Biosens. Bioelectron*. **62**, 140-144.

15. Fila, J., Honys, D., 2012, *Amino Acids*, **43**, 1025-1047.

16. Luo, J., Cote, L. J., Tung, V. C., Tan, A. T., Goins, P. E., Wu, J., Huang, J., 2010, *J. Am. Chem. Soc*. **132**, 17667-17669.

17. Liang, Y., Wang, H., Casalongue, H. S., Chen, Z., Dai, H., 2010, *Nano Res*. **3**, 701-705.

18. Coin, I., Beyermann, M., Bienert, M., 2007, *Nat. Protoc*. **2**, 3247-3256.

19. Chijiwa, T., Mishima, A., Hagiwara, M., Sano, M., Hayashi, K., Inoue, T., Naito, K., Toshioka, T., Hidaka, H., 1990, *J. Biol. Chem*. **265**, 5267-5272.

20. Fox, T., Coll, J. T., Xie, X., Ford, P. J., Germann, U. A., Porter, M. D., Pazhanisamy, S., Fleming, M. A., Galullo, V., Su, M. S., Wilson, K. P., 1998, *Protein Sci*. **7**, 2249-2255.

21. Zhang, J.-H., Chung, T. D. Y., Oldenburg, K. R., 1999, J. Biomol. *Screening* 4, 67.

22. Min, D.-H., Tang, W.-J., Mrksich, M., 2004, *Nat. Biotechnol*. **22**, 717.

23. Knight, Z. A., Gonzalez, B., Feldman, M. E., Zunder, E. R., Goldenberg, D. D., Williams, O., Loewith, R., Stokoe, D., Balla, A., Toth, B., Balla, T., Weiss, W. A., Williams, R. L., Shokat, K. M., 2006, *Cell* **125**, 733-747.

24. Alzani, R., Pedrini, O., Albanese, C., Ceruti, R., Casolaro, A., Patton, V., Colotta, F., Rambaldi, A., Introna, M., Pesenti, E., Ciomei, M., Golay, J., 2010, *Exp. Hematol*. **38**, 259-269.

25. Grimshaw, K. M., Hunter, L. J. K., Yap, T. A., Heaton, S. P., Walton, M. I., Woodhead, S. J., Fazal, L., Reule, M., Davies, T. G., Seavers, L. C., Lock, V., Lyons, J. F., Thompson, N. T., Workman, P., Garrett, M. D., 2010, *Mol. Cancer Ther*. **9**, 1100-1110.

26. Pal, H. C., Sharma, S., Strickland, L. R., Katiyar, S. K., Ballestas, M. E., Athar, M., Elmets, C. A., Afaq, F., 2014, *Plos One* **9**, e86338.

7. Conclusion

In summary, we have demonstrated five different fluorescent sensing systems based on GO for quantitative analysis of biomolecules that were considered as important biological targets in the field of clinical diagnosis and drug discovery. These platforms commonly utilized GO as a super-quencher that was capable of fluorescence quenching across the entire visible spectrum and they were classified into two categories according to each purpose : 1) nucleic acid detection, 2) enzyme activity assay.

First, the nucleic acid detection systems employed artificial PNA probe instead of typical DNA probe in GO based sensor for improved performance, which were impossible to achieve by using conventional DNA probe. Combination of PNA probe and GO enabled double stranded DNA detection without denaturing step and highly effective single mismatch discrimination. Also, by applying BSA in the PNA/GO based system, the detection sensitivity was remarkably improved. Secondly, the enzymatic assay platforms were designed on the basis of the selective fluorescence quenching of dye conjugated to product by GO in a short time and aimed at high throughput fluorometric analysis of target enzymes. These assay platforms aren't restricted by sequence or overall charge of substrate, thus they can be applied to measure the activity of other classes of each enzymes.

These GO based sensor systems are cost/time-effective and technically straightforward. These sensors were designed based on understanding at a molecular level how it works, resulting in noticeable improvement of the sensing performance compared to conventional systems. We believe that the present platforms will become an important assay tool in the field of personalized diagnostics, drug discovery and individual biomolecules related basic research.

Summary in Korean (국문요약)

산화그래핀을 이용한 형광 기반 생분자 분석 플랫폼의 개발

단백질이나 핵산, 지질 등 인체 내 존재하는 생분자들 중 일부는 외부 환경으로부터의 자극 또는 체내 변화에 민감하게 변화하며 이러한 특정 생분자 (생체지표)를 분석하는 것은 특정 질병의 진단뿐만 아니라 치료를 목적으로 하는 신약 개발 분야에서 중요하게 사용되는 수단 중 하나이다. 일반적으로 전기영동, 면역분석법, 항체기반 분석법 등을 이용하여 생분자를 분석하는 방법이 사용되어왔으나 이러한 시스템들은 최근 요구되는 목적에 부합하는 높은 레벨의 분석 사양보다 비교적 낮은 민감도와 정확도를 보이는 경우가 많다. 또한 노동 집약적인 실행이 요구되며, 비효율적인 시간 및 비용의 소모가 있어 대량의 샘플에 대한 분석에 적합하지 않다. 최근 다양한 접근을 통해 기존의 시스템을 대체하면서 보다 높은 성능을 갖는 시스템 개발하기 위한 연구가 진행되고 있으며 특히 그 중 금, 실리카, 탄소등으로 이루어진 나노 크기의 입자를 이용한 시스템의 개발이 활발하게 진행되고 있다. 이러한 나노입자들은 작은 사이즈에 비하여 큰 표면적을 가지고 있으며 이로 인해 같은 원소로 이루어진 큰 사이즈의 물질과는 다른 고유의 특성을 지니게 되므로 이를 이용하여 형광, 전기화학, 분자량분석 또는 표면라만증강에 기반한 다양한 바이오센서 개발이 가능하다. 이들은 기존 분석 시스템에 비하여 간단하고 빠른 검출이 가능하며 보다 높은 검출 성능을 보여주고 있다.

본 연구에서는 생체지표가 되는 다양한 생분자의 정량적 분석을 위하여 산화그래핀을 이용한 새로운 형광기반의 센서를 개발하였다. 산화그래핀은 이차원

탄소구조체인 그래핀에 산화과정을 통해 친수성 작용기를 도입시킨 유도체로 그래핀 자체의 물리적, 광학적 고유특성을 일정 수준으로 유지함과 동시에 수용액에서 잘 분산되기 때문에 나노-바이오분야에서 주목을 받고 있는 나노물질 중 하나이다. 본 연구에서 개발된 플랫폼들은 산화그래핀의 다양한 특성 중 약 20 nm 내에 존재하는 형광염료의 형광신호를 소광시키는 성질에 기반하였으며 형광염료가 부착된 프로브 혹은 효소의 기질을 이용하여 디자인되었다. 이들은 목적에 따라 감염 및 질병의 진단 타겟이 될 수 있는 이중나선 DNA, 단일가닥 DNA 또는 RNA, 유전자의 개체간 단일염기변이의 검출을 위한 핵산분석 시스템과 신약개발의 타겟이 되는 DNA 엑소뉴클레아제와 단백질 키나아제의 분석을 위한 효소활성분석 시스템으로 크게 나누어 볼 수 있다. 공통적으로 기존 분석 시스템들이 가지고 있는 단점을 극복함과 동시에 정량적인 실시간 검출 및 고속대량분석을 목표로 진행되었으며 테스트 과정을 통하여 높은 검출 효율과 다양한 응용가능성을 확인하였다. 이 시스템들은 이후 개인 질병의 진단, 신약개발뿐만 아니라 각각의 생분자에 관한 기초 연구에 중요한 수단이 될 수 있을 것으로 기대된다.

주요어 : 생분석, 산화그래핀, 형광, 고속대량분석방법, 질병진단, 신약개발

학 번 : 2012 – 30076